Selection and characterization of *Arabidopsis thaliana* cohesin and condensin T-DNA insertion mutants

Dissertation

zur Erlangung des akademischen Grades

Doctor rerum naturalium (Dr. rer. nat.)

vorgelegt der

Naturwissenschaftlichen Fakultät I

Biowissenschaften

der Martin-Luther-Universität Halle-Wittenberg

von Frau Andrea Weißleder

geb. am 18.02.1982 in Staßfurt

Gutachter:

Gatersleben, 15.10.2009

ACKNOWLEDGEMENTS

The following work was performed at the Institute of Plant Genetics and Crop Plant Research (IPK), Gatersleben, from January 2006 to June 2009, in the laboratory of Prof. Dr. Ingo Schubert and under the supervision of PD Dr. habil. Veit Schubert.

First I would like to express my gratitude to my supervisor PD Dr. habil. Veit Schubert for giving me the opportunity to work with him, for permanent support, continuous guidance and encouragement.

I am very thankful to Prof. Dr. Ingo Schubert for shearing his knowledge, for the inspiring discussions and his patience with me.

I would like to give my thanks to Dr. Inna Lermontova, Dr. Jörg Fuchs, Dr. Koichi Watanabe, Dr. Gabriele Jovtchev, Izabel Moraes and Stefan Heckmann for their support and their helpful suggestions.

I thank Armin Meister for the help with statistics, Andrea Kunze, Joachim Bruder, Martina Kühne and Rita Schubert for the perfect technical assistance. Special thanks go to Astrid Bruchmüller for providing the *rdr6* mutant line and for the fruitful discussions.
Furthermore, I want to thank Florian Mette for critical reading the dissertation.

I herewith declare that, under supervision, I independently wrote the following doctoral thesis, using none other than the sources and aids listed. Also, during this work, the principles and recommendations in “Verantwortung in der Wissenschaft” (Responsibility in Science), by the Institute of Plant Genetics and Crop Plant Research (IPK), Gatersleben, were observed.
30th of July, 2009

_____ _____

Date Signature

Content

Abbreviations

At1-5	*Arabidopsis thaliana* chromosomes 1 to 5
BAP	6-Benzylaminopurine
bp	base pairs
CAP	chromosome associated protein
cm	centimeter
CenH3	centromeric histone 3
CTCF	CCCTC-binding factor (zinc finger protein)
DAPI	4',6-diamidino-2-phenylindole
DIG	digoxygenine
DNA	deoxyribonucleic acid
DSB	double-strand break
dsRNA	double-stranded RNA
DTT	dithiothreitol
ECO	establishment of cohesion
EDTA	ethylenediaminotetra-acetic acid
ESCO	establishment of cohesion
EYFP	enhanced yellow fluorescent protein
FISH	fluorescence *in situ* hybridisation
GFP	green fluorescent protein
h	hour
H2B	histone 2B
HEAT	Huntingtin, elongation factor 3, the A subunit of protein phosphatase 2A, TOR lipid kinase
HR	homologous recombination
Kan	kanamycin
kb	kilo base pairs
kDa	kilo Dalton
min	minute
ml	milliliter
mM	millimol
mRNA	messenger ribonucleic acid
MTSB	microtubules stabilizing buffer
NASC	Nottingham *Arabidopsis* stock centre
ng	nanogram
NHEJ	non-homologous end-joining
nt	nucleotide
PCR	polymerase chain reaction
pmol	picomol
Pro35S	35S promoter of the cauliflower mosacic virus
PTGS	post transcriptional gene silencing
PPT	phosphinotricine
qRT PCR	quantitative reverse transcription polymerase chain reaction
rDNA	ribosomal DNA
RDR6	RNA-dependent-RNA polymerase 6
RdDM	RNA-directed DNA methylation
RISC	RNA induced silencing complex
RNA	ribonucleic acid
RT	room temperature
RT PCR	reverse transcription polymerase chain reaction

SCC	sister chromatid cohesion
SDS	sodium dodecyl sulfate
sec	second
siRNA	short interfering RNA
SMC	structural maintenance of chromosomes
SSC	sodium chloride sodium citrate buffer
T1	first generation of plants after transformation
T2	second generation of plants after transformation
T-DNA	transfer deoxyribonucleic acid of *Agrobacterium tumefaciens*
TGS	transcriptional gene silencing
Top II	Topoisomerase II
U	unit
UTR	untranslated region of DNA flanking a gene
WAPL	wings apart-like protein
wt	wild type
YFP	Yellow Fluorescent Protein
µl	microliter

1. Introduction

Control of chromosome architecture is an important challenge coped by SMC (structural maintenance of chromosomes) proteins and their interaction partners in all eukaryotes. SMC complexes are necessary for sister chromatid cohesion, condensation of chromatin in nuclear division, DNA repair (reviewed by Nasmyth and Hearing 2005) and they are involved in transcription (Lengronne et al. 2004; Bausch et al. 2007; Bernard et al. 2008; Gullerova and Proudfoot 2008; Parelho et al. 2008; Stedman et al. 2008; Wendt et al. 2008). The diverse functions of SMCs and their interaction partners can be explained by the presence of paralogous genes that evolved during evolution. The wide range of tasks makes SMC complexes to an intensively studied field. Especially in plants only little is known about SMC proteins and their interaction partners.

1.1 SMC complex proteins

Eukaryotes contain three complexes belonging to the evolutionarily conserved SMC protein family: the cohesin, the condensin and the SMC5/6 complex. All three show specialized functions in a variety of organisms. The three SMC complexes developed different functions during evolution. Today´s knowledge is based on studies in budding and fission yeast, *Drosophila melanogaster* (Fallén), *Caenorhabditis elegans* (Maupas), *Xenopus laevis* (Daudin), chicken, mice, and humans.

Two different SMC subunits form the core of each complex. They are arranged as long intramolecular coiled coils with a globular ATPase ‘head’ at one end and a hinge domain at the other end (reviewed by Nasmyth and Hearing 2005; Hirano and Hirano 2006) linking the two SMC subunits in each complex (reviewed by Hudson et al. 2009). Dimerisation of the SMC heads requires ATP binding, while ATP hydrolysis drives the heads apart (Hirano et al. 2001; Hirano and Hirano 2006) according to studies in *Bacillus subtilis var. niger* (Migula). In yeast the head of each SMC subunit binds to the N- or C-terminal end of a kleisin protein, respectively.

Sister chromatid alignment, mediated mainly by cohesins (reviewed by Miyazaki and Orr-Weaver 1994), is defined as “cohesion” by Maguire (1990). After loading by the SCC2/SCC4 complex during replication, sister chromatid alignment is maintained until anaphase (Seitan et al. 2006; Watrin et al. 2006).

Condensins are mainly responsible for chromosome compaction and decatenation during mitosis (D'Ambrosio et al. 2008a). The SMC5/SMC6 complex is involved in somatic and meiotic DNA repair via homologous recombination (Andrews et al. 2005; Palecek et al. 2006). Besides SMC5 and SMC6, six non-SMC subunits named NSE1-NSE6 compose this complex in yeast (McDonald et al. 2003; Pebernard et al. 2004, 2006). The δ-kleisin NSE4 connects both SMC subunits (Sergeant et al. 2005). In *A. thaliana* the SMC5/SMC6 complex shows a similar composition as in yeast (Figure 1) but seems to be lacking the NSE5 and NSE6 subunits (reviewed by Schubert 2009). Like in yeast, SMC5/SMC6 faciliates double-strand break repair by sister chromatid recombination in *A. thaliana* (Watanabe et al. 2009).

The three types of SMC complexes are indispensable for the chromosome organization and function including sister chromatid cohesion, condensation, DNA repair, gene expression and development (reviewed by Nasmyth and Hearing 2005; reviewed by Hirano 2006; Dorsett 2007; Onn et al. 2008; Uhlmann 2008).

Paralogous genes are present for various components of the different SMC complexes allowing them to evolve different functions during evolution of higher plants. Interactions between stalks (coiled coils) of the three SMC complexes and head-head engangement between different complexes are not yet proven but theoretically possible (reviewed by Hirano 2006).

1.1.1 Cohesins

Prokaryotes have no mitotic apparatus but, nevertheless, need to segregate their circular chromosome properly to the daughter cells efficiently. Niki et al. (1991) identified the proteins which promote this process. By searching for mutants showing nucleoid segregation disturbances in *Escherichia coli* they found the *MUK-B* gene encoding a 177 kDa protein essential for the segregation of bacterial chromosomes. The structure of this protein is similar to the SMC proteins found in eukaryotes with globular domains at the N- and C-terminal ends and two long α-helices at the central region. The globular domain at the N-terminus was called Walker A motif and contains an ATP-binding pocket. MUK-B, the bacterial SMC, builds a homodimer and associates with two additional subunits named MUK-E and MUK-F (Yamanaka et al. 1996). Both dimerise via self-association (Gloyd et al. 2007). MUK-F belongs to the kleisin family. Mutations in these genes cause phenotypes with disrupted nucleoid partition (Yamazoe et al. 1999).

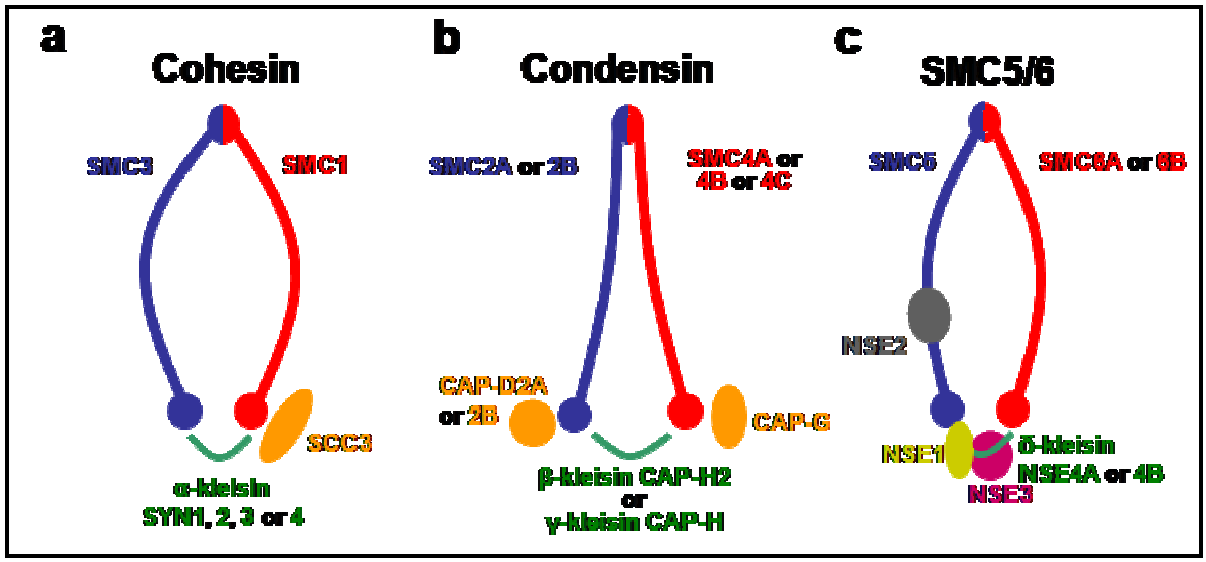

Fig. 1: *A. thaliana* SMC protein complexes, according to review by Schubert 2009. Subunit composition is based on yeast models according to Nasmyth and Hearing (2005) and (Palecek et al. 2006).
a) The cohesin complex consists of SMC1, SMC3, SCC3 and one of the four α-kleisin homologs SYN1-SYN4 in *A. thaliana*.
b) Subunits of the condensin complex can assemble at least two forms: *A. thaliana* presumably has three alternative SMC4 subunits, two alternative SMC2 subunits, two different kleisins named CAP-H (γ-kleisin) and CAP-H2 (β-kleisin), one putative gene encoding the CAP-G subunit and two candidate genes encoding CAP-D2 subunits.
c) The SMC5/6 complexes consist of SMC5, one of the two alternative SMC6 proteins and four NSE proteins (NSE1-NSE4). NSE4 represents the δ-kleisin subunits of the SMC5/6 complex in *S. pombe* (Palecek et al. 2006) and has two homologues, NSE4A and NSE4B in *A. thaliana.*

In *B. subtilis*, the SMCs show a similar structure as in eukaryotes with a head domain, a coiled coil region and a central hinge domain linking the two SMC subunits of the homodimer. SCP-A, a kleisin, and SCP-B are the accessory subunits for the SMC protein in this organism. By labelling of *SCP-A*, *SCP-B* and *SMC* with YFP, it could be shown, that all three subunits (SMC, SCP-A and SCP-B) are required for proper localisation of the SMC complex but the mechanism is still poorly understood (Mascarenhas et al. 2005). One suggestion is that the coiled coil regions might mediate association with DNA. Overproduction results in global chromosome compaction reinforcing the role of SMC in segregation and packing of DNA (Moriya et al. 1998; Melby et al. 1998). Localisation studies revealed that SMC complexes retain in bipolar foci which are suggested as condensation centres. SMC complexes have defined positions on the nucleoid affecting the global compaction of the chromosome (Mascarenhas et al. 2002).

Studies in yeast provided the first insight into the protein complexes cohesin and condensin. In budding yeast the conserved subunits of cohesin SMC1, SMC3, SCC3 and an α-kleisin protein called SCC1 compose the cohesin complex (reviewed by Nasmyth and Hearing 2005; Onn et al. 2008). SCC3, belonging also to the kleisin family, is conserved from yeast to human (reviewed by Losada and Hirano 2005; Onn et al. 2008). It contains a HEAT repeat to facilitate DNA binding and binds to the protein complex by associating with the C-terminal domain of α-kleisin (Toth et al. 1999).

The two cohesin pools present in yeast are loaded at different times during the cell cycle. Loading, moving and removing of cohesins is dynamic throughout the cell cycle and closely related to transcription in yeast (Lengronne et al. 2004; Bausch et al. 2007; Bernard et al. 2008; Gullerova and Proudfoot 2008). Dependent on the adherin SCC2/SCC4, the loading complex for both cohesins and condensins, the first cohesin pool is loaded on centromeres and along chromosome arms in G1 (Ciosk et al. 2000). This pool is able to move from loading sites to loci of transcriptional termination (Lengronne et al. 2004). During pre-anaphase dislocation of cohesin from centromeres, the so called “centromere breathing”, was observed (Ocampo-Hafalla et al. 2007). After separating transiently, sister centromeres associate again by new loading of the second cohesin pool. This phenomenon is caused by tension of the chromosomes during anaphase. The second pool of cohesin is loaded independently of the SCC2/SCC4 loading complex (Ocampo-Hafalla et al. 2007). In the centromere flanking chromatin domains cohesin is concentrated three times stronger than on chromosome arm regions (Blat and Kleckner 1999; Tanaka et al. 1999; Weber et al. 2004; Bernard et al. 2001). Cohesin is enriched around the central spindle forming a cylinder-like structure in mitosis (Yeh et al. 2008). This is important for the bi-orientation of sister chromatids and the intramolecular loop formation of pericentric chromatin mediated by the cohesin complex. Yeast chromosome arms bind cohesin mostly in regions between genes (Laloraya et al. 2000; Glynn et al. 2004). Beside the single kleisin RAD21 (corresponds to SCC1) found in *D. melanogaster* (Vass et al. 2003; Heidmann et al. 2004), yeast and vertebrates contain two α-kleisins. SCC1 is mitosis-specific and its counterpart REC8 acts in meiosis (reviewed by Lee and Orr-Weaver 2001; reviewed by Nasmyth 2001).

In *C. elegans* (Pasierbek et al. 2001) and *Oryza sativa* L., four α-kleisin genes are present and show different functions in somatic cells and during meiosis (Mito et al. 2003; Zhang et al. 2004, 2006; Tao et al. 2007).

In vertebrates, the core components of cohesin complexes are SMC1A or SMC1B, SMC3, SCC1 (RAD21) and SCC3 (SA). They are regulated by the associated factors PDS5 (PDS5A

and PDS5B in mammals), establishment of cohesion protein (ECO1) (ESCO1 and ESCO2 in mammals), the SCC2/SCC4 complex, wings apart-like protein (WAPL) and separase (Skibbens et al. 1999; Hartman et al. 2000; Chen et al. 2002; Kueng et al. 2006). In human, mutations in cohesin genes or genes encoding associated factors cause developmental abnormalities for instance the Cornelia de Lange syndrome (CdLS) (Dorsett 2007; Zhang et al. 2009).

The presence of SMC complexes in all living organisms shows their evolutionarily conserved role in many chromatin related tasks, such as architecture and segregation of chromosomes, DNA repair and gene expression.

In *A. thaliana*, four α-kleisin genes, the *SCC1* homologues *SYN1, SYN2, SYN3* and *SYN4* are found besides the single-copy genes *SMC1*, *SMC3* and *SCC3* (Liu et al. 2002; Lam et al. 2005; Chelysheva et al. 2005). SMC3 may have multiple functions in plants. Using antibodies against SMC3, it could be found at various subcellular compartments (Lam et al. 2005). The four α-kleisins have different functions, in somatic and meiotic tissues. While SYN1 is required for cohesion in meiosis (Bai et al. 1999; Bhatt et al. 1999; Cai et al. 2003), SYN2 and SYN3 seem to play a role in mitosis, as they are expressed mainly in meristematic tissues (Dong et al. 2001). SYN2 has an additional role in DNA repair after UV and ionizing radiation (da Costa-Nunes et al. 2006). SYN3 localisation is visible in the nucleolus suggesting a putative role in controlling rDNA structure, transcription or rRNA processing (Jiang et al 2007). SCC3 is essential for sister chromatid cohesion during mitosis and meiosis (Chelysheva et al. 2005).

Beside the nuclear divisions, sister chromatid cohesion is important for homologous recombination (HR) repair (Palecek et al. 2006). Double-strand breaks (DSBs) are lesions, which can lead to translocations, if they are not repaired correctly (Schubert et al. 2004). In contrast to yeast and vertebrates, sister chromatids in higher plants are frequently separated and show no preferential alignment sites along chromosome arms, whereas sister centromeres stay mostly aligned-up to an endopolyploidy level of 16C in *A. thaliana* (Schubert et al. 2006, 2007, 2008). Extension of alignment sites along sister chromatid arms is variable and leads to the suggestion, that sister chromatid cohesion in higher plants is highly dynamic (Berr et al 2006). After formation of DSBs, cohesins and SMC5/6 complexes are recruited to use the intact sister chromatid for efficient repair (Palecek et al. 2006).

1.1.2 Condensins

Prokayotes contain only one SMC complex but eukaryotes need to change the structure of the chromosomes dynamically. Chromosome architecture maintenance is the most important problem solved by condensin complexes. Recent studies in yeast revealed that condensins play an important role in recruiting and loading non-histone proteins to the chromosomes. Condensins change the topology of DNA to make it permissive for association of proteins. Chromosomes need to stay condensed from prophase to anaphase onset until they arrive at the spindle poles and the new nuclear membrane is formed (reviewed by Hudson et al. 2009). Loading of condensin on yeast chromosomes requires the loading factor SCC2/SCC4 (D'Ambrosio et al. 2008b).

The existing two forms of condensins were identified in different organisms. In condensin I, the SMC proteins bind to the γ-kleisin chromosome-associated-protein (CAP)-H, which was first identified in *Xenopus* (Hirano et al. 1997). The N-terminal end of CAP-H interacts with SMC2 and the C-terminal end with SMC4, thus bringing the ATPase parts of the SMC heterodimer together (reviewed by Hudson et al. 2009).

A third form of condensin has been found only in *C. elegans* until now. This so called condensin I-like complex binds specifically to X chromosomes in hermaphrodites and modulates gene expression to realize dosage compensation (Csankovszki et al. 2009).

In vertebrates, the existing forms condensin I and II consist of the coiled coil forming heterodimer SMC2/SMC4 which is connected by two different kleisins to form a V-like structure (Figure 1) (Sutani et al. 1999; Freeman et al. 2000; Schmiesing et al. 2000; Kimura et al. 2001; reviewed by Nasmyth and Hearing 2005; reviewed by Hudson et al. 2009). CAP-D2, a HEAT repeat-containing protein associates with condensin I (reviewed by Nasmyth and Hearing 2005). In condensin II, identified in vertebrate cells (Ono et al. 2003; Yeong et al. 2003), the two core subunits SMC2 and SMC4 are connected by the β-kleisin CAP-H2. CAP-G acts as the fifth part to stabilise the complex (Dej et al. 2004). In vertebrates, condensin I localises in the cytoplasm until nuclear envelope breakdown (NEBD) and can move on and off the chromosomes, while condensin II is not mobile and localises in the nucleus during the whole cell cycle (reviewed by Hudson et. al 2009). Chromosome condensation in prophase requires condensin II, as condensin I cannot enter the nucleus until NEBD (reviewed by Hudson et. al 2009).

RNAi based depletion of either condensin I or condensin II results in anaphase bridges in mammalian cell cultures (Ono et al. 2004; Gerlich et al. 2006). Condensin complexes are conserved among all eukaryotes.

In *A. thaliana*, the presence of more than one gene for some of the condensin subunits allows, to assemble different condensin complexes (Fujimoto et al. 2005). At least two (probably three) genes encoding SMC4 are found in *A. thaliana* (*SMC4A*, *SMC4B* and *SMC4C*). Two genes each encoding SMC2 (*SMC2A* and *SMC2B*) and CAP-D2 (*CAP-D2A* and *CAP-D2B*) are present in the genome (Figure 1). The subunit variants SMC2A and SMC2B, SMC4A and SMC4B and also the kleisins CAP-H and CAP-H2 are essential for chromosome condensation and segregation during mitosis, meiosis and embryo development in *A. thaliana* (Tzafrir et al. 2002; Liu et al. 2002; Siddiqui et al. 2003, 2006). The two kleisin variants show a different localisation during interphase. CAP-H can be found in the cytoplasm and in the nucleus, while CAP-H2 localises in the nucleus only. Only CAP-H shows the presence of a kleisin-gamma-middle domain which is responsible for localisation of the protein on the chromatin (Fujimoto et al. 2005). *A. thaliana* has one gene with a partial sequence similarity to the *CAP-G* gene but the function of this protein still needs to be elucidated. The function of the SMC4C candidate and the two *A. thaliana* CAP-D2 homologues is unknown so far. In *Drosophila* CAP-D2 is required to stabilise the condensin complex and to resolve sister chromatid cohesion (Savvidou et al. 2005).

1.2 Proteins interacting with cohesins and condensins

For the different tasks of SMC complexes such as establishment, maintenance and dissolution of sister chromatid cohesion, segregation, condensation, transcription, DNA repair, replication and involvement in gene silencing mechanisms a variety of interaction partners are necessary.
In mammals the transcription regulatory zink finger protein CTCF (CCCTC-binding factor) shows the same binding sites as cohesin. CTCF is a transcriptional insulator that can block promoter enhancer interactions by facilitating formation of chromatin loops (reviewed by Gause et al. 2008, Wendt and Peters 2009; Parelho et al. 2008; Stedman et al. 2008; Wendt et al. 2008, McNairn and Gerton 2008).
A. thaliana shows coexpression of cohesins, *C2H2* and *REF6*, which are homologues of *CTCF*. The formation of transcription factories, meaning gene regulation by long-distance interactions, seems to be influenced by insulator proteins like C2H2, REF6 and interacting proteins. These insulators recruit cohesins for transcriptional insulation and influence chromatin condensation (Rudnik 2009).
The cohesin and condensin loading complex SCC2/SCC4 is conserved among all eukaryotes (Seitan et al. 2006; Watrin et al. 2006). Within the *Drosophila* genome, cohesin and Nipped-B (corresponding to the SCC2 subunit of the yeast SCC2/SCC4 loading complex) bind

consistently to the same sites throughout the entire non-repetitive part of the DNA, preferentially to introns in actively transcribed regions (Misulovin et al. 2008). Loading of cohesins and condensins is essential for plant viability, which makes SCC2/SCC4 indispensable. The loading complex also plays a role in organisation of the centromere (Sebastian et al. 2009). Plants mutated in *SCC2* show early embryo lethality and formation of giant endosperm nuclei. RNAi mediated depletion of AtSCC2 results in sterility due to disturbed meiotic chromosome organisation. In detail, the plants show defective homologous pairing, loss of sister chromatid cohesion, missegregation of chromosomes and chromosome fragmentation (Sebastian et al. 2009).

Meiotic cohesion requires the protein SWI1, which has a partial similarity to SMC proteins. SWI1 is required for the establishment of sister chromatid cohesion in gametes. Recombination during early male and female meiosis and the formation of axial elements requires SWI1 in *A. thaliana*. In male meiosis, bivalents cannot be formed without SWI1 at metaphase I. This results in polyads and micronuclei due to premature loss of sister chromatid cohesion (Cai and Makaroff 2001; Mercier et al. 2001, 2003; Agashe et al. 2002; Boateng and Makaroff 2004). *O. sativa* harbers genes homologous to *SWI1* with putative meiotic function (www.arabidopsis.org).

In *A. thaliana* BRU1 is important for structural and functional stability of chromatin. It is involved in chromatin assembly and heterochromatin condensation. BRU1 contributes to postreplicative stability of the epigenetic information, thus linking genetic and epigenetic information and the control of development. *Bru1* mutant plants show a dwarfy phenotype, developmental abnormalities, a very low seed set, a high sensitivity to genotoxic stress, an accidently release of transcriptional gene silencing (TGS), an increased homologous recombination frequency and a disorganised shoot apical meristem due to disturbances in maintaining stem cell identity in this tissue. In some nuclei of mutated plants altered heterochromatin patters with decondensed centromeric heterochromatin can be observed. This protein may play a role in replication and stabilisation of chromatin structure (Takeda et al. 2004).

Recent studies in yeast suggest that various pathways and a multitude of interacting proteins exist for the dissolution of cohesion (Onn et al. 2008). After cohesin dissolution in budding yeast, the remaining amount of cohesion in cohesin deficient mutants depends on the locus analysed. Only at telomeres a complete loss of cohesion has been found. Pericentromeres, rDNA loci and loci on the chromosome arms remain partially aligned because of catenations between the sister chromatids (Díaz-Martínez et al. 2008). Yeast separase and its inhibitor

securin are indispensable for the separation of sister chromatids in nuclear divisions. By degrading securin, separase cleaves almost all cohesins to separate chromatids during anaphase (Uhlmann 2007). Cohesin removal from meiotic chromosomes requires the *Arabidopsis* separase homolog AESP (Liu and Makaroff 2006).

DNA repair needs dynamic cohesion to facilitate postreplicative homologous recombination-repair of double-strand breaks (DSBs) by local pairing of a damaged chromatid with its intact sister (reviewed by Ström and Sjögren 2007; Onn et al. 2008). Cohesin accumulates at DSB ends, to mediate *de novo* cohesion in yeast (Ström et al. 2004, 2007; Ünal et al 2004; Cortes-Ledesma and Aguilera 2006) and human (Kim et al. 2002). First the SMC5/6 complex is loaded to the breakpoint and recruites cohesin afterwards (Palecek et al. 2006; Potts et al. 2006; reviewed by Cortes-Ledesma et al. 2007; reviewed by Murray and Carr 2008). The positional sister chromatid alignment is increased after X-irradiation when the AtSMC5/SMC6 complex is intact in *A. thaliana* (Watanabe et al. 2009).

1.3 Life cell imaging of chromatin in interphase and during nuclear division

The phenomenon of cell division (mitosis) was first described by Walther Flemming (1878). Cell division including nuclear division is of great biological importance to maintain the chromosomal set. Consequences of mistakes can be dramatic. To avoid breaking of chromosomes, sister chromatid cohesion and condensation of chromatin are required during mitosis (reviewed by Miyazaki and Orr-Weaver 1994; reviewed by Cobbe and Heck 2000).

The longstanding argument that *in vitro* experiments do not directly reflect the situation in a living organism can be overcome by life cell imaging. This can provide a critical insight into the fundamental nature of cellular and nuclear functions, especially due to the rapid advances that are currently being witnessed in fluorescent protein technology. Thus, live cell imaging has become a requisite analytical tool in most cell biology labs (Komari and Hiei 1996, Levitt et al. 2009).

Autofluorescence from chlorophyll, lignified cell walls, vacuolar contents or callose in case of stressed tissue turn life cell imaging in plants into a real challenge. The choice of the proper emission wavelength is important especially for leaf tissue.

Fluorescent tagged recombinant proteins represent a powerful tool for in vivo studies. Many variants of coloured fluorescence proteins are available today. In this study DsRed and YFP were chosen as markers. DsRed was extracted from the oral disk of the reef coral *Discosoma striata* (Matz et al. 1999) and shows a higher stability compared to the often used GFP. The

DsRed protein was used successfully for expression in mammalian cells (Bevis et al. 2002), in higher plants (Dietrich et al. 2002) and in yeast (Rodrigues et al. 2001). Also in filamentous ascomycete fungi DsRed was shown to be a good marker (Mikkelsen et al. 2003).

YFP is a synthetic variant of GFP (Chalfie 1994; Sheen et al. 1995; Tsien et al. 1998), which was derived from the bioluminescent jellyfish *Aequorea victoria* (Murbach and Shearer). These markers fused to a protein of interest allow tracing in space and time by fluorescence microscopy. To analyse the consequences of mutations in nuclear proteins during cell division and interphase, chromatin labelling is necessary. Therefore, histones such as H2B are well established markers for microscopical tracking of nuclei. In centromeres, canonical histone H3 is replaced by the centromere-specific histone H3 (CenH3), which was first discovered in human as centromeric protein A (CENP-A) (Palmer et al. 1987). *Arabidopsis* CenH3 was isolated later (Talbert et al. 2002). Tracking of centromeres via fluorescent proteins can be done using recombinant CenH3.

Simultaneous transformation with chromatin and centromere specific markers provides a direct insight into two important structures during mitosis *in vivo*. Co-transformation was shown to be successful on RNA level by using the Northern blot technique in *A. thaliana* (Radchuk et al. 2005) but detailed analysis of single nuclei was not done.

1.4 T-DNA lines of *A. thaliana*

Agrobacterium tumefaciens (Smith and Townsend) allows transformation of plant genomes. From its Ti plasmid, the genes responsible for tumor induction were removed and genes providing antibiotic resistance and/or markers that are fused to a gene of interest are inserted (Buchholz and Thomashow 1984). This is one reason to make *A. thaliana* to a model organism for molecular analyses. An important resource is the collection of >250 000 T-DNA insertion lines (http://signal.salk.edu/cgi-bin/tdnaexpress). For >90% of *A. thaliana* genes, a mutant line can be found in the collection. The T-DNA insertion can cause a loss of gene expression allowing reverse genetic approaches (Alonso and Stepanova 2003). It is very likely, to find more than one insertion of T-DNA after transformation within the genome, especially when hypervirulent *Agrobacterium* strains were used (Alonso et al. 2003). In this case it has to be proven, that the effect of the mutation is a real consequence of an insertion in the gene of interest and not a side-effect of the second T-DNA locus in another gene. Multiple insertions bear also multiple CaMV 35S promoters, which are a part of the T-DNA. This can cause silencing of other expression constructs, which are inserted addidionally (Daxinger et al. 2008).

1.5 Aim of this work

Cohesin and condensin are multi subunit complexes that are well studied in yeast and mammals. In plants detailed analysis is lacking. T-DNA lines were selected, to interrupt the putative cohesin- and condensin genes, as well as genes encoding interacting proteins. The function of the cohesin and condensin subunits and proteins interacting with them was investigated.

Selection of T-DNA lines

According to sequence similarity to the cohesin and condensin genes in yeast, the respective candidate genes were identified in *A. thaliana*. To apply a reverse genetic approach, T-DNA insertion lines interrupting the putative cohesin- and condensin genes were selected from the SALK, GABI and SAIL collection.

Confirmation of T-DNA lines

First the lines were genotyped, to find out if the mutation is homozygously lethal. In this case only heterozygous plants can be selected. PCR fragments using a primer annealing on the left border of the T-DNA and a gene-specific primer were sequenced to confirm the position of the T-DNA in the gene of interest. Further confirmation was needed according to the mRNA expression of the respective genes. Homozygous mutant plants were analysed by RT PCR for the presence or absence of the mRNA and for presence of a truncated transcript upstream or downstream of the T-DNA. For the lines which could only be selected as heterozygous, real-time PCR was performed, to measure the exact expression level of the intact allele. Additionally, the number of the integrated T-DNA loci was identified by Southern blot hybridisation using a T-DNA specific probe.

Transformation and life cell imaging to analyse genome stability

Lines with a T-DNA position in the coding region of the respective genes were transformed with Pro35S-H2B-DsRed to visualize the whole chromatin in red and Pro35S-EYFP-CenH3 to label the centromeres in yellow. After observing very low frequencies of expression of both constructs within one nucleus, the strategy was changed. The confirmed T-DNA lines were transformed only with Pro35S-H2B-YFP to label the chromatin in yellow. In the transformed mutant lines mitotic divisions and interphase chromatin structure were analysed in root tips *in vivo* and compared to wt. To confirm the results observed *in vivo*, seedlings of untransformed mutant lines and wt as control were incubated with DAPI to visualize the chromatin. The importance of the components belonging to the cohesin and condensin complex and three interacting proteins for genomic stability in interphase and mitosis was investigated.

2. Materials & Methods

2.1 Plant Material and Genotyping

The SALK T-DNA insertion lines in ecotype Columbia (Col) background were selected from the Salk Institute Genomic Analysis Laboratory (http://signal.salk.edu/cgi-bin/tdnaexpress) (Alonso et al. 2003) and provided by the Nottingham Arabidopsis Stock Centre (http://nasc.nott.ac.uk/). GABI (Genomanalyse im biologischen System Pflanze) T-DNA mutants (in Col-0) were generated in the context of the GABI-Kat program and provided by Bernd Weisshaar (MPI for Plant Breeding Research, Cologne, Germany) (http://www.gabi-kat.de/) (Rosso et al. 2003). One mutant line out of the SAIL (Syngenta Arabidopsis Insertion Library) collection was kindly provided by Daniel Riggs (Department of Botany, Devision of Life Science, University of Toronto, Canada). The mutant line deficient in the RNA-dependent-RNA polymerase 6 (RDR6) was selected out of the SALK collection (SALK_001394).

Seeds were germinated on agar and cultivated in soil under short day conditions (8-h-light/16-h-dark) at 21 °C. Genomic DNA was isolated from rosette leaves and used for PCR-based genotyping to identify hemizygous and homozygous T-DNA insertion mutants. The PCR primers used for genotyping are listed on Supplementary Table 1, 4 and 7 and their positions are shown together with the corresponding gene structure (http://mips.gsf.de/ (MAtbB v2.0) in Figures 4, 7 and 10. PCR using the gene-specific primer sets yielded DNA fragments of ~1 kb representing the wild-type alleles. The PCR fragments specific for the T-DNA insertion allele yielded PCR products of ~0.5 kb. The positions of T-DNA insertion were confirmed by sequencing the PCR-amplified T-DNA junction fragments obtained with GoTaq Polymerase from Promega, Mannhein Germany. (Supplementary Tables 2, 5 and 8) Sequencing of PCR products was done by AGOWA GmbH using ABI 3730xl sequencing run with a read length up to 1000 nt (PHRED20 quality).

Sequences were aligned using ‘MultAlign’ (http://bioinfo.genotoul.fr/multalin/multalin.html). The following databases were used for sequence comparisons and BLAST (Basic Local Alignment Search Tool) analyses: NCBI – http://www.ncbi.nlm.nih.gov/BLAST/

TAIR – http://www.arabidopsis.org/Blast/index.jsp

2.2 mRNA Expression Analyses

Total RNA was isolated from rosette leaves using the RNeasy plant mini kit (QIAGEN) according to manufacturer's instructions. Reverse transcription was performed using a First Strand cDNA Synthesis Kit (Fermentas, St. Leon-Rot) and 1 µg of total RNA as starting material.

Semiquantitative and Real-time PCR primers used to amplify transcripts are shown in Supplementary Table 3, 6 and 9. Real-Time PCR with SYBR® Green was used to quantify the abundance of transcripts within 1µg RNA using an iCycler from BIORAD. Initial denaturation time was 5 min at 95 °C. Then, 40 cycles were run with 10 sec denaturation at 95 °C, 20 sec annealing at 60 °C and 20 sec elongation at 72 °C. Actin2 served as a standard.

For Semiquantitative RT-PCR, the following program was used: initial denaturation: 2 min at 95 °C, then 40 sec denaturation at 95 °C, 30 sec annealing (depending on primer sequences 55 °C – 59 °C), 40 sec elongation for 35 cycles, 5 min final elongation. Elongation factor 1α served as a standard.

2.3 Restriction digestion, gel electrophoreses of genomic DNA and non-radioactive Southern hybridisation

Southern hybridisation was performed according to Southern (1975). Detection was done using the non-radioactive method described by Accotto (1998). 3 µg of genomic DNA from plants with T-DNA insertion and from wt as negative control were digested over night with the restriction enzymes *KpnI* or *HindIII* (Fermentas, St. Leon-Rot) for the SALK lines, *XapI* or *PaeI* (Fermentas, St. Leon-Rot) for GABI lines at 37 °C. The restriction enzymes were selected according to their restriction patterns in the T-DNA. These enzymes showed a single restriction side inside of the respective T-DNA and do not restrict the corresponding hybridisation probe. A second restriction side was found in the surrounding genomic sequence resulting in a DNA fragment of an expected size, if the position of the T-DNA is known. The digested DNA was size-fractionated by gel electrophoresis (1 % agarose in TBE buffer, 4 h at 80 V). A Digoxigenin-labeled DNA Molecular Weight Marker (Roche Diagnostics, Penzberg) was used for comparison of the fragment size. The gel was denatured in denaturation buffer (1.5 M NaCl, 0.5 M NaOH) for 30 min, neutralized in neutralization buffer (1.5 M NaCl, 1 M TrisHCl, pH 7.2, 0.001 M EDTA) 15 min twice, then blotted onto Hybond-N+ membrane (GE Healthcare, Buckinghamshire, UK) by transfer in 20x SSC

overnight. The DNA was fixed to the membranes by a UV Stratalinker 1800 (Stratagene, La Jolla, USA). Prehybridisation and hybridisation were performed according to the manufacturer's instructions using the DIG Easy Hyb Granules (Roche Diagnostics, Penzberg). Labeling of the PCR probes with Digoxigenin was done with the PCR DIG Probe Synthesis Kit (Roche Diagnostics, Penzberg). Washing off the unspecifically bound probes was done twice 15 min in high stringency washing buffer I (0.5x SSC, 0.5% SDS) and twice 15 min in high stringency washing buffer II (0.1x SSC, 0.1% SDS). Before blocking, the membrane was washed for 5 min in maleic acid buffer (100 mM maleic acid, 150 mM NaCl, pH 7.5) containing 0.3 % Tween 20 (Sigma-Aldrich, Steinheim). Blocking Reagent was used for nucleic acid hybridisation and detection (Roche Diagnostics, Penzberg). For detection, the antibody Anti-Digoxigenin-AP-Fab-Fragments (Roche Diagnostics, Penzberg) was used according to the manufacturer's instructions. CSPD ready-to-use reagent (a chemiluminescent substrate for alkaline phosphatise that enables extremely sensitive and fast detection of biomolecules by producing visible light) was used for detection (Roche Diagnostics, Penzberg).

Amersham Hyperfilm^{TM} ECL was used under red-light conditions in the darkroom to visualize the emitted chemiluminescence according to the manufacturer´s instructions (GE Healthcare, Buckinghamshire, UK).

According to the different vectors for T-DNA insertions specific probes were designed for hybridisation. Insertion lines provided by the GABI collection contain the vector pAC161. A probe was designed specific for the right border of the T-DNA covering 496 bp.

The SALK institute used the pBIN-pROK vector to create the mutant lines. For these lines the CaMV 35S promoter sequence was used, to design a probe specific with a length of 374 bp. Primer sequences for amplification of hybridisation probes are listed in Supplementary Table 10.

The Syngenta mutant line was provided by Dan Riggs (University of Toronto, Canada) and Southern hybridisation was performed in his lab (Siddiqui et al. 2006).

2.4 Transformation of *A. thaliana*

To transform *A. thaliana* plants, the simplified "floral dip" method was used according to Clough and Bent (1998). Siliques and opened flower buds were removed from flowering plants, because only closed flower buds can be transformed by *A. tumefaciens*. The bacterial culture was grown for 2 days at 28° C until an OD of 1.7 measured at 600 nm. After

centrifugation the bacterial pellet was resuspended in infiltration medium (5 % Sucrose, 0.0187 µM Benzylaminopurin (BAP), pH 5.7) containing 1 % Acetosyringone, a secondary plant metabolite secreted after wounding, and Silwet 0.05 % L-77 (Lehle Seeds, Round Rock, USA) to improve cuticular penetration. The flower buds were dipped into the medium and the plants were stored vertically under wet and dark conditions over night. Then the plants were put into an upright position under long day light conditions. Seeds were harvested and transformants selected on plates containing MS medium (Murashige and Skoog 1962) suitable antibiotics or herbicides. Double transformation was done using a mixture of two *A. tumefaciens* strains, containing Pro35S-H2B-DsRed and Pro35S-EYFP-CenH3 constructs, respectively (Figure 4). DsRed was fused to the histone H2B and YFP to CenH3, the centromeric histone H3. After transformation of the fusion constructs, the whole chromatin is marked in red and the centromeres appear as yellow dots in the nuclei of transgenic plants.

The fused Pro35S-EYFP-CenH3 sequence was cloned into the pLH7000 vector and the fusion sequence Pro35S-H2B-DsRed was cloned into pLH9000 (www.dna-cloning-service.de) (Figure 2). All cloning experiments were performed by I. Lermontova.

Seeds were surface sterilized and germinated under long day conditions (16 h light at 20 °C, 8 h dark at 18 °C) on selective MS medium (Murashige and Skoog 1962) containing 16 µg/ml PPT for selection of Pro35S-EYFP-CENH3 and/or 50 µg/ml Kan for Pro35S-H2B-DsRed or Pro35S-H2B-YFP. Effects of mutations on mitoses were analysed in root tips of eight to 14 days old plantlets *in vivo* in the T2 generation.

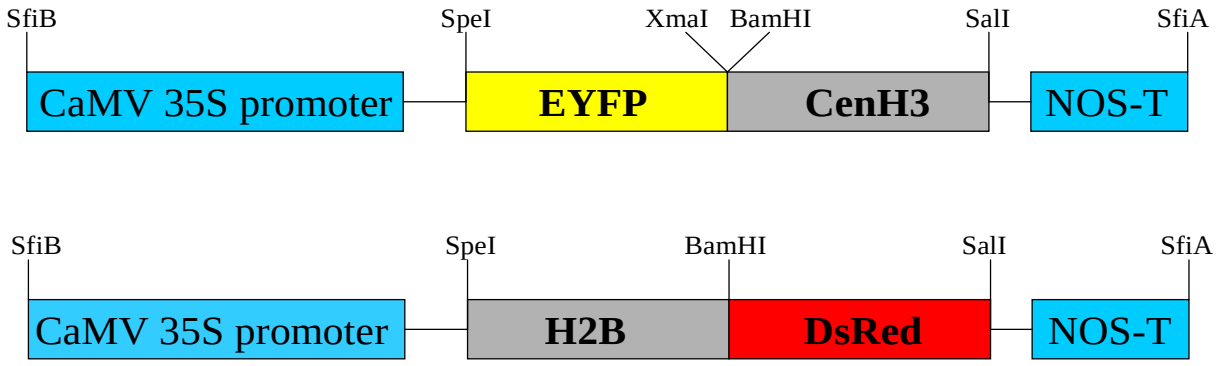

Fig. 2: Constructs for the *A. thaliana* double transformation. EYFP was fused to the sequence of the centromeric histone CenH3 in a 35S promoter – Nopaline Synthase (NOS) terminator expression vector; the histone H2B was fused to DsRed into the same vector type.

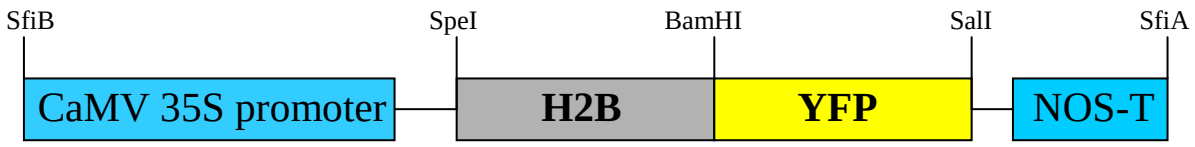

Fig. 3: Construct structure for the *A. thaliana* single transformation. The histone H2B was fused to YFP in a 35S promoter – Nopaline Synthase (NOS) terminator expression vector. This construct was kindly provided by Frédéric Berger (Ecole normale supérieure de Lyon France).

2.5 Fixation and DAPI staining of seedlings

For the confirmation of the *in vivo* results, 3 days old seedlings were fixed and stained with DAPI to visualize the chromatin. Mitoses were analysed in cotyledons of squashed seedlings. Untransformed seedlings of Col wt and mutants were grown four days under long day conditions (16 h light at 21 °C, 8 h dark at 18 °C) on filter paper and fixed in ethanol/acetic (3:1) acid between 10 and 12 o'clock am, because cell division activity is highest at this time (Schubert et al. unpublished). Fixation solution was washed out after 20 h incubation with 2xSSC (3 times 5 min). Digestion with PCP enzyme mixture (2.5 % pectinase, 2.5 % cellulase Onozuka R-10, and 2.5 % pectolyase dissolved in MTSB) was done for 2 h at 37 °C, to soften the tissue. DAPI (1.5 µg/ml in 2xSSC) staining was optimal after 1.5 h incubation at RT in the dark to avoid bleaching. Then, seedlings were put on a slide, mounted in 5 µl Vectashield and covered with a cover slip. 14 individual seedlings were analysed per mutant line and compared to wt.

2.6 Microscopic evaluation, image processing and statistics

Analysis of *in vivo* YFP and DsRed fluorescence signals was performed with an inverted Axiovert 100 TV epifluorescence microscope (Zeiss, Jena) using a 63x/1.4 apochromate objective and a CV-M300 black and white camera (JAE Corporation, Tokyo, Japan), or using a confocal laser-scanning-microscope LSM 510 META (Zeiss, Jena) with a laser of 488 nm. The Zeiss Axiovert 100 TV microscope was integrated into a Digital Optical 3D Microscope system (Schwertner GbR, Jena) to check the signals. Images were captured separately for each fluorochrome using appropriate excitation and emission filters. For detection of DAPI the filterset F36-513, for YFP F36-720 and for DsRed F36-750 was used (AF Analysentechnik, Tübingen). The images were merged using Adobe Photoshop 6.0 software (Adobe Systems, San Jose, USA). DAPI stained meristems of fixed seedlings were analysed with an Axiophot epifluorescence microscope (Zeiss, Jena) using a 100x/1.45 α plan-fluar

objective (Zeiss, Jena) and a 3-chip Sony DXC-950P color camera. This microscope was integrated into a Digital Optical 3D Microscope system (Schwertner GbR, Jena). Differences in expression after double transformation and single transformation were analysed by counting of nuclei in freshly cutted root and leaf material after DAPI staining. YFP and DsRed fluorescing nuclei were compared with the number of DAPI stained nuclei and significant differences were calculated using the two-sided Fisher´s Exact Test.

The frequencies of anaphase bridges in mutants compared to wt were calculated applying the two-sided Fisher´s Exact Test. From heterozygous mutants three days old seedlings could not be genotyped after fixation, DAPI staining and squashing the cotyledon tissue on the slight. Therefore, the anaphase bridge frequencies were grouped according to a significance table for the expected distribution based on Fisher´s exact test. The exact 95% binomial confidence intervals for the corresponding bridge frequencies were calculated with the QUICKBASIC program for exact and mid-p confidence interval for a binomial proportion (Fagan 1996). Two examples of the mid-p confidence intervals can be found in Supplementary Figure 3, displaying only heterozygous mutants and wt derived from a heterozygous parent plant. Supplementary Figure 4 shows the seedling distribution of a heterozygous *SWI1* patent plant segregating in heterozygotes, wts and one homozygous plant. Homozygous plants mutated in *SWI1* were sterile.

3. Results

All analysed *A. thaliana* genes encoding subunits of the cohesin complex, the condensin complex, as well, as the three analysed interacting proteins are relevant for correct procedure of mitosis. Some of these genes seem to be required additionaly for meiosis and cause sterile plants in case of homozygosity. But meiosis was not analysed in detail in this study. To analyse mitosis in mutant plants, life cell imaging allowed the detection of consequences of the mutations on cellular level.

For the different cohesin and condensin candidate genes altogether 15 and 17 T-DNA insertion lines were analysed, respectively. The SCC2/SCC4 cohesin and condensin loading complex was analysed using two T-DNA insertion lines interrupting the *SCC2* gene. As interacting proteins for cohesin the *SWI1* gene and for condensin *BRU1* was analysed. Presence and position of the T-DNA were confirmed by genotyping via PCR using gene-specific and T-DNA specific primers. PCR fragments amplified from the LB of the T-DNA and the surrounding gene sequence were sequenced. The positions of the primers are illustrated in Figure 4, 7 and 10. Primer sequences are listed in Supplementary Tables 1, 4 and

7. The genotyping PCR products were aligned with the corresponding gene sequence (Supplementary Tables 2, 5 and 8) and the T-DNA sequence, respectively. Mutations which were homozygously lethal could be selected only as heterozygous lines. The segregation of mutants occurred in a non-mendelian segregation value. mRNA expression of homozygous mutants was analysed by RT PCR to confirm the absence or mutation of the respective transcripts. Quantitative real-time RT PCR was used to determine the expression level in heterozygous lines. Primers used for amplification of cohesin cDNA are listed in Supplementary Table 3. Condensin cDNA was amplified using the primers listed in Supplementary Table 6 and the primers for cDNA amplification of the genes encoding interacting proteins can be found in Table 9.

The confirmed lines, showing no or aberrant transcripts of the corresponding genes compared to wt were double transformed with Pro35S-H2B-DsRed and Pro35S-EYFP-CenH3. The double transformation strategy was changed into single transformation with Pro35S-H2B-YFP after observing very low expression frequencies. Eight of the mutant lines showed an increased number of anaphase bridges in the life cell imaging approach. To confirm this result, untransformed mutant lines were DAPI stained and cotyledons showed similar bridge frequencies like root tips *in vivo*. The lines which showed not enough fluorescence expression were analysed by DAPI staining. Significant increase in the anaphase bridge frequency compared to wt was observed in 14 out of 21 mutant lines (Table 1).

3.1 Cohesins

For the seven genes encoding the cohesin complex components, 15 T-DNA lines were found. Two of them were found in introns, twelve in exons and one upstream of the coding region of a gene (Figure 4). Alignments of PCR fragments with the corresponding gene can be found in Supplementary Table 2. The two SMC subunits, as well as SCC3 and SYN3, one of the four α-kleisin candidates, are essential for survival of *A. thaliana*. T-DNA lines inserted in these genes could only be selected as heterozygous. In these lines an upregulation of transcription of the intact allele was observed (Table 1). Homozygous plants mutated in *SYN1*, the meiotic α-kleisin were sterile. Analysis of transcription of homozygous lines via RT PCR is illustrated in Figure 5. Expression of Pro35S-H2B-YFP correlates negatively with the number of T-DNA loci found by Southern hybridisation (Figure 6). The number of T-DNA loci had no influence on the amount of anaphase bridges.

	Gene Symbol	Locus	T-DNA lines	No. of T-DNA loci	Habit	Fertility	Zygosity	% expression of mRNA [a]	Expression of H2B-YFP	% anaphase bridges		max. no. of bridges	Segregation (number of plants)[d] wt : he : ho
Cohesin										*in vivo* root tip[b]	fixed cotyledons[c]		
	SMC1	At3G54670	SALK_017437	8	wt-like	fertile	he	78.2	weak	0	2.4	1	1:1.5 (137)
			GABI_269E12	1	wt-like	fertile	he	90.7	strong	4	2.4	1	1:3 (105)
	SMC3	At2G27170	SALK_015308	8	wt-like	fertile	he	90.4	weak	0	2.9	1	1.6:1 (84)
			SALK_087935	2	wt-like	fertile	he	97.8	strong	n.d.	n.d.	n.d.	1:3.2 (21)
			GABI_498B03	1	wt-like	fertile	he	87	strong	2.7	2.6	1	1:1.5 (61)
	SYN1	At5G05490	SALK_137095	4	smaller	sterile	ho	absent	weak	n.d.	5.7	1	1:4:1.9 (69)
			SALK_006687	3	smaller	sterile	ho	absent	weak	n.d.	3.1	1	7.3:14:1 (89)
	SYN2	At5G40840	SALK_015096	2	wt-like	fertile	ho	absent	strong	n.d.	n.d.	n.d.	n.d.
			SALK_044851	4	wt-like	fertile	ho	absent	strong	12.5	9.8	2	n.d.
	SYN3	At5G16270	SALK_119629	5	wt-like	fertile	ho	wt-like	n.d.	n.d.	n.d.	n.d.	n.d.
			GABI_095A10	1	wt-like	fertile	he	76.8	n.d.	n.d.	23.4	2	2.7:1 (115)
	SYN4	At3G59550	SALK_076116	6	wt-like	fertile	ho	truncated	medium	13.6	18.8	3	n.d.
			SALK_130085	3	wt-like	fertile	ho	truncated	strong	12.5	10.8	5	n.d.
			SALK_020171	2	wt-like	fertile	ho	truncated	n.d.	n.d.	15.3	2	n.d.
	SCC3	At2G47980	SALK 021769	2	wt-like	fertile	he	83.5	n.d.	n.d.	14.5	2	1:1 (100)
Condensin	*SMC2A*	At5G62410	SALK_052322	2	wt-like	fertile	ho	truncated overexpression	strong	22.6	15.6	3	n.d.
			SALK_103701	1	wt-like	fertile	he	92.2	n.d.	n.d.	n.d.	n.d.	1:4 (20)
			SALK_103691	1	wt-like	fertile	he	79.2	n.d.	n.d.	n.d.	n.d.	2.4:1 (94)
			SALK_095685	4	wt-like	fertile	ho	truncated	n.d.	n.d.	n.d.	n.d.	n.d.
	SMC2B	At3G47460	SALK_101627	n.d.	wt-like	fertile	ho	wt-like	n.d.	n.d.	n.d.	n.d.	n.d.
			SALK_101643	2	wt-like	fertile	ho	absent	strong	15.6	11.6	2	n.d.
			SALK_030653	2	wt-like	fertile	ho	absent	n.d.	n.d.	n.d.	n.d.	n.d.
	SMC4A	At5G48600	SALK_002313	5	wt-like	fertile	he	101.6	n.d.	n.d.	n.d.	n.d.	1:1.3 (32)
			SALK_002371	n.d.	wt-like	fertile	ho	wt-like	n.d.	n.d.	n.d.	n.d.	n.d.
			SALK_002392	n.d.	wt-like	fertile	ho	wt-like	n.d.	n.d.	n.d.	n.d.	n.d.
			SAIL_86D02	1	wt-like	fertile	he	85.4	strong	11.5	14.5	3	2.1:1 (65)
	SMC4B	At5G08010	SALK_105826	n.d.	wt-like	fertile	ho	wt-like	n.d.	n.d.	n.d.	n.d.	n.d.
	CAP-H	At2G32590	SALK_072400	4	wt-like	fertile	he	100	n.d.	n.d.	4.2	2	2:1 (33)
			SALK_017766	2	wt-like	fertile	he	90.8	strong	12.3	14.9	3	1.3:1 (37)
	CAP-H2	At3G16730	SALK_059304	1	wt-like	fertile	ho	absent	strong	9.8	10.5	2	n.d.
	CAP-D2A	At3G57060	SALK_077796	n.d.	wt-like	fertile	ho	wt-like	n.d.	n.d.	n.d.	n.d.	n.d.
Interacting Proteins	*SWI1*	At5G51330	GABI_206H06	1	wt-like	sterile	ho	truncated overexpression	strong	21.7	21 (he), 43.8 (ho)	3	1.9:3.3:1 (105)
	SCC2	At5G15540	SALK_058767	7	wt-like	fertile	he	97.1	weak	n.d.	n.d.	n.d.	1:1.2 (189)
			SALK_151609	3	wt-like	fertile	he	95.2	n.d.	n.d.	22.9	2	1:3.3 (43)
	BRU1	At3G18730	SALK_034207	4	smaller, fasciation	low seed set	ho	absent	n.d.	n.d.	20	2	n.d.
	Col	wild type	wild type	0	wt	fertile		100	strong	1.7	2.6	1	

Tab. 1: Characterization of all analyzed T-DNA insertion mutants corresponding to the cohesin, condensin and interacting genes.
[a] expression in rosette leaves analyzed by semiquantative RT-PCR or real-time PCR (%) in comparison to wt Columbia.
[b] anaphase bridges were counted in T2 plants expressing Pro35S-H2B-YFP.
[c] bridge values correspond to mutant plants containing no Pro35S-H2B-YFP construct after DAPI staining.
[d] Segregation wild type (wt):heterozygous (he):homozygous (ho) plants, if the mutation is homozygous lethal, only wt and he could be counted.
n.d. – not done

3.1.1 SMC1 and SMC3 are essential for plant viability

To interrupt the *SMC1* gene, two T-DNA insertion lines were found, which were both located in the fifth intron of the gene. Sequencing confirmed the annotated position given in the database (http://signal.salk.edu/cgi-bin/tdnaexpress). Southern hybridisation revealed at least 8 loci of T-DNA in line SALK_017437. The GABI collection provided the second line, GABI_269E12, which turned out to be a single T-DNA insertion line according to Southern hybridisation. For analysis of the dimerisation partner of SMC1, SMC3, three lines were found. SALK provided two lines with location in the third (SALK_015308) and eighth (SALK_087935) exon. Line SALK_015308 showed at least eight loci of T-DNA and SALK_087935 showed two loci of T-DNA. The third T-DNA insertion line, GABI_498B03, showed a single locus of the T-DNA in the eleventh exon (Figure 4). No homozygous line for *SMC1* and *SMC3* could be selected. All heterozygous plants were fertile and showed no obvious habit that differed from wt. Quantitative real-time PCR was applied to measure the transcript levels of the heterozygous *SMC1* and *SMC3* alleeles. The observed strong upregulation in order to compensate the mutated allele is in accordance with the fact that *SMC1* and *SMC3* are indispensable for viability of *A. thaliana*. Transcription levels reached from 78 % to 98 % of expression compared to wt (Table 1).

3.1.2 α-kleisin proteins evolved different functions

Two insertion lines were found in the SALK collection mutating *SYN1* encoding the meiotic kleisin of the cohesin complex (Bai et al. 1999; Bhatt et al. 1999; Cai et al. 2003). One was located in the eighth (SALK_137095) and the second in the 15th exon (SALK_006687). Homozygous mutation in *SYN1* caused sterile plants which were smaller than wt. Homozygotes did not segregate in the expected mendelian 1 : 2 : 1 (wt : heterozygous : homozygous) ratio. They were observed more seldomly. The segregation was 7 : 14 : 1 (n = 89 plants).

Southern hybridisation revealed four (SALK_137095) and three (SALK_006687) T-DNA loci. Transcription of *SYN1* was completely absent in homozygous mutant plants (Figure 5).

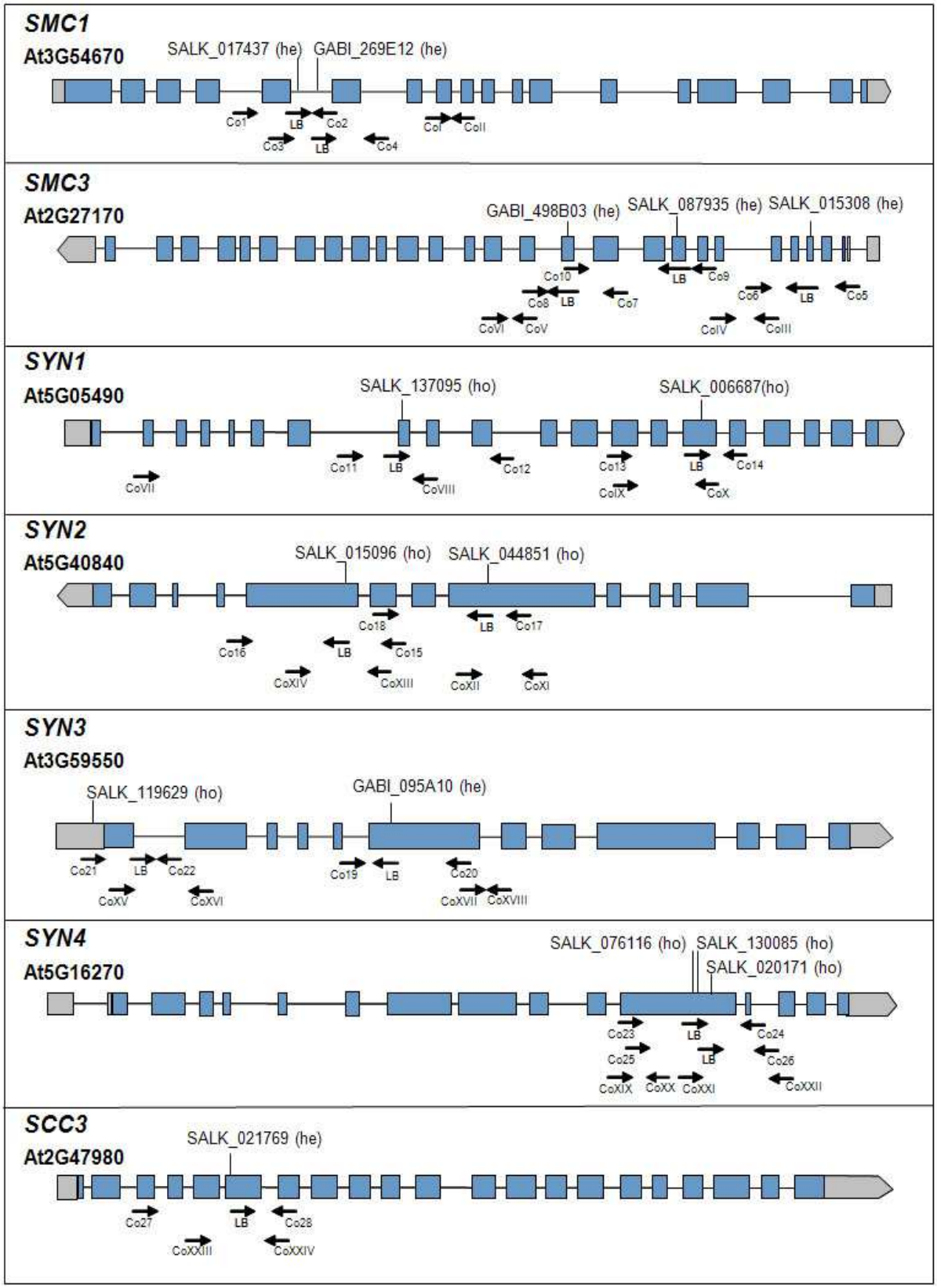

Fig. 4: Structures of cohesin genes. Blue boxes represent exons. UTRs are shown as grey boxes. Confirmed positions of the T-DNA insertions (SALK and GABI lines) are indicated with the black lines. Homozygous lines are marked with ho and heterozygotes with he. The positions of the genotyping primers are shown by the black arrows with arabic letters. Primers used for expression analysis by RT PCR or real-time PCR are marked with roman letters.

Two homozygous lines were confirmed from the SALK collection mutating *SYN2*. Line SALK_044851 was found in the sixth exon and SALK_015096 was located in the eleventh exon. Both showed two loci of T-DNA and complete absence of the *SYN2* transcript. The habit of homozygous mutant plants did not differ from wt and fertility was not influenced by mutating *SYN2*.

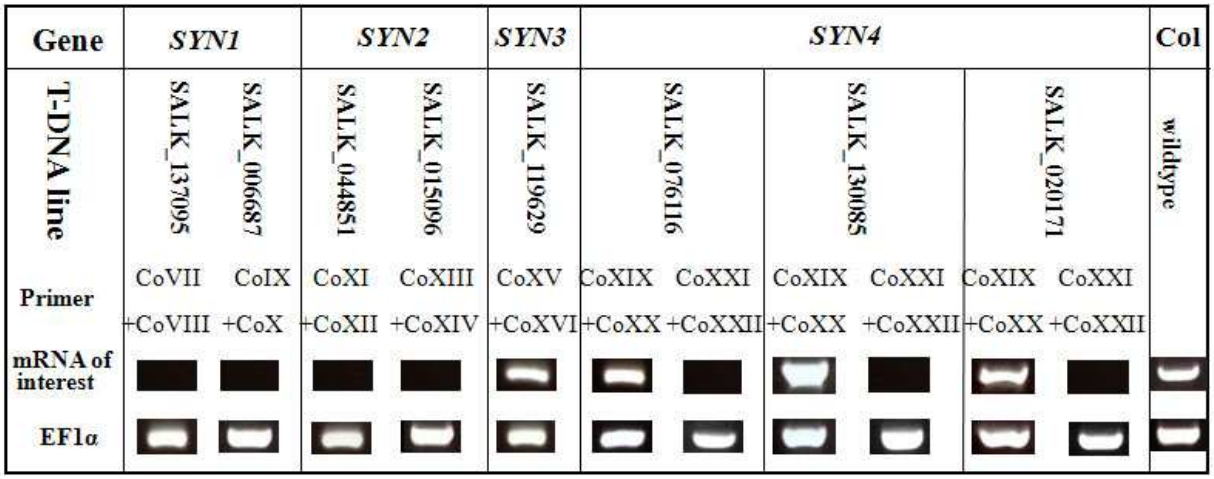

Fig. 5: RT PCR of homozygous T-DNA lines mutating the α-kleisin genes of the cohesin complex. Expression patterns of the α-kleisin mutants *syn1*, *syn2*, *syn3* and *syn4*; only one representative sample is shown for the wt accession Columbia. Mutant lines *syn1* and *syn2* show complete absence of the transcript. The *syn3* T-DNA insertion is located upstream of the coding region and shows a wt-like transcript. Elongation factor 1α is served as control. The primer positions are indicated in Figure 4.

To mutate the third α-kleisin candidate gene, *SYN3*, one homozygous line was identified (SALK_119629). According to sequencing, the T-DNA was located 188bp upstream of the transcription start point. RT PCR revealed a wt-like transcript for *SYN3* in this line (Figure 5). Probably the T-DNA has no effect on the transcription of *SYN3* because the promoter sequence might be located more near to the start codon. The second line, GABI_095A10, segregated in heterozygous plants only. Homozygous plants from this line were not viable. This insertion line with a T-DNA location in the sixth exon showed ~77% of wt transcription, measured by quantitative real-time RT-PCR. Segregation of mutant plants was observed in a 3.4 : 1 ratio (wt : heterozygous plants; n-115). These heterozygous mutants showed a wt-like habit and were fertile.

For *SYN4* the SALK collection provided three lines with T-DNA insertions in the eleventh exon. All three homozygous mutants produced a truncated transcript. This truncated mRNA was coding *SYN4* until the T-DNA insertion in exon 11. Southern hybridisation revealed that

line SALK_076116 had five, SALK_130085 three and SALK_020171 two loci of integrated T-DNA. Unfortunately, no single T-DNA insertion line could be found but side effects of T-DNAs which were not located in *SYN4* were excluded as all three lines showed similar behaviour in the analysis of mitosis.

The four different α-kleisin homologs evolved specialized functions during plant evolution. SYN1 is essential for meiosis (Bai et al. 1999; Bhatt et al. 1999; Cai et al. 2003), SYN2 plays an important role in mitosis (Dong et al. 2001) and SYN3 is involved in the organisation of rDNA structure (Jiang et al. 2007). The function of SYN4 is unknown so far and elucidated in this study.

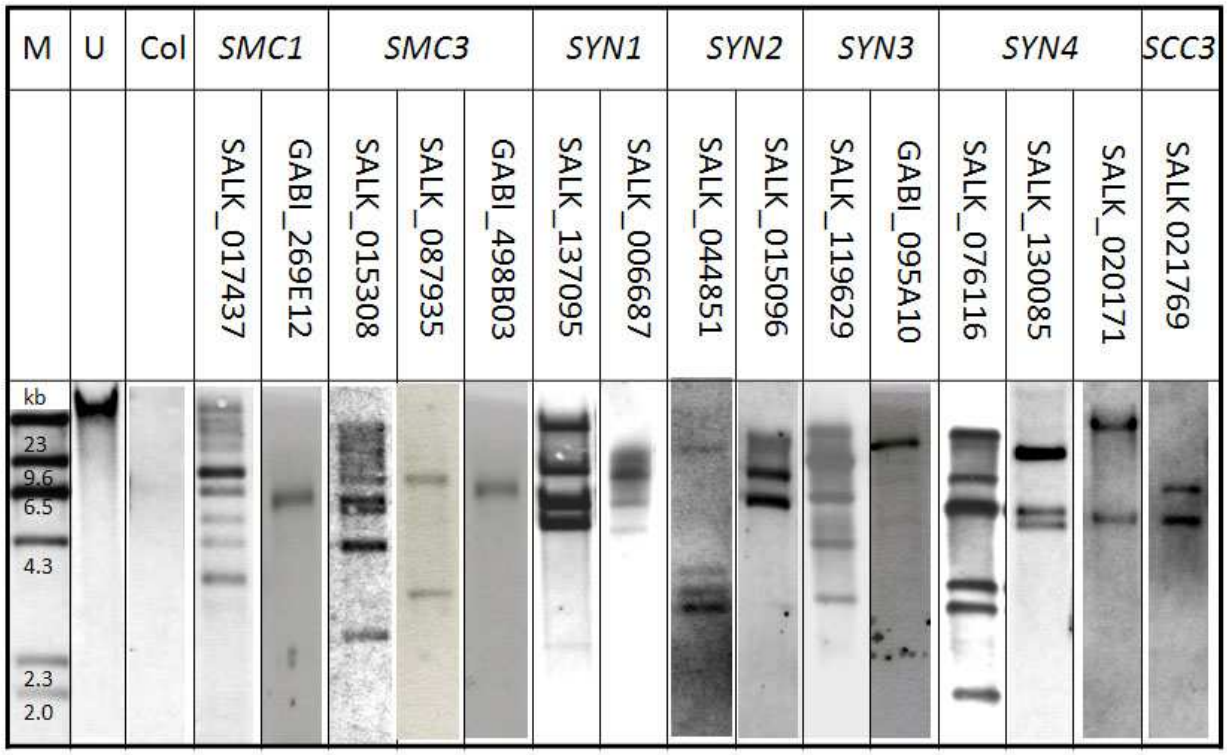

Fig. 6: Southern hybridisation of cohesin T-DNA lines. Three µg of genomic DNA were digested with KpnI. U represents undigested genomic DNA of a representative mutant plant. The wt Columbia does not contain the target DNA. The T-DNA lines from SALK contain at least two up to eight loci of the SALK T-DNA. All three GABI lines contain only a single locus of the T-DNA mutating *SMC1*, *SMC3* and *SYN3*.

3.1.3 SCC3 is essential for plant viability

The HEAT repeat containing subunit SCC3, which is required for stabilisation of the cohesin complex in yeast (Toth et al. 1999), was analysed with line SALK_021769. Only heterozygous mutants could be selected. The mutation in the *SCC3* gene is homozygously lethal in *A. thaliana*, indicating the essentiality of SCC3 for viability. The T-DNA was integrated in the sixth exon of the gene. Southern hybridisation revealed two loci of T-DNA. The expression of the intact *SCC3* allele was upregulated to 83.5% (Table 1). Habit and fertility of mutant plants were not different from wt.

3.2 Condensin

Out of the nine genes encoding the condensin complex subunits, only five could be analysed. Selection of T-DNA insertion lines mutating *SMC4B*, *CAP-D2A*, *CAP-D2B* and *CAP-G* was not successful up to now. The lines found for *SMC4B* and *CAP-D2A* revealed a T-DNA position outside of the coding region and revealed a wt-like transcript. For *CAP-D2B* and *CAP-G* no T-DNA insertion line was found.

Four T-DNA insertions were found in introns, seven in exons, two lines were found upstream of the respective coding region and three downstream of the coding region of a gene (Figure 7). The positions of primers for genotyping and expression analysis of mutated genes are shown also in Figure 7. Alignments of PCR fragments with the corresponding gene sequence are shown in Supplementary Table 5. Sequences of primers for genotyping PCR, RT PCR and real-time PCR are illustrated in Supplementary Tables 4 and 6, respectively. Analysis of expression in homozygous T-DNA insertion lines mutating respective condensin genes is shown in Figure 8. The expression values in heterozygous lines measured by quantitative real-time PCR can be found in Table 1. The numbers of T-DNA copies determined by Southern hybridisation with respective T-DNA probes are shown in Figure 9.

The presence of at least two homologous genes encoding the SMC proteins, kleisin components and CAP-D2 subunits of the condensin complex allows *A. thaliana* to assemble different condensin complexes. Mutation in *SMC2A*, *SMC4A* and *CAP-H* were lethal if homozygous, pointing out the necessity of these genes for plant viability.

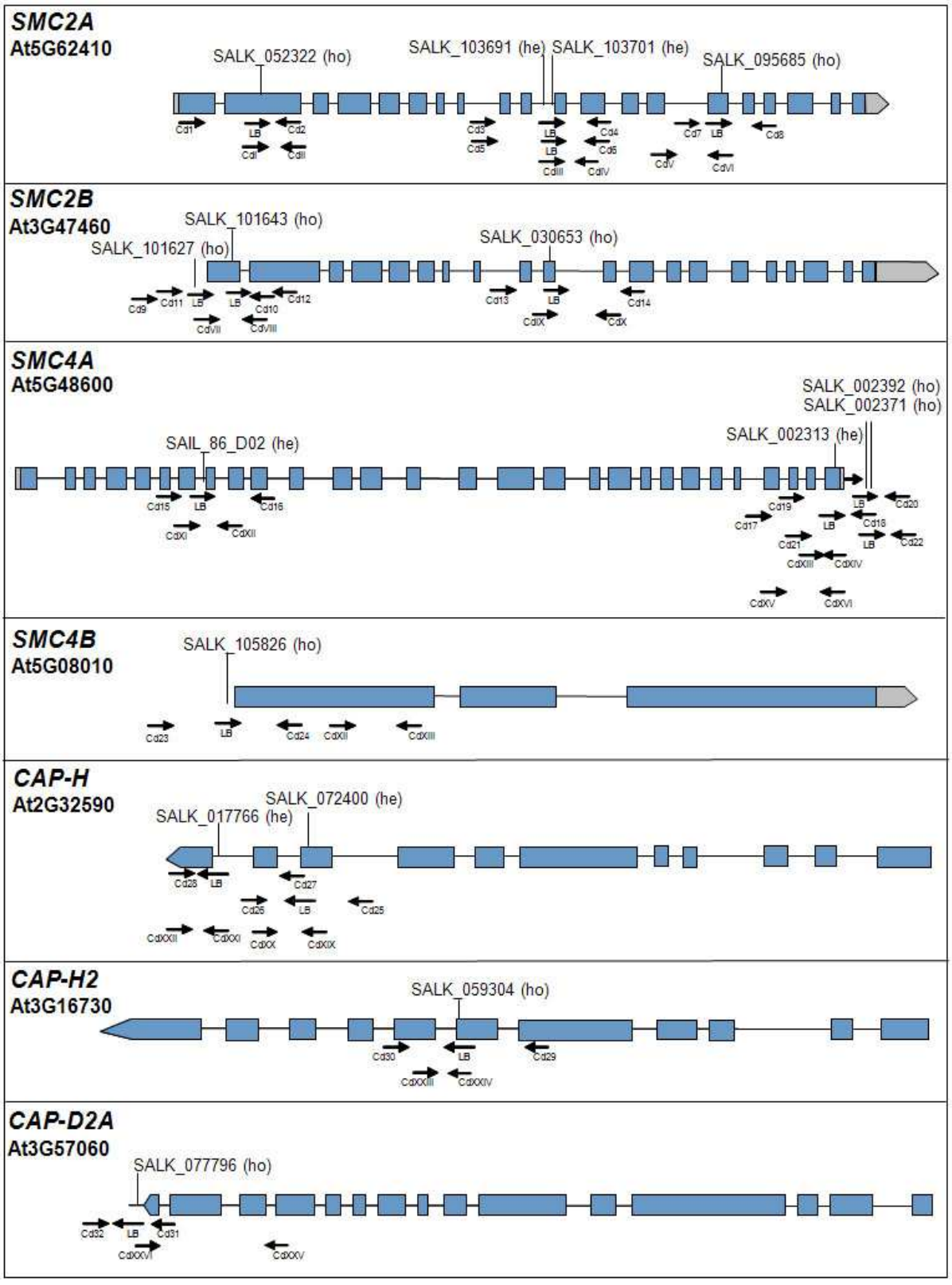

Fig. 7: Structures of condensin genes. Blue boxes represent exons. UTRs are shown as grey boxes. Confirmed positions of the T-DNA insertions (SALK and SAIL lines) are indicated with black lines. Homozygous lines are marked with ho and heterozygotes with he. The positions of the genotyping primers are shown by the black arrows with arabic letters. Primers used for expression analysis are labelled with roman letters.

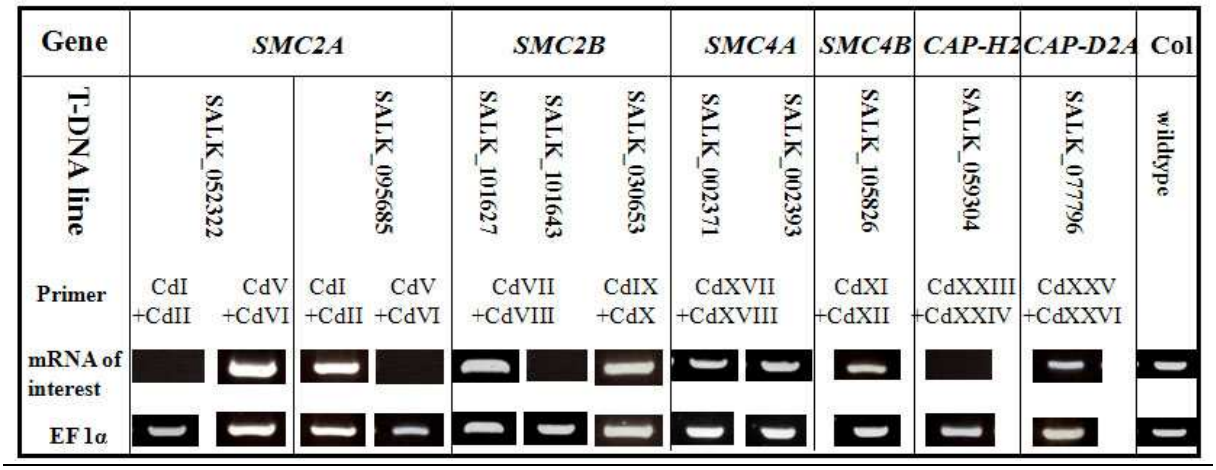

Fig. 8: RT PCR of homozygous T-DNA lines mutating condensin genes. Expression patterns in leaves of homozygous mutant lines. Only one representative sample is shown for the wt accession Columbia (Col). SALK_052322 shows a slight overexpression of the *SMC2A* gene downstream of the T-DNA insertion due to the 35S promoter. A partially functional truncated mRNA is also expressed in the *SMC2A* mutant line SALK_095685. Both *SMC4A* T-DNA insertions are located downstream of the coding region and show a wt-like transcript. The *SMC4B* T-DNA insertion is located upstream of the coding region and shows a wt-like transcript. The line mutating *CAP-H2* shows complete absence of the transcript. The *CAP-D2* T-DNA insertion is located downstream of the coding region and shows a wt-like transcript. Elongation factor 1 α is served as control.

3.2.1 *SMC2A* can compensate the mutation in *SMC2B* but not *vice versa*

In *A. thaliana*, two homologous genes encoding SMC2 are present. The nomenclature *SMC2A* corresponds to At5G62410 and *SMC2B* corresponds to At3G47460. For both genes homozygous mutants were selected. NASC provided the line SALK_052322 with a T-DNA in the second exon of *SMC2A* and line SALK_095685 is mutated in the 15th exon. Both could be selected as homozygous mutant lines and showed a truncated transcript. In SALK_052322 a slight upregulation of expression downstream of the T-DNA could be observed. This could be caused by the 35S promoter in the SALK T-DNA (Daxinger et al. 2008). Southern hybridisation revealed two and four loci of T-DNA in line SALK_052322 and line SALK_095685, respectively. In addition, two heterozygous T-DNA lines with a single T-DNA insertion with location in the 10th intron of *SMC2A* were selected (SALK_101691 and SALK_101701). Both lines showed upregulation in order to compensate the missing allele. The production of truncated transcripts in both homozygous lines (SALK_052322 and SALK_095685) could explain the heterozygosity of lines SALK_101691 and SALK_101701. As in both homozygous lines only a small part of the protein is missing, the truncated

transcript may be translated into a partial functional protein, which can close the condensin ring. *SMC2A* is essential and can compensate *SMC2B* but not *vice versa*. For mutating *SMC2B*, three lines were found in the SALK collection. Line SALK_101627, with a T-DNA position located upstream of the coding region showed a wt-like transcript. A second line was found with a T-DNA in the first exon and selected as homozygous (SALK_101643). The high homology (90% at the protein level) (Siddiqui et al. 2003) of both *SMC2A* and *SMC2B* did not allow, to design unique primer pairs annealing only on one of the genes at the region from exon seven to exon twelve (Supplementary Figure 1). In case of the insertion site of the homozygous line SALK_030653, a wt-like transcript was observed. By sequencing it was obvious that the amplified fragment was not from *SMC2B* but from the homolog *SMC2A*.

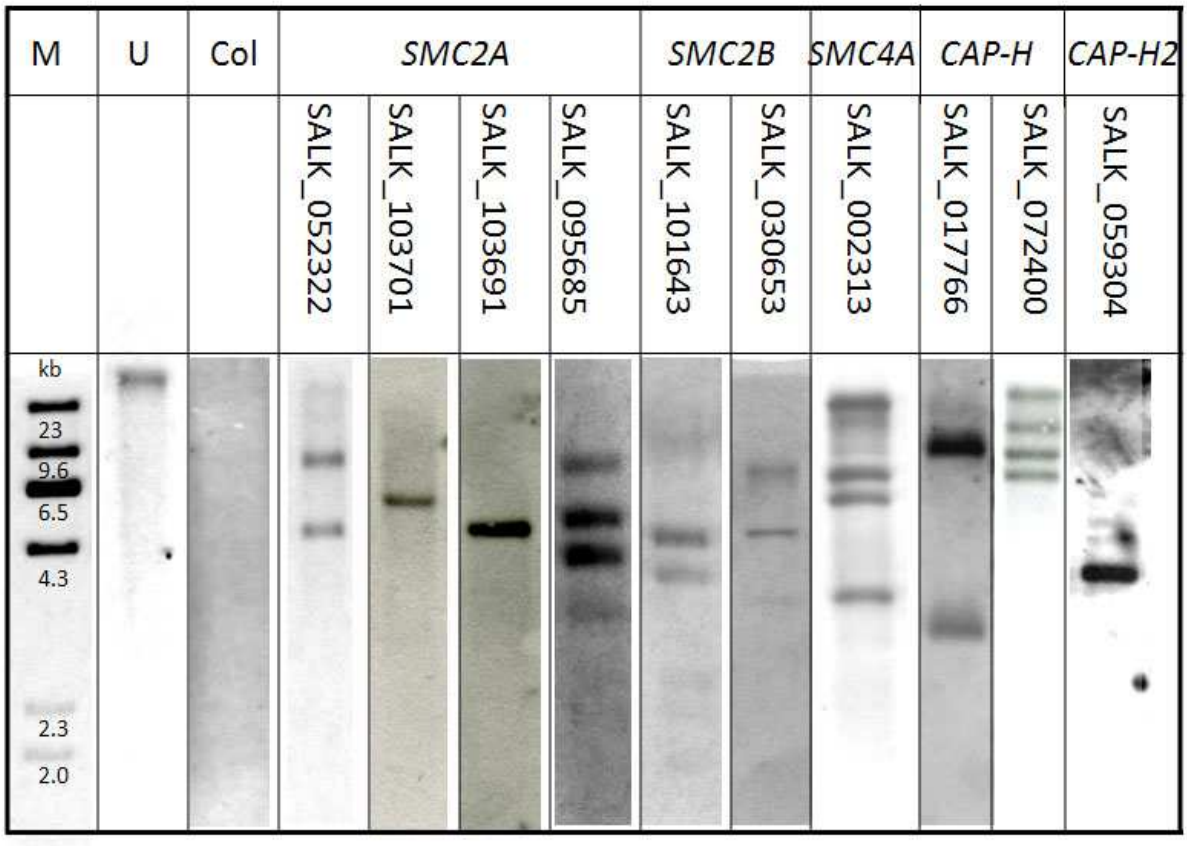

Fig. 9: Southern hybridisation of condensin T-DNA lines. Three µg of genomic DNA were digested with KpnI. U represents undigested genomic DNA of a representative mutant plant. The wt Columbia (Col) does not contain the target DNA. Single loci of T-DNA were found for one line of *SMC2A* and *CAP-H2*, respectively. The other lines showed between two and five loci of SALK T-DNA.

3.2.2 SMC4A is essential for plant viability

The *Arabidopsis* genome contains at least two homologs of the *SMC4* gene. A third homolog, *SMC4C*, is not proven to encode a condensin SMC subunit, as it shows homology to the *SMC3* component of the cohesin complex as well. Therefore, it was not included in this study. *SMC4B* can not compensate for *SMC4A*. Both genes differ strongly in DNA sequence and length. *SMC4A* shows nearly a doubled size with 3796 bp, while *SMC4B* has a cDNA length of 1822 bp (Supplementary Figure 2). To determine the effects of mutating *SMC4A*, four lines were analysed. Two of them showed a location of T-DNA downstream of the coding region. Both lines SALK_002371 and SALK_002392 were selected as homozygous lines. Transcription of *SMC4A* was observed like wt showing no alteration in mRNA level in both lines. For line SALK_002313 only heterozygous plants could be selected. The T-DNA was located in the last exon of *SMC4A* and real-time PCR revealed a transcription level like in wt. This upregulation of expression of the intact *SMC4A* allele indicates the requirement of the gene for plant viability.

Daniel Riggs (Department of Botany, Devision of Life Science, University of Toronto, Canada) provided one T-DNA insertion line from Syngenta (SAIL_86D02) for analysis of *SMC4A*. SAIL_86D02 showed a T-DNA insertion at the end of the seventh intron and could be selected only as heterozygous. This line showed 85% of the wt transcript level of *SMC4A*. According to Southern hybridisation, which was performed in Daniel Rigg´s laboratory, SAIL_86D02 contains the T-DNA only in the *SMC4A* gene with at least two transgenes in tandem array (Siddiqui et al. 2006).

For analysis of *SMC4B*, only one T-DNA insertion line was found. The SALK database provided this line as homozygous T-DNA insertion line interrupting the promoter sequence but after sequencing it was obvious that the insertion was located 311bp upstream of the transcription start point. The line showed a wt-like transcript of *SMC4B* analysed by RT PCR indicating no effect of the T-DNA on transcription of *SMC4B*. Thus, detailed analysis of the *SMC4B* homolog could not be done.

3.2.3 γ-kleisin Cap-H is essential and can compensate the function of β-kleisin Cap-H2

The SMC heterodimer can bind different kleisin proteins. In vertebrates condensin I requires the CAP-H subunit, a γ-kleisin, and condensin II requires CAP-H2, a β-kleisin (Hirano et al. 1997; Ono et al. 2003; Yeong et al. 2003). NASC provided two T-DNA insertion lines

mutating the *CAP-H* gene. Both could be selected only as heterozygous mutants. SALK_017766 showed a T-DNA location in the tenth intron and two loci of T-DNA. Line SALK_072400 with an insertion in the ninth exon of the gene revealed four loci of T-DNA. Both lines showed transcript levels from 90.8% - 100% of wt *CAP-H* transcription. This indicates that *CAP-H* is essential for plant viability.

To mutate *CAP-H2*, only one mutant line could be found in the SALK collection with a single insertion in the sixth exon. It could be selected as homozygous loss-of-function line that showed no *CAP-H2* transcript. The habit and fertility of mutant plants did not differ from wt. This suggested that CAP-H containing condensin complexes can compensate the lack of CAP-H2 containing complexes, but not *vice versa* because the mutation in *CAP-H* was homozygously lethal.

3.2.4 *A. thaliana* contains two candidate genes encoding CAP-D2

Database search revealed two candidate genes (*CAP-D2A*: At3G57060 and *CAP-D2B*: At4G15890) encoding CAP-D2 in the *A. thaliana* genome.

Only one insertion line mutating the gene *CAP-D2A* was found in the database. SALK_077769 showed a position of T-DNA downstream of the coding region of *CAP-D2A* and was selected as homozygous line. The analysis of the *CAP-D2A* expression in this line revealed a wt-like transcript. Obviously, it seems that the T-DNA at this position has no effect on the expression of *CAP-D2A*. Analysis of the possible function of this gene could not be done within this study.

CAP-D2B represents the second homolog encoding this HEAT repeat-containing protein required for stabilisation of the condensin complex in *D. melanogaster* (Savvidou et al. 2005). Unfortunately, no T-DNA insertion line could be selected mutating *CAP-D2B* up to now. Thus, analysis of the function of *CAP-D2B* in *A. thaliana* could not be done.

3.3 Proteins interacting with cohesins and condensins

For analysis of the three interacting proteins SWI1, SCC2 and BRU1, altogether four T-DNA insertion lines were found. In the GABI collection the respective line for analysis of *SWI1* was found. This protein was shown to be involved in the axial element formation during meiosis (Mercier et al. 2001, 2003) but mitotic tissue was not yet analysed in *swi1* mutant plants. Two lines mutating *SCC2*, a subunit of the cohesin and condensin loading complex,

were found in the SALK collection. Only one line with insertion in the *BRU1* gene was available and selected out of the SALK collection. Homozygous T-DNA lines for *BRU1* and *SWI1* were analysed regarding the transcription of the respective gene by RT PCR (Figure 11). In heterozygous lines mutating *SCC2* the transcript level was measured by quantitative real-time PCR (Table 1). The number of T-DNA loci is depicted in Figure 13.

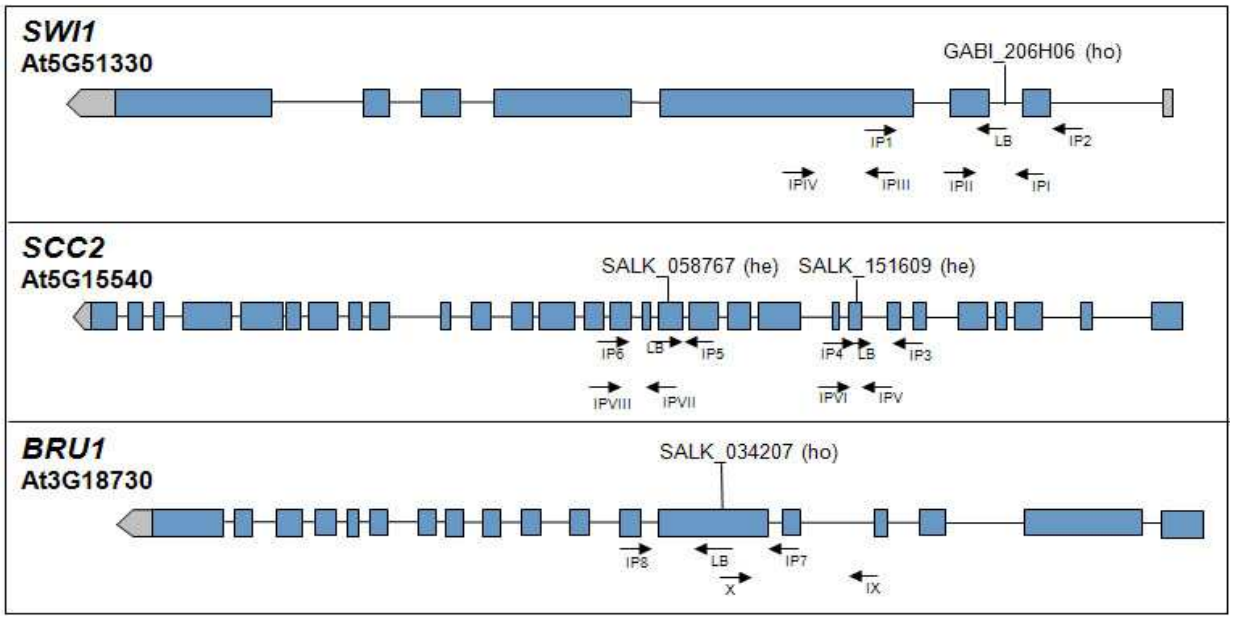

Fig. 10: Gene structures of cohesin and condensin interacting proteins SWI1, SCC2 and BRU1. Blue boxes represent exons. UTRs are shown as grey boxes. Confirmed positions of the T-DNA insertions (SALK- and GABI lines) are indicated with the black lines. Homozygous lines are marked with ho and heterozygotes with he. The positions of the genotyping primers are shown by the black arrows with arabic letters. Primers used for expression analysis are labelled with roman letters.

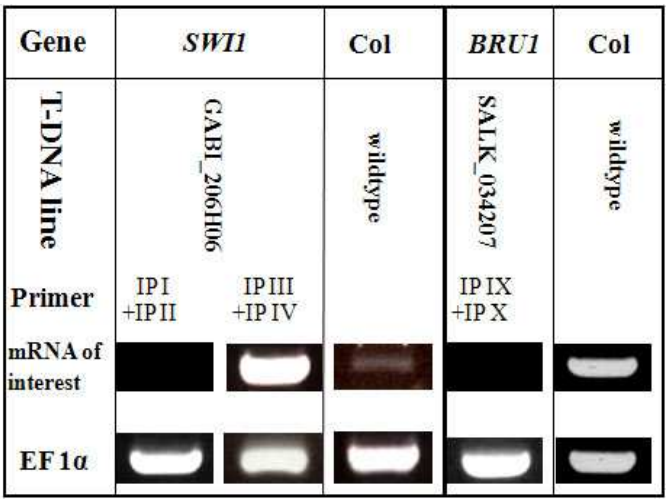

Fig. 11: RT PCR of homozygous T-DNA lines mutating genes coding for proteins interacting with cohesin (SWI1) and condensin (BRU1). The *SWI1* gene showed a low expression in wt leaves. In line GABI_206H06 a strong overexpression of the *SWI1* gene was visible downstream of the T-DNA. This truncated mRNA did not prevent the mutant sterility. In the *bru1* mutant line SALK_034207 no *BRU1* mRNA was detectable.

3.3.1 SWI1 is essential for fertility and genome stability

Homozygous plants mutated in *SWI1* were completely sterile. GABI_206H06, with a single insertion in the first intron showed an overexpression downstream of the T-DNA. This could be due to the 35S promoter in the right border of the T-DNA. This overexpression did not prevent the mutant sterility because the truncated mRNA was lacking the first exon and therefore, obviously an essential domain of the protein.

3.3.2 SCC2 is indispensable for plant viability

The loading complex consisting of SCC2 and SCC4 was analysed by T-DNA insertion in *SCC2*. Two T-DNA lines were found in the SALK collection. The T-DNA was located in the eighth (SALK_151609) and 13th exon (SALK_058767). The two lines could only be selected as heterozygous and showed an expression level of ~88% of wt transcription indicating the essentiality of SCC2. Southern hybridisation revealed three and seven loci of T-DNA for line SALK_151609 and line SALK_058767, respectively.

3.3.3 Plants mutated in *BRU1* show developmental abnormalities

BRU1 was shown to be involved in centromere condensation (Takeda et al. 2004) therefore it was included into this study. NASC provided an insertion line to analyse *BRU1* as interaction partner for condensin. Line SALK_034207, with a T-DNA insertion in the sixth exon of the gene, could be selected as homozygous and showed complete absence of the *BRU1* transcript. Southern hybridisation revealed four loci of T-DNA. Homozygous *bru1* mutants showed an irregular branching pattern and fasciation in roots, stems, shoots and flowers. Organs were fused resulting in a brush-like structure of siliques. Furthermore, plants were smaller than wt and had a very low seed set (Figure 12).

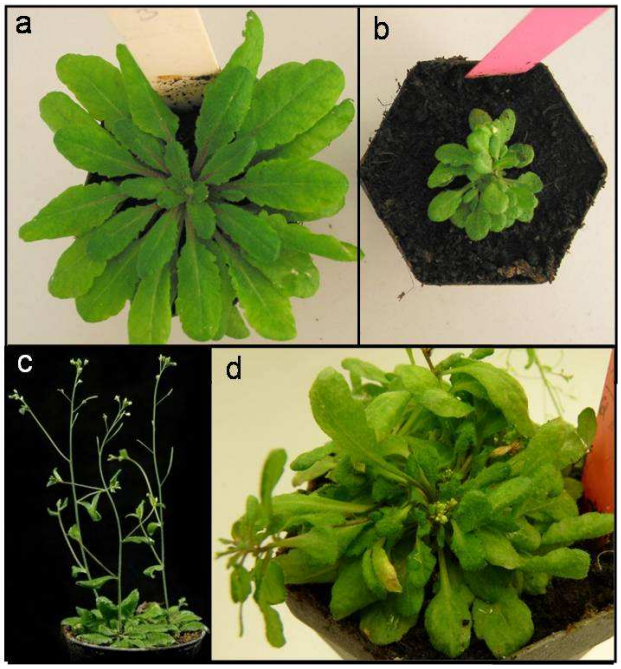

Fig. 12: Habit of *bru1* mutants. Col wt (a) and *bru1/bru1* (b) 6 weeks after germination under short day conditions; Col wt (c) and *bru1/bru1* (d) 11 weeks after germination under long day conditions, flowers appeared but showed secondary rosettes and fused flowers. Homozygous as well as heterozygous mutants showed a very low seed set.

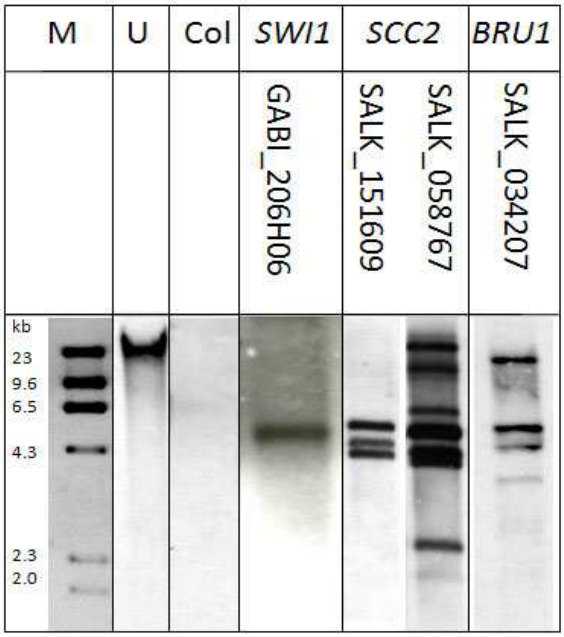

Fig. 13: Southern hybridisation of T-DNA lines mutating genes coding for proteins interacting with cohesin and condensin. Three µg of genomic DNA were digested with KpnI. U represents undigested genomic DNA of a representative mutant plant. The wt Columbia (Col) does not contain the target DNA. A single locus of T-DNA was found for GABI_206H06. The lines mutating *SCC2* showed three and seven loci of the SALK T-DNA, respectively. The *bru1* mutant contains four loci of T-DNA.

3.4 *In vivo* studies to analyse genome stability

The confirmed mutant lines were transformed with fluorescence tagged constructs encoding recombinant histones (Pro35S-H2B-DsRed, Pro35S-EYFP-CenH3, Pro35S-H2B-YFP) to visualize mitoses in root tip meristems. The first strategy was to label the centromere with Pro35S-EYFP-CenH3 and the whole chromatin with Pro35S-H2B-DsRed. Unfortunately, no lines expressing both constructs stably could be selected. Therefore, the mutant lines were

transformed only with a single construct (Pro35S-H2B-YFP). For some of the lines it was not possible to select transformants expressing the Pro35S-H2B-YFP construct stably. Therefore, seedlings were fixed and stained with DAPI to analyse the consequences of the mutations on cell divisions. Seedlings derived from heterozygous plants could not be genotyped after fixation and were classified according to their bridge values using the QUICKBASIC program for exact and mid-p confidence interval for a binomial proportion (Fagan 1996). The classification of *SYN3/syn3* and *SWI1/swi1* mutants is depicted in Supplementary Figure 3 and 4. Furthermore, using untransformed seedlings for DAPI staining, it should be determined whether the expression of the Pro35S-H2B-YFP construct *per se* had an influence on the frequency of anaphase bridge formation. The Pro35S-H2B-YFP cassette did not affect the amount of anaphase bridges (Table1). Plants mutated in cohesin or condensin genes or genes encoding one of the interacting proteins SCC2, SWI1 and BRU1 showed an increased frequency of anaphase bridges. In some mutants, micronuclei were visible as the consequence of non-disjunction due to anaphase bridges.

3.4.1 Pro35S-EYFP-CenH3 and Pro35S-H2B-DsRed double transformants do not stably express both constructs simultaneously

Simultaneous *Agrobacterium* transformation with Pro35S-EYFP-CenH3 and Pro35S-H2B-DsRed constructs provided only 14 out of 80 T1 plants, which expressed both constructs partially in root and leaf tissue (Figure 14). No double transformed line stably co-expressing both fusion constructs in all nuclei could be selected neither from transformed wt, nor mutant plants. Therefore, double transformation was not useful to generate stably expressing transgenic mutant lines for analysis of mitotic divisions and interphase nuclei.

Expression frequencies were different between meristematic and differentiated tissues, but similar in differentiated root and leaf tissue of the double transformants (Figure 14 and 15). In meristematic tissue only 0.4% and 1.4% of the nuclei showed expression of both constructs simultaneously in *syn4* mutants and wt plants, respectively. Pro35S-EYFP-CenH3 was mainly expressed in the root tip, while Pro35S-H2B-DsRed showed high expression in the differentiated tissue of elongated root. The expression frequencies in the *syn4* mutants were compared between different tissues and with wt using the *t*-test. Significant differences ($P \leq 0.001$) were observed between meristematic and differentiated tissues (elongated root and leaf). Here, opposite expression frequencies of Pro35S-EYFP-CenH3 compared to Pro35S-

H2B-DsRed were observed. The root tip meristem expressed the Pro35S-EYFP-CenH3 construct in 59.0% and 83.2% of nuclei in homozygous *syn4* mutants and wt, respectively. Only ~4% of nuclei in the elongated root expressed Pro35S-EYFP-CenH3 in mutant and wt plants. The highest expression in the elongated root was observed with Pro35S-H2B-DsRed showing 68.6% and 93.4% of nuclei with expression in *syn4* mutants and wt, respectively. The two expression cassettes inhibited the expression of each other in the different root tissues.

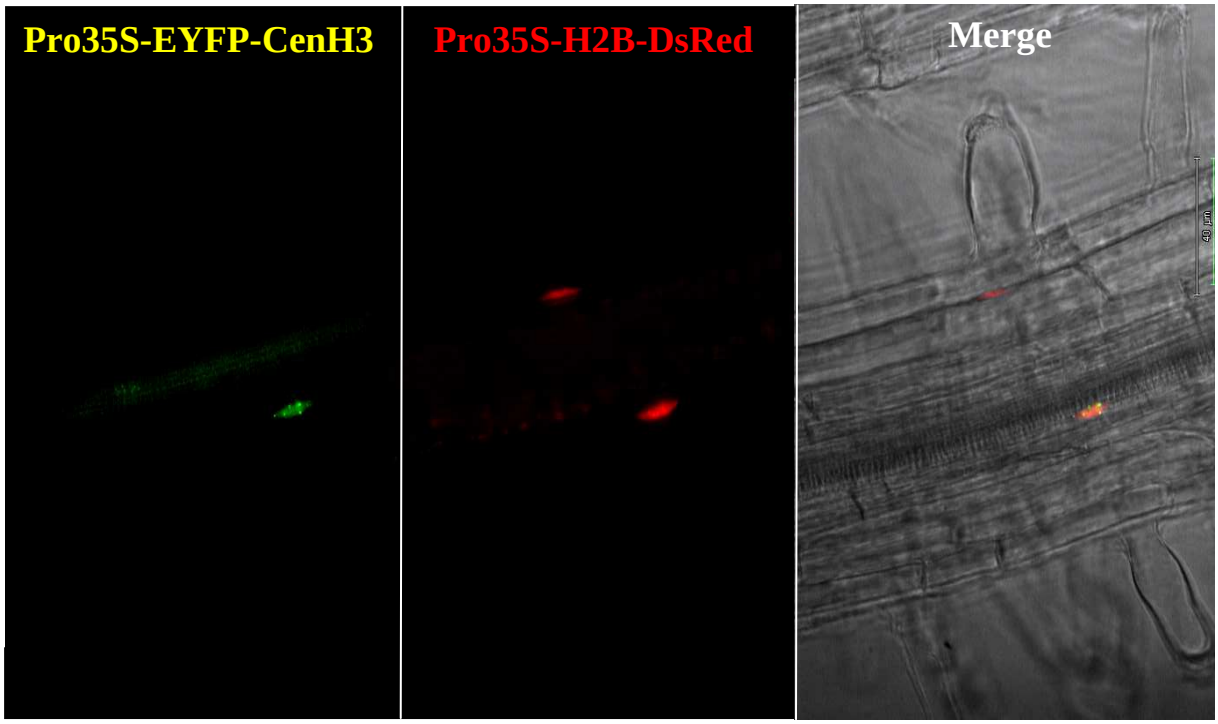

Fig. 14: Expression of Pro35S-EYFP-CenH3 and Pro35S-H2B-DsRed in double transformed *syn4* mutant line SALK_076116. One of the very rare nuclei expressing both fluorescence constructs simultaneously was found in elongated root tissue. The meristematic tissue showed only 0.4% of the nuclei expressing both constructs together in plants mutated in *SYN4* and 1.4% in wt plants.

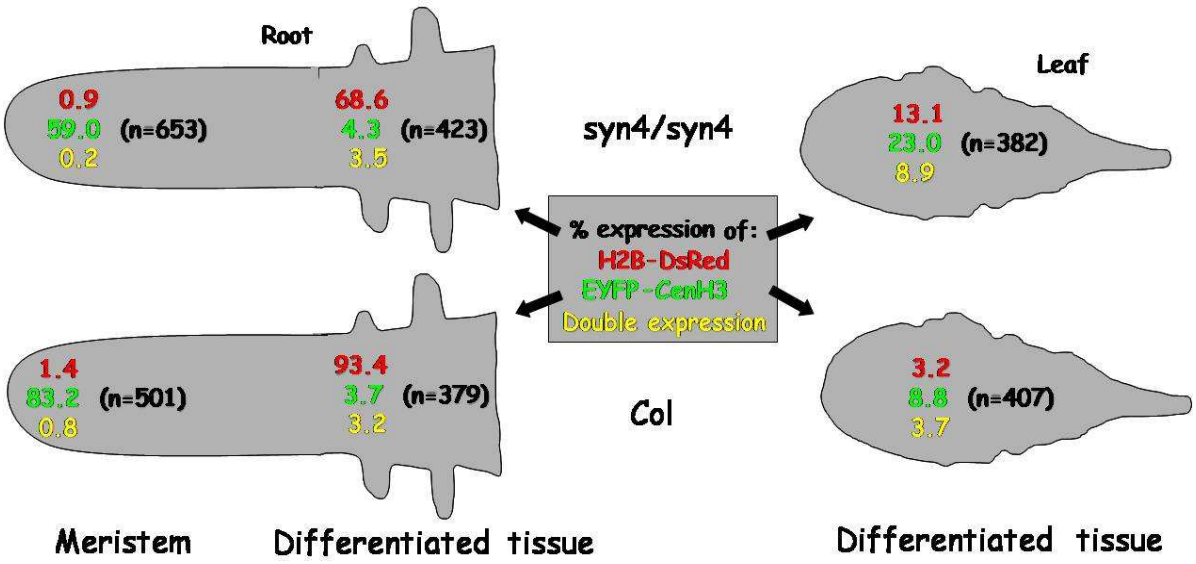

Fig. 15: Expression frequencies after double transformation with Pro35S-EYFP-CenH3 and Pro35S-H2B-DsRed in *syn4* mutant line SALK_076116 and wt. Nuclei were counted in freshly cut material of root tips, elongated roots and leaf tissue after DAPI incorporation 16 days after germination. n = number of nuclei pooled from analysis of ten T2 plants. Double expression of both constructs is significantly ($P \leq 0.001$) higher in differentiated tissue (leaf and elongated root), than in root meristem but not significantly different between leaf and elongated root.

For exact measurement of expression values, quantitative real-time PCR was applied to compare a homozygous *syn4* cohesin mutant line (SALK_076116) containing six loci of SALK T-DNA with wt. Due to the small size of *A. thaliana* roots, it was not possible to divide the tissues in meristematic and differentiated root tissue for RNA isolation. Therefore, RNA was isolated from 15 pooled seedlings 14 days after germination and the expression difference of transgenes between homozygous *syn4* mutants and wt was measured. The highest expression values were obtained after wt single transformation. Transgene transcript levels were reduced in the double transformed seedlings in comparison to single transformants but did not reflect the low degree of co-expression of *in vivo* fluorescence. After double transformation *syn4* mutants showed only 63% (Pro35S-H2B-DsRed) and 54.7% (Pro35S-EYFP-CenH3) compared to the transcript level of double transformed wt plants, respectively. Double transformed *syn4* mutant plants showed only 30.1% (Pro35S-EYFP-CenH3) and 42% (Pro35S-H2B-DsRed) of the transcript levels of single transformed wt plants on mRNA level, respectively. Single transformed mutant plants showed 70.4% of the transcript levels compared to wt. It was obvious, that *syn4* mutants, which contain six loci of T-DNAs in addition to the unknown number of fluorescence expression cassettes, showed a reduced expression in comparison to wt after double transformation as well as after single

transformation (Figure 16). The lowest expression was present in the *syn4* mutant line after double transformation. The reduced expression compared to wt can be taken as an indicator of silencing due to multiple T-DNA insertions in the mutants. SALK T-DNA constructs contain the 35S promoter, which can induce silencing of other expression cassettes (Matzke et al. 2003; Daxinger et al. 2008). Due to the identical promoter and terminator regions of the two fluorescence expression constructs, it seems that the two constructs were prone to simultaneous silencing. Especially in mutant plants containing six loci of T-DNA in addition to the two fluorescence expression cassettes only very rarely both constructs were expressed within one nucleus simultaneously. Assuming a progressive onset of silencing, the observation that older plants (six weeks) showed no fluorescence at all supports this idea.

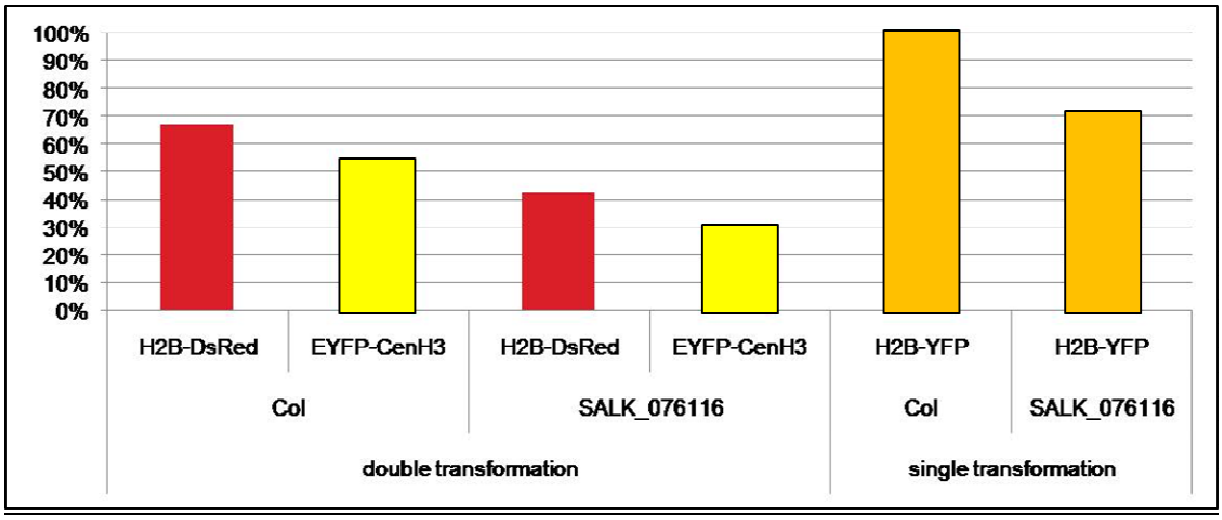

Fig. 16: Expression after Pro35S-H2B-DsRed and Pro35S-EYFP-CenH3 double transformation compared to single transformation with Pro35S-H2B-YFP in *syn4* mutant and wt seedlings. All values are relative to *ACTIN2* as a housekeeping gene. Pro35S-H2B-YFP expression in wt was regarded as 100%.

To test, whether Post-Transcriptional-Gene-Silencing (PTGS) causes the silencing in the double transformants, RNA-Dependent-RNA-Polymerase 6 (RDR6) deficient plants were transformed with the same constructs. RDR6 plays a crucial role in the RNA silencing response in plants. RDR polymerases participate in natural defence against plant viruses. Plants mutated in *RDR6* show stable expression of transgenes (Wassenegger and Krczal 2006; Diaz-Pendon 2007; Butaye et al. 2004). The *rdr6* mutant line suppresses PTGS effects. Around 4000 seeds were surface-sterilized after transformation but only one plant grew on the selective medium containing two antibiotics (Kan and PPT) reflecting a transformation

efficiency of only 0.025%. The transformation rate observed in wt plants was 2% meaning one transformant among 50 seeds. The only transformant of the *rdr6* line showed neither expression of Pro35S-H2B-DsRed, nor of Pro35S-EYFP-CenH3. Maybe the action of mechanisms others than PTGS were responsible for the suppressing of both constructs but one single transformant was not conclusive enough.

3.4.2 Single transformation with Pro35S-H2B-YFP

Due to the low simultaneous fluorescence expression after double transformation, single transformation with Pro35S-H2B-YFP was applied to allow visualization of individual root tip mitoses *in vivo*. Strong fluorescence expression was detectable in nearly all nuclei and allowed to analyse a high number of divisions. Homozygous *syn4* mutants showed 97.5% of nuclei expressing Pro35S-H2B-YFP in root meristems.

In leaf tissue expression was visible in nearly 90% of nuclei. In wt 100% of nuclei expressed the construct in root tissue (Figure 17). Only very few nuclei (0.5%) showed no expression in leaf tissue in wt. Significant differences of expression were observed between wt and mutant in leaf tissue ($P \leq 0.01$) and in the elongated root ($P \leq 0.1$) using the two-sided Fisher Exact Test.

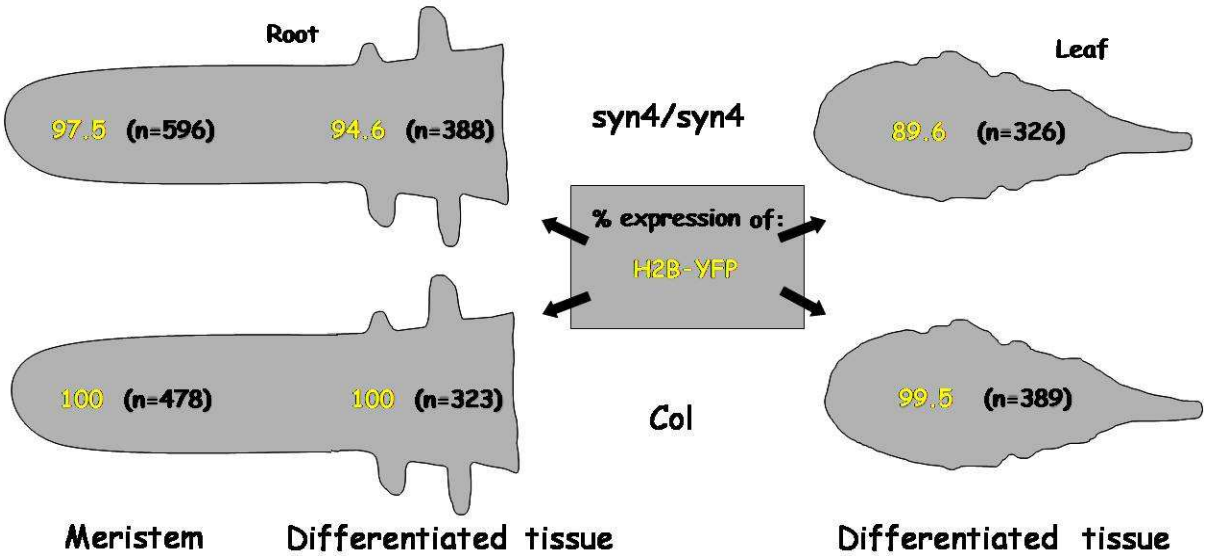

Fig. 17: Expression frequencies after single transformation with Pro35S-H2B-YFP in *syn4* mutant line SALK_076116 and wt. No significant differences between meristem and differentiated tissues and between mutant and wt were observed.

In vivo analysis of *SMC1/smc1* and *SMC3/smc3* mutants could be done only in the T-DNA lines provided by GABI, which showed a single locus of the T-DNA. Pro35S-H2B-YFP expression was very rare in the lines SALK_017437 and SALK_015308, containing at least eight loci of T-DNA construct within the CaMV 35S promoter sequence (Figure 6). The GABI T-DNA also contained the 35S promoter but the number of T-DNAs in the genome seemed not to reach the threshold for *trans*-inactivation of the fluorescence expression cassette. Silencing of the Pro35S-H2B-YFP expression cassette seemed to inhibit the *in vivo* fluorescence in the SALK lines. After six weeks, no Pro35S-H2B-YFP expression could be observed in any of the transgenic plants, suggesting onset silencing effects.

Transformants of the heterozygous *SMC1* mutant line GABI_269E12 showed a frequency of anaphase bridges of 4.4%. This displays no significant difference compared to wt. Analysis of mitosis in three days old seedlings of the untransformed mutant lines revealed a wt-like frequency of anaphase bridges of 2.4% in SALK_017437 and GABI_269E12, 2.6% in GABI_498B03 and 2.9% in SALK_015308. Col wt showed on average 2.6% anaphase bridges.

In heterozygous *SYN1* mutants no significant increase in the frequency of anaphase bridges could be observed in three days old seedlings after DAPI staining in comparison to wt. Homozygous mutants were observed very rarely with a segregation of 7 : 14 : 1 (wt : he : ho) and therefore, only heterozygous mutants could be analysed after DAPI staining. The frequency of mitotic errors did not differ significantly from wt in heterozygous plants. It is possible that homozygous mutants, which were sterile, would show more severe consequences on mitosis. The expression of Pro35S-H2B-YFP was very rare in meristems, which severely limited the *in vivo* analysis. Due to the presence of three to four T-DNAs, which contain the CaMV 35S promoter, in the SALK line, it is likely that the Pro35S-H2B-YFP expression cassette is silenced in these lines. Complete absence of YFP expression after six weeks supports this hypothesis.

The homozygous loss of function of *SYN2* results in a frequency of 12.5% anaphase bridges analysed *in vivo* in root tips. Untransformed seedlings lacking SYN2 show 9.8% anaphase bridges after DAPI staining, implicating the necessity of this kleisin for proper mitosis. Maximally two bridges per nuclear division were found.

In vivo analysis of heterozygous plants mutated in *SYN3* could not be performed. All 21 transformants that were selected on Kanamycin-containing medium after Pro35S-H2B-YFP transformation contained no SALK T-DNA insertion. Hence, it was only possible to analyse

mitoses in seedlings after DAPI staining. Up to three anaphase bridges were found per division in line GABI_095A10. In total 21.9% of anaphases showed chromosome bridges.
Root tips of homozygous *syn4* mutants showed a bridge frequency of 13.6% in line SALK_076116 *in vivo*. After DAPI staining of seedlings 18.8% bridged anaphase chromosomes were observed with a maximum of three bridges per division. Line SALK_130085 showed 10.8% anaphase bridges and up to five bridges in one mitosis (Figure 18). In line SALK_020171 15.3% bridges were observed, showing not more than two bridges per division. All three lines display a significant increase of bridge frequency compared to wt.
Heterozygous *SCC3* mutants showed 15.9% anaphase bridges with a maximum number of two bridges per division in three days old seedlings (Figure 18). Selection of proper lines after transformation with Pro35S-H2B-YFP was not successful. Only two plants grew on the selective marker medium, which were confirmed as wt after PCR genotyping.

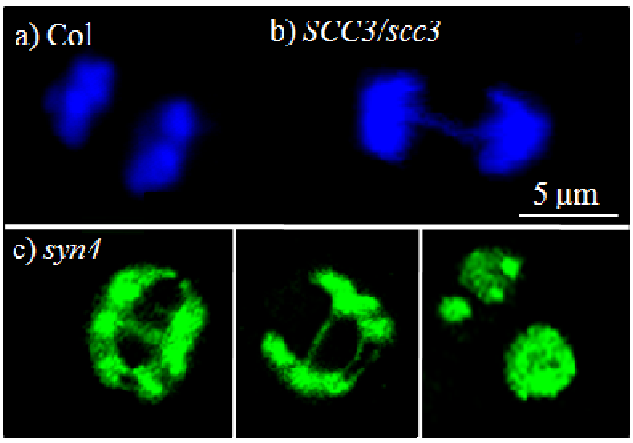

Fig. 18: Representative examples for disturbed mitoses in cohesin mutants. a) Col wt anaphase without bridges after DAPI staining of cotyledon tissue. b) Anaphase of *SCC3/scc3* mutant with one anaphase bridge in DAPI stained cotyledons. c) Pro35S-H2B-YFP transformed *syn4* mutant. Up to five anaphase bridges were observed within one cell in root tips. Micronuclei were the consequence of non-disjunction (left).

Also condensin mutants revealed an increased occurrence of anaphase bridges in root tips and cotyledons of three days old seedlings leading to genomic instability. Representative condensin mutants for the genes *SMC2A* and *SMC2B, SMC4A* and both kleisins *CAP-H* and *CAP-H2* display a significant increase in anaphase bridge frequency in root tips as well as in cotyledons of three days old seedlings compared to wt. SMC2A seems to be very important for mitotic divisions. Pro35S-H2B-YFP expressing root tips of line SALK_052322 revealed 22.6% anaphase bridges and in cotyledons of fixed seedlings 15.6% of anaphases showed bridges. In addition to the increased amount of anaphase bridges, *smc2A* mutants showed 18% of meristematic nuclei with abnormal shapes (Figure 19). It seems that the daughter nuclei stay connected after mitosis due to the high amount of anaphase bridges. The truncated transcript detected in this line can not code for a functional protein and the homolog SMC2B can not compensate completely the truncated SMC2A protein. Nevertheless, homozygous

mutants for both *SMC2* homologs are viable indicating that at least a partial compensation mechanism or the present truncated *SMC2A* mRNA provides some minimal function. Analysis of mitoses in *smc2B* mutants revealed an appearance of anaphase bridges of 11.6% in the line SALK_101643 in fixed seedlings and 15.6% in Pro35S-H2B-YFP expressing root tips with a maximum of two bridges in one anaphase.

Also SMC4A is required for genome stabilisation. 14.5% anaphase bridges in fixed seedlings and 11.5% in root meristems *in vivo* shows that even a slight reduction (~15%) in the transcript level of *SMC4B* results in mitotic disturbances.

Analysis of mitoses in plants mutated in *CAP-H* revealed a significant increase in bridge frequency of 14.9% in line SALK_017766 and of 14.7% bridges in SALK_072400 in three days old seedlings. Both *cap-H* mutants showed up to three bridges per division. Even a slight decrease (~10%) in *CAP-H* expression resulted in disturbed mitoses visible as anaphase bridges and micronuclei (Figure 19). Mutants of the second kleisin candidate of condensin, *CAP-H2* (SALK_059304) could be selected as homozygous. The consequences of *cap-H2* mutation were not as severe as the *cap-H* mutations on divisions. Chromosome bridges in the *cap-H2* mutant line (SALK_059304) were observed in 10.5% of anaphases in fixed seedlings. *In vivo* 9.8% of anaphases showed chromosome bridges. The *cap-H2* mutants showed not more than two chromosome bridges per anaphase.

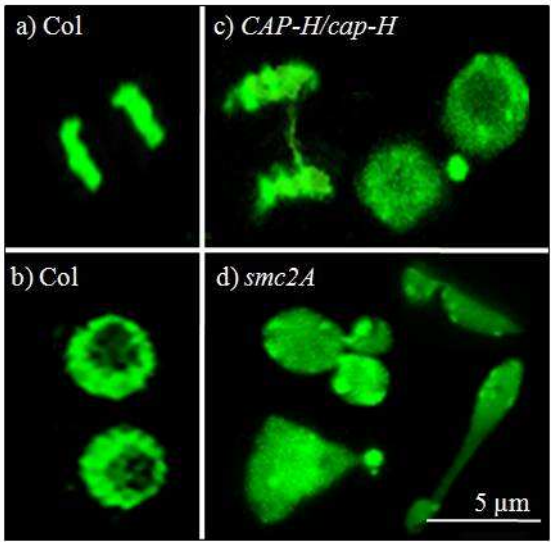

Fig. 19: Representative examples for disturbed anaphases and interphases in root tips of condensin mutants. Plants were transformed with Pro35S-H2B-YFP. a) Anaphase in wt without bridges. b) Interphase structure of meristematic wt nuclei. c) *CAP-H/cap-H* mutant (SALK_017766) shows one anaphase bridge and a micronucleus as the consequence of non-disjunction. e) Nuclei of *smc2A* mutant line SALK_052322 with abnormal shapes.

In addition to cohesins and condensins also the proteins interacting with them were analysed regarding the occurrence of anaphase bridges. SWI1, essential for the formation of axial elements during meiosis (Mercier et al. 2001, 2003) is also necessary for mitosis. The Pro35S-H2B-YFP transformed mutant line showed an anaphase bridge frequency of 21.7% in root

tips. DAPI stained seedlings revealed 21.0% anaphase bridges in heterozygous plants and even 43.8% in one single putative homozygous plant. Because of sterility of the homozygous plants, seedlings were derived from a heterozygous plant and classified according to their bridge values (Supplementary Figure 4). Up to three chromosome bridges were found in one division.

Mutation in the cohesin and condensin loading complex were lethal if homozygous. *SCC2* expression in heterozygous plants was upregulated up to ~88%. Nevertheless, effects of this reduction in *SCC2* mRNA impaired mitoses. No mutant line expressing Pro35S-H2B-YFP in meristems could be selected. Thus, analysis of mitoses could be performed only in DAPI stained seedlings. A bridge frequency of 22.9% was observed showing up to two bridges per division.

Due to the strongly reduced seed set in homozygous plants mutated in *BRU1*, transformation with Pro35S-H2B-YFP could not be performed. Analysis of mitoses was done using three days old seedlings, which showed a frequency of 20.0% anaphase bridges with not more than two bridges in one anaphase.

The Pro35S-H2B-YFP transformation does not influence the anaphase bridge frequency, because there are no differences between the Pro35S-H2B-YFP expressing mutant lines and the mutant lines after DAPI-staining without the Pro35S-H2B-YFP expression cassette.

4. Discussion

Sister chromatid cohesion and chromosome condensation are indispensable for survival of eukaryotes. Efficient repair of double-strand breaks (DSBs) is also essential to maintain genome stability. Correct DSB repair via Homologous recombination (HR) between sister chromatids requires cohesin complexes to use the intact sister chromatid for repair of the damaged one in addition to the SMC5/6 complex in yeast, mammals and plants (Sjörgen and Nasmyth 2001; Ünal et al 2004; Potts et al. 2006; Watanabe et al. 2009). HR (Figure 20) is required for maintenance of the genome integrity (Pacher et al. 2007). In this study, a line of evidence is provided that the cohesin complex is required for efficient repair of DSBs by HR in *A. thaliana*.

Furthermore, DSBs can be repaired by non-homologous end-joining (NHEJ) somatic cells of eukaryotes (Figure 21). Homologous sequence information does not play a major role in this process of DSB rejoining. A few nucleotides of homology are enough for the annealing reaction (Puchta 2005). This process can lead to translocations and other lesions. Both

mechanisms share common steps and combinations between HR and NHEJ are also present in plants (Puchta 2005). DSB repair can start with the HR pathway and as final rejoining process NHEJ can be used (Gorbunova and Levy 1999).

Phosphorylation of the histone H2A at serine 129 recruites the cohesin complex to DSB sites and is necessary for repair by HR and NHEJ in yeast (Ünal et al 2004; Pacher et al. 2007). Cohesin mutations impair efficient HR because of insufficient sister chromatid alignment. Misrepair due to separated sister chromatids because of mutated cohesin genes or genes encoding interacting proteins may result into dicentric and acentric chromatids (Figure 22). DSBs and misrepair can arise between different chromosomes. Theoretically only 50% of reciprocal chromatid translocations are visible as chromosome bridges, because only asymmetric translocations result in dicentric and acentric fragments.

The condensin complex is required for chromosome contraction from prophase to metaphase and to resolve associations between sister chromatids by recruiting chromatin remodelling proteins such as Topoisomerase II (Top II) (reviewed by Hudson et al. 2009). Top II is necessary for resolution of catenations between sister chromatids prior to segregation (Pasierbek et al. 2003). An important function of condensin is, to regulate that non-histone proteins associate correctly with chromatin (reviewed by Hudson et al. 2009). In condensin mutants the anaphase bridges may arise due to non-disjunction of sister chromatids which failed the in resolution of associations like catenations and entanglements (Figure 23).

In addition, proteins interacting with cohesin and condensin are required for correct nuclear divisions or processes which are required prior to segregation for instance DSB repair. SWI1 was shown to be involved in axial element formation in meiosis and in the formation of RAD51 foci (Mercier et al. 2003) indicating interaction with cohesins and mediating alignment of chromosomes and DSB repair by HR. The loading of both cohesin and condensin is dependent on the SCC2/SCC4 loading complex in yeast and *Drosophila* (Seitan et al. 2006; Watrin et al. 2006). In *A. thaliana* the loading complex is essential for plant viability possibly by mediating sister chromatid cohesion via loading of cohesins and chromosome condensation by loading of condensins. Furthermore, BRU1 is necessary for centromere condensation and control of the epigenetic information in *A. thaliana*. Plants mutated in *BRU1* show a high sensitivity to genotoxic stress (Takeda et al. 2004). Interaction of BRU1 with the condensin complex seems to be important for developmental control in plant growth. Condensation of chromatin needs to be regulated at the correct time and locus. It is possible that BRU1 is involved in this regulation by interaction with condensin

complexes and thus, mediating chromatin condensation of heterochromatin for instance centromeric repeats.

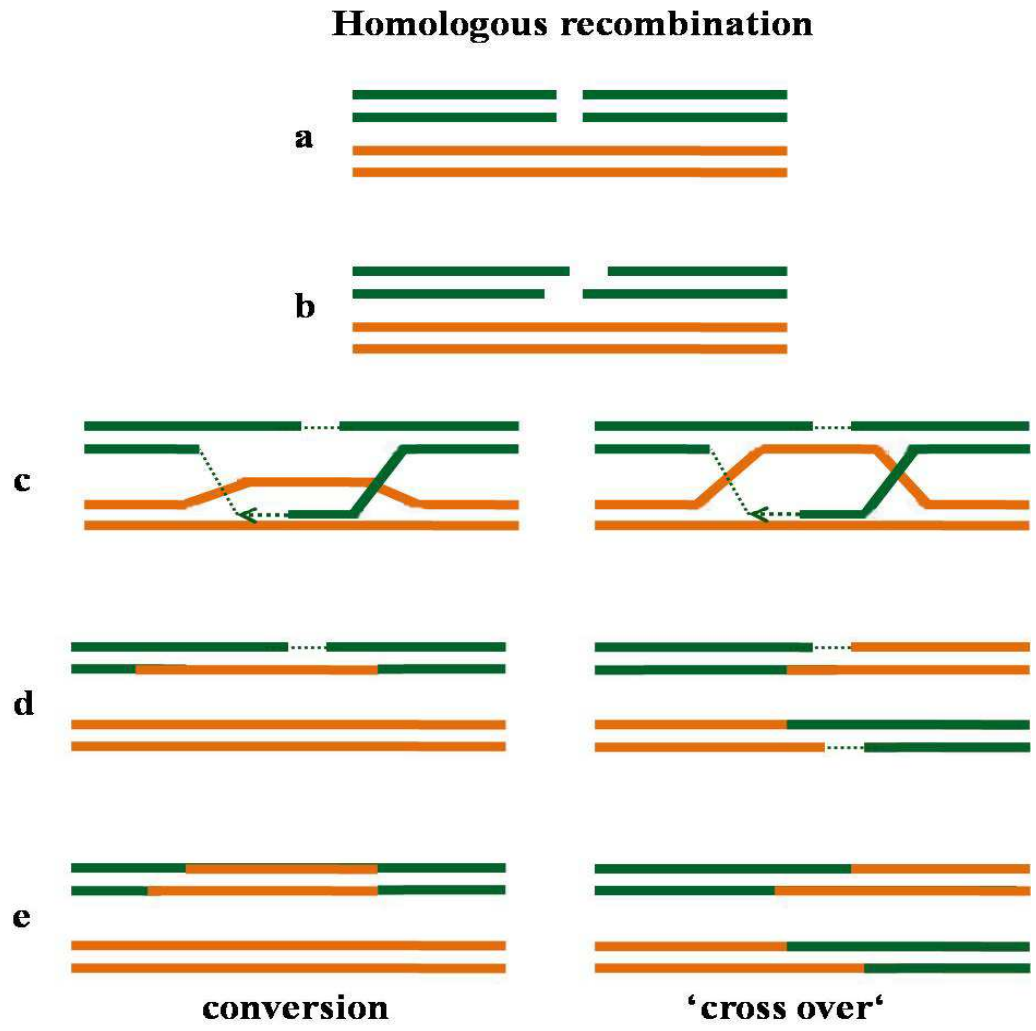

Fig. 20: DSB repair via HR in somatic plant cells (according to Puchta 2004). After DSB induction (a), breaks can be closed via synthesis dependent strand annealing (SDSA) (left). An exonuclease catalyzes 3`-single strand overhangs at DSB ends (b). At the homologous double-strand e.g. the sister chromatid (orange), a D-loop is built by invasion of a free 3` end (c). After repair synthesis (d) at the template of the homologous strand the ends are ligated together again resulting in a gene conversion (e). A special HR mechanism is the allelic HR (right). A double holliday-junction is formed (c), either between homologous chromosomes-resulting in a cross over or between sister chromatids-resulting in a sister chromatid exchange (SCE). Gaps are filled by DNA synthesis (d). The originally broken sister chromatid (green) is ligated to the homologous chromosome or sister chromatid (orange) (e).

4.1 Disturbed cohesion and misrepair cause somatic anaphase bridges

The cohesion of sister chromatid centromeres is required in prophase of mitosis for correct chromosome segregation and for the correct repair of double-strand breaks via HR during G2 phase of the cell cycle. In addition to cohesin, also SMC5/6 and condensin complexes, as well as the replication- and transcription machinery seems to be involved in sister chromatid cohesion. In repetitive chromatin regions with specialized functions (centromeres, telomeres and rDNA loci) distinct mechanisms for sister chromatid cohesion can be found like catenations or entanglements (reviewed by Losada 2007). It was indicated, that in human cells telomere cohesion of sister chromatids is mediated by an association between the cohesin subunit SCC3 and components of telomeric chromatin (Canudas et al. 2007).

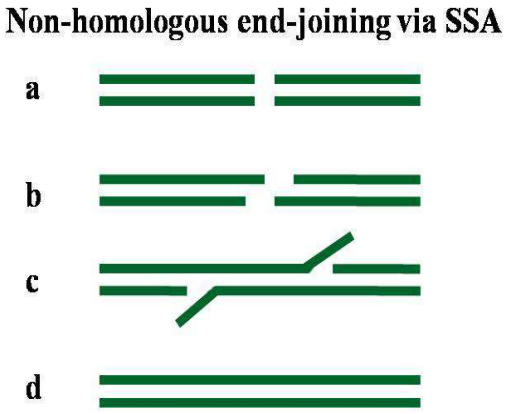

Fig. 21: DSB repair in somatic plant cells via single strand annealing (SSA) (according to Puchta 2004). SSA belongs to the NHEJ repair pathway. A DSB is induced (a). Exonuclease produces 3`-single strand overhangs at DSB ends (b). If complementary sequences are present they can anneal and produce a chimeric DNA-molecule (c). Overhanging ends are restricted resulting in deletions. In case that there are no complementary sequences present, homology of only three nucleotides is enough for the annealing reaction (d) and putative single-stranded regions are filled by DNA synthesis.

After semi-conservative replication, DNA molecules are catenated and therewith aligned without need for cohesin (Díaz-Martínez et al. 2008), but during replication also cohesin mediated cohesion is established after cohesin loading via SCC2/SCC4 during G1. ETG1 and CTF18 are evolutionary conserved replisome factors required for cohesion establishment during this process (Takahashi et al. 2009 submitted). Furthermore, cohesins are required for correct repair of DSBs by HR (Ünal et al 2004; Pacher et al. 2007). Sister chromatid exchange (SCE) was shown to be the preferred pathway for accurate repair in yeast and mammals (Kadyk and Hartwell 1992; Johnson and Jasin 2000; Gonzalez-Barrera et al. 2003). Cohesin complexes are essential for repair of DSBs by SCE in *S. cereviseae* (Cortes-Ledesma and Aguilera 2006). If no or not enough functional cohesin is present in the nucleus to align sister chromatids sufficiently, DSBs might be misrepaired by using NHEJ or HR of ectopic

homologous sequences instead of HR between allelic sequences. *A. thaliana* sister chromatids show 30% separation along chromosome arms (Schubert et al. 2006). Thus, cohesins are required to align sequences of sister chromatids for efficient repair of DSBs by HR during G2 phase. Ligation of different DSBs at non-allelic positions via NHEJ may lead to translocations between chromosome arms resulting in di- and acentric chromatids (Pacher et al. 2007), when ligations are asymmetric. Only 50% of reciprocal translocations become visible as anaphase bridges when asymmetric ligation of chromatids occured. During mitosis the two centromeres of dicentric chromatids can be pulled towards different cell poles forming chromosome bridges during anaphase. Pulling forces of the mitotic spindle or the new cell wall cuts the bridged chromosome into two pieces. Acentric chromosome fragments remain between the daughter nuclei forming micronuclei at telophase. A DSB, if interfering with replication may result in a fusion between sister chromatids forming a chromatid bridge during the next mitosis similar to the break-fusion-break cycle first described by McClintock (1953). Three and more bridges in one anaphase may represent a misrepair of DSBs between sister and non-sister chromatids during G2.

Lines containing a mutation in *smc1* or *smc3* showed no significant increase of chromosome bridges. These mutations were homozygously lethal and could only be selected as heterozygotes. The allele of the respective gene without mutation (*SMC1* or *SMC3*) was upregulated to a level comparable to wt. Analysis of alignment frequencies along chromosome arms by fluorescence *in situ* hybridisation (FISH) showed in *smc1* and *smc3* mutants no significant differences in comparison to wt (Schubert et al. 2009). Consequently, also the anaphase bridge frequency did not differ significantly from wt. To reduce the expression level of *SMC1* or *SMC3*, RNAi lines might be helpful for further analysis.

In yeast and metazoa two different α-kleisins evolved, one for mitosis and one for meiosis (reviewed by Lee and Orr-Weaver 2001; reviewed by Nasmyth 2001), while higher plants (*A. thaliana* and rice) contain four α-kleisins. These four paralogs developed organ-specific functions, but can compensate each other partially (reviewed by Schubert 2009).

The homozygous mutation in the meiotic α-kleisin subunit SYN1 causes sterility in *A. thaliana* (Bai et al. 1999; Bhatt et al. 1999; Cai et al. 2003). Analysis of homozygous *syn1* mutants could not be done due to the very low number of homozygotes. The segregation of mutants was 7 : 14 : 1 (wt : he : ho). Mitotic disturbances did not differ significantly from wt in heterozygous mutants but to draw final conclusions on the role of SYN1, analysis of homozygous mutants would be necessary. Plants mutated in *SYN1* showed increased sister

chromatid separation after X-irradiation compared to wt indicating the requirement of cohesin complexes for correct DSB repair (Watanabe et al. 2009).

Plants mutated in *SYN2* showed varying alignment values along sister arms indicating a locus-specific impact if this α-kleisin (Schubert et al. 2009). The elevated amounts of anaphase bridges in *syn2* mutant lines indicate the necessity of this cohesin subunit for correct repair of DSBs.

SYN3 represents an α-kleisin with a specialized role in maintenance and transcription of rDNA structure and processing of rRNA (Jiang et al. 2007). A mutation in this gene was homozygously lethal and the expression of the intact allele in heterozygous mutants was upregulated to ~77% indicating the importance of this gene. This reduction in the amount of SYN3 resulted in ~23% of mitoses with anaphase bridges. Reduced amount of SYN3 might change the rDNA structure and cause elevated amounts of incorrect DSB repair resulting in translocations. The *Arabidopsis* genome contains two chromosome domains encoding ribosomal proteins. These nucleolus organisator regions (NORs) are located on chromosome two and four. If the rDNA structure cannot be maintained due to lack of SYN3, DSBs which arise during G2 might be misrepaired. Asymmetric translocations may result into dicentric chromatids and anaphase bridges in these mutants.

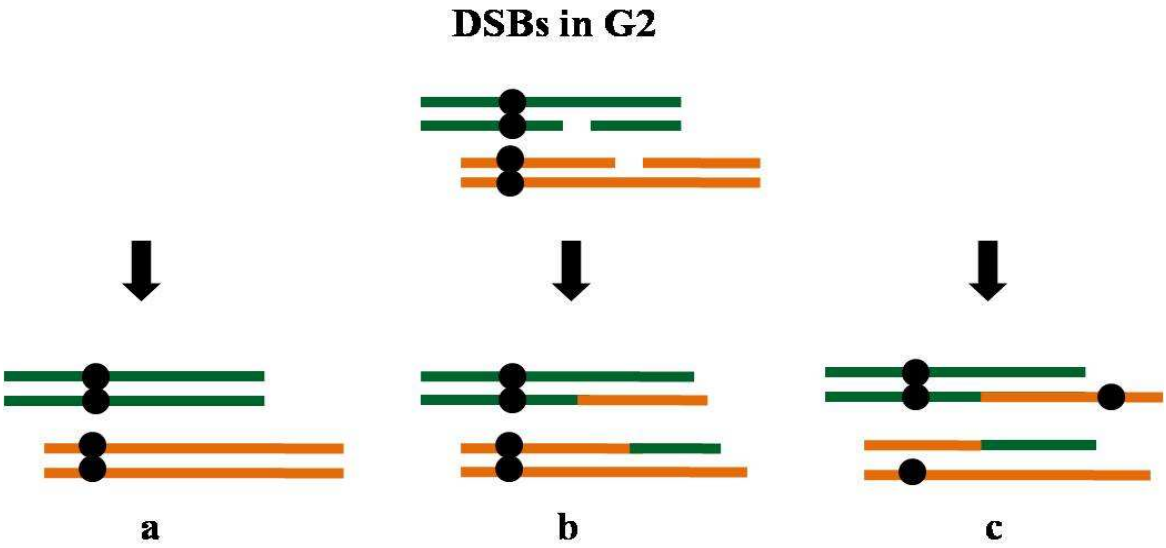

Fig. 22: Misrepair between chromosomes in G2 phase (according to Traut 1991). Repair of DSBs in chromosomes in G2 result in **a)** the restoration of original chromosomes **b)** in a symmetric reciprocal exchange between chromosome arms **c)** in a dicentric and an acentric chromatid via asymmetric exchange. Dicentrc chromatids can be pulled towards different cell poles in anaphase and become visible as anaphase bridge. Theoretically only 50% of asymmetric and reciprocal translocations become visible as anaphase bridges. Centromeres are shown as black balls.

SYN4 is required for chromosome arm and centromere cohesion (da Costa-Nunes et al. 2006). Centromere cohesion is very important prior to anaphase. SYN4 is involved in centromere- and arm cohesion as the separation frequencies were elevated in *syn4* mutants (Schubert et al. 2009). Centromere separation is a drastic consequence of mutated *SYN4*. The truncated transcript present in *syn4* mutants might not produce a completely functional protein, as an anaphase bridge frequency of ~11-19% was observed.

The SCC3 protein is essential and mutations are homozygously lethal in *A. thaliana*. The number of anaphase bridges was significantly increased to 14.5% compared to wt in *scc3* mutants. Similar results were observed after RNAi depletion of SCC3 resulting in mitotic and meiotic anaphase bridge formation in *C. elegans* (Pasierbek et al. 2003). SCC3 is involved in sister chromatid arm alignment (Schubert et al. 2009) and might be necessary for correct repair of DSBs as well.

The genomic instability found in several cohesin mutants provides new aspects of the function of cohesin not only in sister chromatid cohesion but also in facilitating double-strand break repair. Misrepair of double-strand breaks due to reduced availability of cohesin might be the phenomenon causing the chromosome bridges in *A. thaliana* cohesin mutants. In future, the cohesin mutant lines can be analysed for sensitivity to genotoxic stresses, such as X-ray irradiation (Watanabe et al. 2009) or DSB inducing chemicals. This might reveal the involvement of cohesins in DSB repair via HR by mediating sister chromatid cohesion.

Immunolocalisation studies identified SMC proteins also in the cytoplasm. Mammalian centrosomes contain SMC1 (Austin et al. 2009). SMC3 was found in the cytoplasm and along the spindle from metaphase to telophase in *A. thaliana* during mitosis and meiosis (Lam et al. 2005). This suggests also non-chromatin related functions of cohesin.

In yeast, *Drosophila* and mammals cohesin together with CTCF insulator proteins is involved in the regulation of gene expression and development by interaction with enhancer sequences (reviewed by Gause et al. 2008, Uhlmann 2008; Wendt and Peters 2009). In *Arabidopsis* two candidate genes encode insulator proteins with homology to CTCF. *C2H2* and *REF6* are homologues of CTCF, which show co-expression with cohesin genes during the cell cycle (Rudnik 2009) but the involvement in gene expression needs further confirmation in *A. thaliana*.

4.2 Condensins are required for correct chromosome segregation

As condensin is involved in proper spindle-kinetochore attachment and bipolar orientation of *S. cereviseae* chromosomes via realization of inter chromatid release and chromosome contraction (Yong-Gonzalez et al. 2007), mutations in condensin coding genes result in genome instability. In vertebrate condensin mutants it was shown, that the inner centromeric chromatin structure is decondensed, affecting the stiffness of the centromere (Ribeiro et al. 2009).

The *A. thaliana* genome contains several putative genes for the different components of the condensin complex. This allows a combination of various complexes, which can realize specialized functions during the cell cycle (reviewed by Schubert 2009). The condensin complex was called “architect of mitotic chromosomes” by Hudson et al. (2009). The proper loading of proteins onto the chromosomes requires a permissive DNA topology which might be created by the condensin complex (reviewed by Hudson et al. 2009). This SMC complex is necessary for the formation of higher order chromatin and plays an important role in recruiting proteins required for the formation of compact chromosomes. Especially the recruitment of Top II is important prior to anaphase. This enzyme disentangles interwined sister chromatids, which can not be separated in anaphase if they are still catenated or entangled. In case of incomplete condensation, sister chromatids might twist around each other, inhibiting correct chromosome segregation (Pasierbek et al. 2003). Furthermore, condensin is required for complete cohesin removal and for the resolution of chromosome associations prior to segregation (Hirota et al. 2004). Chromatin bridges in anaphase are the consequence of mutations in condensin subunits (Hirano 2005).

Also loss-of-function mutants, incomplete transcripts or reduced expression of condensin genes impair mitosis in *A. thaliana* as shown in this work. As the homozygous mutation in *SMC2A* inhibits the formation of a correct condensin complex, remaining cohesion might hold the sister chromatids together and result in high amounts of chromosome bridges in anaphase. Similar effects were observed in RNAi studies using mammalian cell cultures. Either condensin I or condensin II deficiency resulted in chromosome bridges (Ono et al. 2004; Gerlich et al. 2006). In vertebrates it was shown that depletion of SMC2 results in a high frequency (~20%) of anaphase bridges (Vagnarelli et al. 2006). Yeast metaphase chromosomes lacking condensin showed dramatic differences in the behavior of the kinetochores. Sister kinetochore movements were uncoordinated, due to the disturbed morphology of the inner centromere chromatin and not the protein structure of the kinetochore itself (Gerlich et al. 2006).

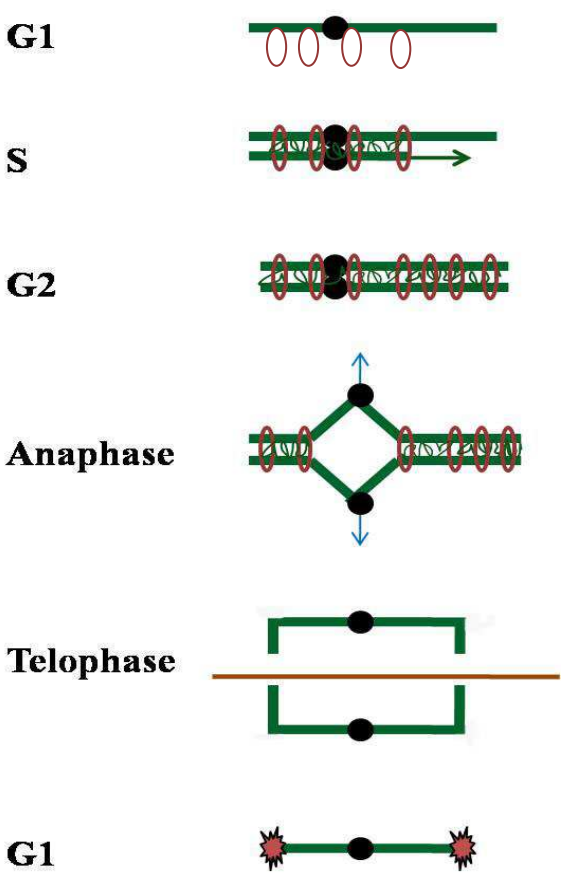

Fig. 23: Failure in resolution of entanglements and cohesion in condensin mutants during the mitotic cell cycle leading to two chromosome bridges (according to Pasierbek et al. 2003). In G1 only one chromatid is present and cohesins (red ovals) are loaded. During replication in S-phase sister chromatid cohesion is established. Sister chromatids become entangled and catenated in G2 (thin green line between chromatids). Microtubuli (blue arrows) try to separate the sister chromatids in anaphase by pulling the centromeres (black balls) apart. Resolution of cohesion, entanglements and catenations prior to segregation fails in condensin mutants. Thus, sister chromatids cannot be separated and become visible as anaphase bridges. In telophase the cell wall (brown line) cuts the bridged chromatids and creates DSBs (red asterisks).

In yeast cells lacking condensin, the Cell Untimely Torn (CUT) phenotype was visible after defective chromosome segregation. This prevented the completion of cytokinesis and was first described in fission yeast (Hirano et al. 1986). The cells showing a CUT phenotype cannot complete cytokinesis and stay connected after cell division. *A. thaliana* mutants deficient in SMC2A showed a similar phenotype in root tip cells (Figure 19) indicating incomplete cytokinesis.

The two homologs encoding SMC2 show different compensation effects. *SMC2A* can compensate the mutation in *SMC2B* but not *vice versa*. The mutation in *SMC2A* is homozygously lethal but *SMC2B* is dispensable for plant viability. The high homology at the protein level (Siddiqui et al. 2003) indicates a duplication event that occurred recently during the evolution of *A. thaliana* but SMC2B is not a completely functional protein as SMC2A. *SMC2B* shows at the cDNA level nearly 50 bp less than *SMC2A* at the start point of the coding region indicating a specialized domain which is only present in *SMC2A* (Supplementary Figure 1).

A similar situation is true for the two *SMC4* homologs. SMC4A is essential for plant viability but SMC4B seems to be dispensable. The selection of additional T-DNA lines with mutated

smc4B revealed also homozygous mutants (data not shown) indicating a minor role of the *SMC4B* homolog in comparison to *SMC4A*. The sequence similarity of the *SMC4* homologs is low at the cDNA level. Also the lengths of the transcripts are different. *SMC4A* shows nearly doubled the length compared to *SMC4B* (Supplementary Figure 2).

The two kleisins CAP-H and CAP-H2 show different effects after mutation. The γ-kleisin CAP-H is essential for plant viability and can partially compensate the mutation in the β-kleisin CAP-H2. This could be due to the unique kleisin-γ middle domain in CAP-H. Through this domain CAP-H is able to localise at different compartments in the cell. In interphase it localises in the cytoplasm while CAP-H2 shows always localisation in the nucleus (Fujimoto et al. 2005). This suggests that both kleisins and especially CAP-H evolved different functions during evolution. In *Drosophila cap-H2* mutants the formation of interphase chromosome territories is intermingled (Hartl et al. 2008). *A. thaliana* chromosomes are organizd in well defined chromosome territories in interphase (Pecinka et al. 2004), similar what has been found in mammals (Manuelidis 1985; Cremer et al. 1988) and other plant species (Leitch et al. 1990). If the chromosomes are intermingled and cannot occupy discrete nuclear regions due to the lack of CAP-H2, DSB repair via HR can be disturbed due to the large distance between sister chromatids preventing correct alignment required for repair.

Unfortunately, no T-DNA mutants for the condensin subunits SMC4B and CAP-D2A and CAP-D2B could be selected up to now.

4.3 Correct cell division requires the proteins SWI1, BRU1 and the cohesin and condensin loading complex SCC2/SCC4

The dynamic chromosome architecture cannot be mediated only by the various SMC complexes. Additional proteins interact with the cohesin and the condensin complexes.

The protein SWI1 is essential for axial element formation in meiosis in *A. thaliana*. During male meiosis *swi1* mutants show a precocious loss of sister chromatid cohesion, suggesting a role of SWI1 in cohesion maintenance. SWI1 is required for plant fertility (Mercier et al. 2001, 2003).

Also mitosis or processes prior to mitosis require SWI1 as shown in different tissues of *A. thaliana* mutants. Cotyledons deficient in SWI1 cannot perform mitosis correctly and show increased numbers of chromosome bridges in anaphases. In root tips lacking SWI1 the number of defective anaphases was even higher. Furthermore, SWI1 is involved in sister

chromatid arm alignment analysed by FISH (Schubert et al. 2009). The disturbed alignment impairs proper repair of DSBs.

SWI1 is expressed in G1 and S phase (Mercier et al. 2001, 2003). At this time point the loading and establishment of sister chromatid cohesion is done. In addition, SWI1 was shown to be essential for axial element formation in meiosis, mediating plant fertility. It is possible that SWI1 is involved also in the establishment of sister chromatid cohesion prior to mitosis. How SWI1 interacts with cohesin is not elucidated up to now. Furthermore, plants mutated in *SWI1* impair the formation of RAD51 foci indicating recombination defects in meiosis (Mercier et al. 2003). May be SWI1 is involved also in HR repair of DSBs by interacting with cohesins and mediating sister chromatid cohesion.

A second gene similar to *SWI1* is present in the *A. thaliana* genome (At5G23610). It has not yet been analysed functionally (reviewed by Schubert 2009). The strong effects (sterility and elevated number of anaphase bridges) of the *SWI1* mutation suggest that At5G23610 obviously can not compensate the mutation in the *SWI1* gene.

The biological importance of cohesin- and condensin interacting proteins is also obvious in human diseases. Patients with Cornelia de Lange syndrome have mutations in cohesin genes or genes encoding the cohesin and condensin loading complex SCC2/SCC4. The mutation causes developmental problems and mental retardation (Dorsett 2007; Barber et al. 2008).

The loading and distribution of both cohesin and condensin along chromosomes is realized by the SCC2/SCC4 complex in yeast and *Drosophila* (Seitan et al. 2006; Watrin et al. 2006). By mutating the *SCC2* gene of *A. thaliana*, it was obvious that this mutation was homozygously lethal and even a slight reduction in the transcript level of *SCC2* (~88% of wt level) resulted in mitotic disturbances in heterozygous mutants. The genomic instability in these mutants pointed out the importance of the correct expression level of the cohesin and condensin loading complexes. Reduced availability of SCC2 results in an elevated frequency of anaphase bridges. *A. thaliana* centromere cohesion and organisation is also affected by the loading complex (Schubert et al. 2009; Sebastian et al. 2009). Depletion of *SCC2* by RNAi results in disturbed meiotic chromosome organisation and sterility, visible as defective homologous pairing, loss of sister chromatid cohesion, missegregation of chromosomes and chromosome fragmentation (Sebastian et al. 2009), supporting the impact of SCC2 on cell divisions.

Structural and functional stability of chromatin requires BRU1 interacting with the condensin complex in *A. thaliana*. Stability of the epigenetic information after replication is controlled by BRU1. By loosing of developmental control, *bru1* mutants are dwarfy and show

developmental abnormalities (Takeda et al. 2004). Chromosome bridges in anaphases were visible in one out of five mitoses. This indicates an important role for BRU1 in segregation of mitotic chromosomes or prior to segregation. By controlling epigenetic information, BRU1 might be necessary for stability of heterochromatic regions. The centromeric chromatin appears decondensed in *bru1* mutants (Takeda et al. 2004). The centromere represents an important structural part of the nuclear division. Due to the loss of the centromere condensation chromosomes might have problems to form a stable structure inhibiting appropriate disjunction in anaphase. Similar as in condensin mutants, chromatids in *bru1* plants might twist around each other due to lack of condensation. These entanglements may result into anaphase bridges when the chromatids should be separated.

4.4 Life cell imaging allows visualization of cell divisions *in vivo*

Visualization of growth in real time and single cell tracking is used to understand the spatiotemporal dynamics in the cell. The different techniques for non-invasive protein labelling and/or interaction studies in different tissues open an amazing field to cell biologists. Fluorescence labelling opens the possibility to detect single molecules due to its high sensitivity (Levitt et al. 2009; Reddy and Roy-Chowdhury 2009).

In living roots YFP and DsRed can serve as molecular markers which can be visualized dynamically. Fluorescent tagginf of recombinant proteins, such as histones, allows direct insight into processes in the plant cell (Chen and Li 2005). Histone H2B, as one of the core histones, is a useful marker for chromatin localisation.

In this present work the initial approach was to label two different chromatin domains (the centromere and the chromosome arms) by simultaneous expression of differentially labelled histone variants. This strategy failed as expression of both markers rarely occurred and was visible only in few nuclei indicating silencing caused by a high number of T-DNAs containing 35S promoters present in mutant lines after double transformation. An excess of mRNAs produced by overexpression due to the strong 35S promoter can induce RNA-mediated silencing pathways leading to histone methylation and heterochromatic silencing in *Arabidopsis* (Zilberman et al. 2003). The length of short interfering RNAs (siRNAs) mediates the pathway of silencing. 21-22 nucleotide (nt) siRNAs suppress gene expression post-transcriptionally by mediating mRNA degradation. Longer siRNAs (24-26 nt) lead to homologous DNA methylation (Hamilton et al. 2002). Transcriptional gene silencing (TGS) can be the result of RNA-directed DNA methylation (RdDM) if promoter sequences are

targeted by homologous RNA molecules (Mette et al. 1999, 2000) (Figure 24). The presence of the 35S promoter sequences in T-DNA insertion lines can lead to *trans*-inactivation of other 35S promoter-controlled expression cassettes elsewhere expression cassettes in the genome (Daxinger et al. 2008). The absence of robust reporter gene expression indicated silencing in the SALK mutant lines containing more than one T-DNA insert especially after double transformation with Pro35S-H2B-DsRed and Pro35S-EYFP-CenH3 constructs. This made the analysis of mitoses with double labelled chromatin (chromosome arms and centromere) impossible. Especially in homozygous *syn4* mutant plants it was obvious that the expression of both fluorescence constructs was reduced in comparison to double transformed wt plants. Therefore, single transformation with Pro35S-H2B-YFP was performed to reduce the number of transgenes present in the plant genome after transformation. 100% of wt nuclei of wt nuclei expressed the construct in root tissue. Plants mutated in *SYN4* showed a slight reduction in expression compared to wt. In leaf nuclei 90% displayed a fluorescence signal, indicating that more than one T-DNA insertion strongly enhances the probability of silencing. After six weeks under short day conditions no Pro35S-H2B-YFP fluorescence at all was detectable any more in these single transformants, further underlining the hypothesis of a silencing process. In the lines containing more than six T-DNAs, expression of the Pro35S-H2B-YFP cassette was reduced to a level that the analysis of mitoses *in vivo* was inhibited.

Simultaneous expression of transgenes can be present as shown by the Northern blot technique in *A. thaliana* after double and triple-transformation (Radchuk et al. 2005). But expression frequencies of single nuclei cannot be compared with a blotting method based on homogenized tissue. Also in this study, expression of the two transgenes was present after double transformation in homogenized seedling tissue measured by quantitative real-time PCR. Unfortunately, the two constructs Pro35S-H2B-DsRed and Pro35S-EYFP-CenH3 were expressed in different tissues. The Pro35S-EYFP-CenH3 expression was restricted to the meristematic cells in the root tip while the Pro35S-H2B-DsRed fluorescence expression was mainly visible in the elongated root. One construct seems to inhibit the expression of the other may be due to the similarity of promoter and terminator sequences in both cassettes. In contrast, the use of the native promoters for recombinant protein expression with different fluorescence tags was more successful in *A. thaliana* (Reddy and Roy-Chowdhury 2009). Co-expression of fluorescence tagged proteins in multiple colours allows to analyse protein interaction or developmental studies for any organism if the native promoters are used (Levitt et al. 2009). In tobacco BY-2 cells simultaneous expression of fluorescent tagged CenH3 under the control of the strong constitutive 35S promoter and GFP-α-tubulin with the native

promoter was visible within one cell (Kurihara et al. 2008). This shows that co-expression of recombinant proteins can be successful if different promoters are used.

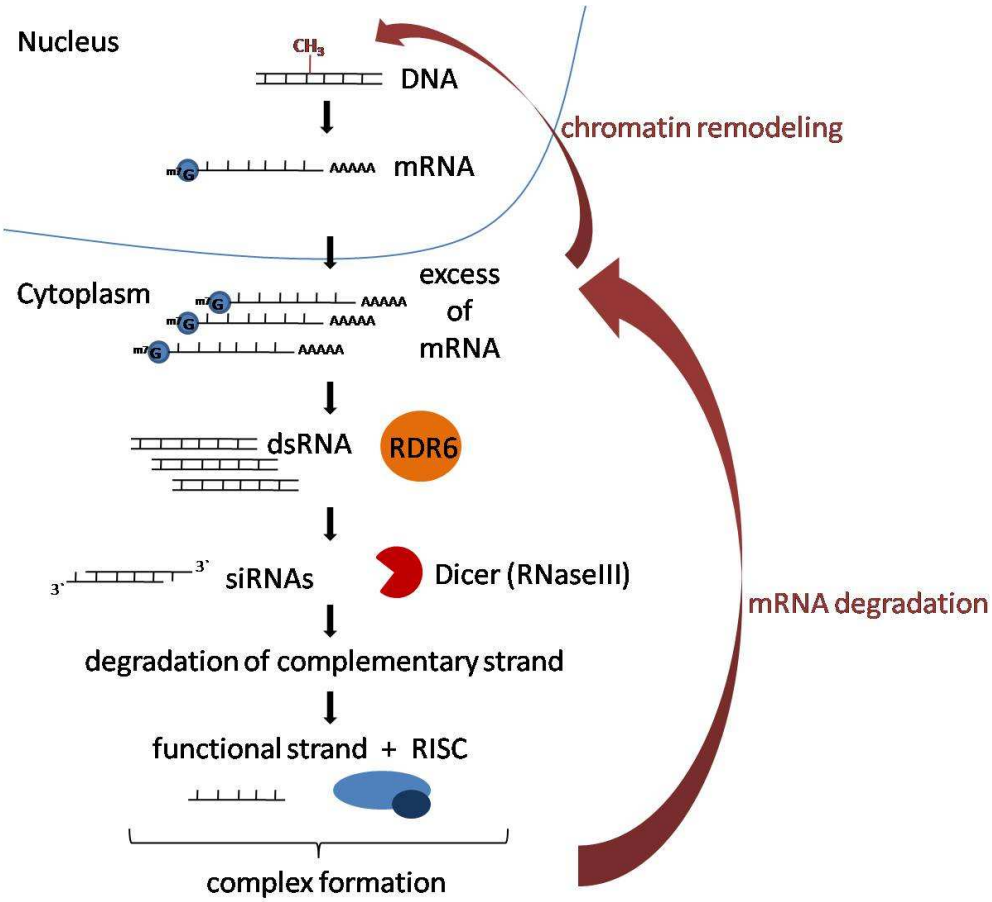

Fig. 24: RNA-mediated silencing pathways in plant development (accoring to Verdel et al. 2009; Ellendorff et al. 2008; Kuhlmann et al. 2006). Large amounts of mRNAs produced due to overexpression by the strong constitutive 35S promoter are recognized by the RDR6-polymerase. RDR6 transcribes double-stranded RNA (dsRNA) molecules out of the excess of mRNA. The RNaseIII activity termed dicer cleaves the dsRNA into short interfering RNAs (siRNAs) with 3´-overhangs. RISC is activated, degrades the complementary strand and forms a complex with the functional strand of the siRNAs leading to mRNA degradation by target recognition (binding to the complementary mRNA strand) and/or chromatin remodelling of the respective promoter sequence (DNA methylation). The protein expression is suppressed.

The observed tissue-specific differences in expression of transgenic marker constructs and the "switching off" after a few weeks of life time suggested silencing effects. To test, whether Post Transcriptional Gene Silencing (PTGS) was responsible for silencing of the constructs, homozygous mutant plants deficient in the RNA-Dependent-RNA-Polymerase 6 (RDR6)

(Wassenegger and Krczal 2006; Diaz-Pendon 2007; Li et al. 2005) which are known to be impaired in PTGS (Butaye et al. 2004) were transformed with the same constructs (Pro35S-H2B-DsRed and Pro35S-EYFP-CenH3). Due to the very low transformation rate observed with of this mutant line, only one single transformant could be selected. This plant showed no fluorescence expression. May be mechanisms other than PTGS are responsible for the silencing of both constructs but only one transformant is not sufficient to conclude. The suggestion that Transcriptional-Gene-Silencing (TGS) is the responsible mechanism requires further analysis.

4.5 T-DNA insertion lines are a powerful tool for reverse genetics but require detailed determination of T-DNA position, copy number, and effect on expression of the interrupted gene

The availability of T-DNA lines for nearly any gene of interest of *A. thaliana* allows the application of reverse genetics. Nevertheless, these lines often do not show a complete loss-of-function of the gene. Insertions can be located in introns and might be spliced out during the RNA processing pathway. For optimal `knocking out` the gene of interest, the T-DNA should be located in the middle of the coding region. Otherwise truncated transcripts could disturb the analysis by producing a partial functional protein. The 35S promoter in the T-DNA of SALK and GABI lines can cause overexpression of the respective protein downstream of the T-DNA. Due to this, insertions at the transcription start might result in opposite effects than loss-of-function of the respective gene (Rosso et al. 2003). Insertions upstream of the coding region can have an effect on the transcription, if they are located in a promoter or enhancer. Downstream of the coding region locates the terminator which can effect the transcription as well if interrupted by a T-DNA. Untranslated regions (UTRs) are important for mRNA processing. T-DNA insertions in these domains might disturb the production of a functional protein (Ülker et al. 2008). To conclude on the function of a gene of interest, it is important to select more than one mutant line per gene if available. When the mutant lines show similar effects, side effects from other integrated T-DNAs can be neglected.

Among the 35 lines analysed, only eight lines were confirmed as a complete loss-of-function of the respective genes. Four lines showed a truncated transcript upstream of the T-DNA. In two lines an overexpression was found downstream of the T-DNA. One was provided from GABI and one from SALK. This can be explained by the strong constitutive 35S promoter included in the T-DNAs which might enhance the endogenous expression level of the

respective gene. The pAC161 vector in GABI-kat lines was originally generated for activation tagging and overexpression of *A. thaliana* genes (Rosso et al. 2003). However, not all potentials of these activation tagged lines were used. Transgenic overexpressors are an interesting tool in *A. thaliana*, as many genes are too large for easy cloning. The unknown function of a protein might be elucitated by it´s overexpression in the same way as by its loss-of-function. But if the researcher´s purpose is the loss-of-function of a gene, side-effects can make the analysis difficult.

5. Summary

Sister chromatid cohesion, chromosome condensation, DNA repair, recombination and transcription are indispensable processes for all eukaryotes. SMC (structural maintenance of chromosome) protein complexes and proteins interacting with them are essential for these tasks (reviewed by Nasmyth and Hearing 2005.)

First studies in yeast showed, that cohesin complexes consist of the subunits SMC1, SMC3, SCC3 and the α-kleisin SCC1 to close the ring (reviewed by Nasmyth and Hearing 2005). In *A. thaliana* four α-kleisins were found and named SYN1-SYN4. SYN1 represents the meiotic α-kleisin (Bai et al. 1999; Bhatt et al. 1999; Cai et al. 2003). Cohesins mainly facilitate sister chromatid cohesion (Liu et al. 2002; Lam et al. 2005; Chelysheva et al. 2005). Condensins with the subunits SMC2, SMC4, CAP-D2, CAP-G and the β-kleisin CAP-H2 or the γ-kleisin CAP-H are responsible for chromosome condensation and segregation in mitosis and meiosis (Hirano and Hirano 2006).

Interaction partner for cohesin and condensin is the SCC2/SCC4 loading complex (Seitan et al. 2006; Watrin et al. 2006). SWITCH1 (SWI1) is required for meiotic sister chromatid cohesion (Mercier et al. 2001, 2003) and was therefore included in this study. As interaction partner of condensin BRUSHY1 (BRU1) was analysed, as it was shown to be required for heterochromatin condensation (Takeda et al. 2004).

This study was focussed on the two SMC complexes cohesin and condensin and proteins interacting with them in *Arabidopsis thaliana* (L.) Heynh.

T-DNA insertion mutants for the putative cohesin- and condensin genes were selected and analysed regarding their habit, fertility, mRNA expression and copy number of T-DNAs. In addition, three cohesin and condensin interacting proteins were analysed. Selection of homozygous mutant lines was only possible for the α-kleisin genes *SYN1*, *SYN2* and *SYN4* belonging to the cohesin complex, and for two of the condensin genes *SMC2* and *CAP-H2*,

because there are two paralogs for each of them in *A. thaliana*. Mutation in the genes encoding proteins interacting with cohesin (SWI1) and condensin (BRU1) could also be selected as homozygous. For *SMC1, SMC3, SCC3, SCC2, SMC4* and *CAP-H* only heterozygotes could be selected showing between 75-100% of wt transcript level. These proteins are essential for plant viability. *CAP-D2* and *CAP-G* mutants could not be analysed, as there were no suitable T-DNA lines available mutating these genes.

The confirmed mutant lines were transformed simultaneously with Pro35S-H2B-DsRed and Pro35S-EYFP-CenH3 to visualize the chromatin and the centromeres during mitosis and interphase, respectively. Very low expression frequencies of both fluorescence constructs were observed. The expression correlated negatively with the number of T-DNAs in the genome. Both fluorescence expression cassettes are identical in promoter and terminator, which leads to the suggestion that post-transcriptional gene-silencing occured. Afterwards the mutant lines were transformed only with Pro35S-H2B-YFP. The mutants were studied regarding the occurrence of disturbances in mitotic divisions and interphase in a life cell imaging approach. For further confirmation DAPI staining of untransformed seedlings was done to exclude an influence of the Pro35S-H2B-YFP transformation on cell divisions. Observations were similar after DAPI staining and Pro35S-H2B-YFP transformation.

Mutations in cohesin genes *SYN2, SYN3*, *SYN4* and *SCC3* resulted in an increased number of anaphase bridges, emphasizing the importance of these genes for correct nuclear division. Chromatid bridges in anaphase are the result of non-disjunction. This may occur if the homologous recombination (HR) repair mechanism is disturbed due to the lack of cohesin. After formation of double-strand breaks (DSBs), non-homologous end-joining is used for repair, which can lead to translocations. Asymmetric translocations result in dicentric and acentric fragments. Dicentric chromatids can be pulled towards opposite poles by the mitotic spindle and become visible as anaphase bridges.

Micronuclei were the result of disturbed mitoses in *syn2* and *syn4* mutants. The heterozygous *SMC1* and *SMC3* mutants showed nearly wt transcript level and did not differ significantly from wt in the occurrence of mitotic errors. Heterozygous *SYN1* mutants showed no significant increase in the frequency of anaphase bridges but homozygous mutants were sterile, confirming the meiotic function of SYN1.

Similar effects were observed in condensin mutants. Increased number of anaphase bridges were visible in *smc2, smc4/SMC4, cap-H/CAP-H and cap-H2* mutants. Condensin mutants impair the resolution of attatchments such as catenations between the sister chromatids prior to segregation. The complete cohesin removal from chromosomes and the recruitment of

Topoisomerase II (Top II) require condensins (reviewed by Hudson et al. 2009). Top II resolves catenations which impair correct segregation. Furthermore, sister chromatids in condensin mutants might twist around each other due to their incomplete condensation inhibiting correct disjunction in anaphase.

Plants mutated in genes encoding proteins interacting with cohesin (SWI1) and condensin (BRU1) and in the cohesin and condensin loading complex (SCC2/SCC4) showed severe disturbances in mitoses with anaphase bridge frequencies reaching from 20% (*bru1*) and ~23% (*SCC2/scc2*) up to ~44% in one single homozygous plant mutated in *SWI1*. The results indicate the necessity of every subunit of the cohesin and condensin complex and also the interacting proteins SWI1, BRU1 and SCC2 for nuclear divisions and plant viability.

With the 35 T-DNA lines analysed in this study, an overview is given about the possibilities to apply cytogenetic methods. But also the side-effects which can occur and may disturb the analysis like the silencing of fluorescence expression in T-DNA lines were observed.

6. Zusammenfassung

Schwesterchromatidenkohäsion, Chromosomenkondensation, DNA-Reparatur, Rekombination und Transkription sind unentbehrliche Prozesse für alle Eukaryoten. SMC (Structural Maintenance of Chromosomes) Eiweiß-Komplexe und Proteine, die mit ihnen interagieren, sind essentiell für diese Aufgaben (Nasmyth and Hearing, 2005.) Diese Arbeit befasst sich mit den zwei SMC-Komplexen Kohäsin und Kondensin und mit interagierenden Proteinen in *Arabidopsis thaliana*.

T-DNS Insertionsmutanten für alle putativen Kohäsin- und Kondensingene wurden bezüglich Habitus, Fruchtbarkeit, mRNA Expression und der Anzahl der T-DNS Kopien untersucht. Zusätzlich wurden drei Proteine, die mit dem Kohäsin- und/oder dem Kondensinkomplex interagieren, analysiert.

Kohäsinkomplexe bestehen aus den Untereinheiten SMC1, SMC3, SCC3 und einem der α-Kleisine SYN1-SYN4. SYN1 repräsentiert das Meiose-spezifische α-Kleisin (Bai et al. 1999; Bhatt et al. 1999; Cai et al. 2003). Kohäsinkomplexe realisieren insbesondere die Schwesterchromatidenkohäsion. Kondensine mit den Untereinheiten SMC2, SMC4, CAP-D2, CAP-G und dem β-Kleisin CAP-H2 oder dem γ-Kleisin CAP-H sind für die Kondensation der Chromosomen und deren Segregation in Mitose und Meiose verantwortlich (Nasmyth und Hearing 2005; Hirano und Hirano 2006).

Interaktionspartner für Kohäsine und Kondensine ist der SCC2/SCC4 Ladekomplex (Seitan et al. 2006; Watrin et al. 2006). SWITCH1 (SWI1) wird für die meiotische Schwesterchromatidenkohäsion benötigt (Mercier et al. 2001, 2003) und wurde deshalb in diese Studie mit einbezogen. Als Interaktionspartner für Kondensine wurde BRUSHY1 (BRU1) analysiert, da es an der Heterochromatinkondensation beteiligt ist (Takeda et al. 2004).

Die Selektion homozygoter Mutantenlinien war nur für die α-Kleisin Gene *SYN1*, *SYN2* und *SYN4* der Kohäsinkomplexe möglich. Mutationen in den entsprechenden Kondensingenen brachten homozygote Linien für *SMC2* hervor, da in *A. thaliana* zwei homologe Gene für SMC2 kodieren. Homozygote Mutationslinien konnten ebenfalls für *CAP-H2*, *SWI1* und BRU1 selektiert werden. Für *SMC1*, *SMC3*, *SCC3*, *SCC2*, *SMC4* und *CAP-H* konnten nur heterozygote Linien selektiert werden, welche 75-100% der Wildtyp-Expression zeigten. Diese Gene sind essentiell für das Überleben der Pflanze. *CAP-D2* und *CAP-G* Mutationen konnten nicht analysiert werden, da zum Zeitpunkt der Selektion keine entsprechenden T-DNA Insertionslinien erhältlich waren.

Die bestätigten Mutantionslinien wurden gleichzeitig mit Pro35S-H2B-DsRed und Pro35S-EYFP-CenH3 transformiert, um das Chromatin und die Zentromere wähend der Mitose und in der Interphase sichtbar zu machen. Es waren nur sehr geringe Co-Expressionsfrequenzen beider Konstrukte zu beobachten. Die Expression korrellierte negativ mit der Anzahl im Genom vorhandener T-DNAs. Da die Konstrukte der beiden Fluoreszenz-Expressionskassetten in Promoter und Terminator identisch sind, liegt die Vermutung nahe, dass Post-transkriptionelle Gen-Stillegung vorliegt. Die T-DNS Linien wurden anschliessend nur mit einem Chromatin-markierendem Konstrukt (Pro35S-H2B-YFP) transformiert. Die mutierten Pflanzen wurden in einem Lebend-Zell-Beobachtung Versuch bezüglich des Auftretens von Störungen in mitotischen Teilungen und in der Interphase untersucht. Zur weiteren Bestätigung der Ergebnisse wurden untransformierte Sämlinge der T-DNS Insertionslinien einer DAPI-Färbung unterzogen, um einen Einfluss der Transformation mit Pro35S-H2B-YFP auf die Zellteilungen auszuschliessen. Die Beobachtungen nach der DAPI-Färbung waren nahezu identisch mit denen nach der Transformation.

Die Folge der Mutationen in den Kohäsingenen *SYN2*, *SYN3*, *SYN4* und *SCC3* waren fehlerhafte Mitosen mit Anaphasebrücken. Dies zeigt die Bedeutung dieser Gene für eine korrekte Kernteilung. Chromatidenbrücken in der Zellteilung sind die Folge einer Nicht-Trennung der Schwesterchromatiden. Dies kann auf Grund eines gestörten Reparaturmechanismus bei der homologen Rekombination durch das Fehlen intakter

Kohäsinkomplexe auftreten. Nachdem Doppelstrangbrüche entstanden sind, werden diese mit Hilfe der nicht-homologen End-Verknüpfung geschlossen, was zu Translokationen führen kann. Asymmetrische Translokationen resultieren in dizentrische und azentrische Fragmente, welche zu beiden entgegengesetzten Polen der mitotischen Spindel gezogen werden können und als Anaphasebrücken sichtbar werden.

Mikrokerne waren das Ergebnis der gestörten Mitosen in den *syn2* und *syn4* Mutanten. Die heterozygoten *SMC1* und *SMC3* Mutanten zeigten nahezu das Expressions-Niveau der Wildtyppflanzen und zeigten entsprechend keine signifikanten Unterschiede im Auftreten von mitotischen Fehlern. Heterozygote *SYN1* Mutanten zeigten keinen signifikanten Anstieg der Anaphasebrückenfrequenz, aber homozygote Mutanten waren steril, was die meiotische Funktion von SYN1 bestätigt.

In Kondensin Mutanten wurden ähnliche Effekte beobachtet. Eine erhöhte Anzahl von Anaphasebrücken war in *smc2, smc4/SMC4, cap-H/CAP-H* und *cap-H2* Mutanten sichtbar. Das Auftreten von Chromatidenbrücken in den Kondensin Mutanten ist vermutlich auf eine fehlende Auflösung von Verbindungen wie z. B. Verkettungen zwischen den Schwesterchromatiden zurückzuführen. Kondensin wird für die Rekrutierung der Topoisomerase II und anderer Nicht-Histon-Proteine benötigt (Hudson et al. 2009). Desweiteren können sich die Schwesterchromatiden auf Grund der unvollständigen Kondensation in Mutanten ineinander verdrehen,so dass ihre korrekte Trennung in der Anaphase verhindert wird.

Fehlerhafte Mitosen wurden ausserdem in Pflanzen beobachtet, welche mutierte Gene aufwiesen, die für Kohäsin (SWI1) und Kondensin (BRU1) interagierende Proteine kodieren, sowie für den Köhäsin- und Kondensin Ladekomplex (SCC2/SCC4). Diese Ergebnisse zeigen die Notwendigkeit jeder einzelnen Untereinheit der Kohäsin- und Kondensin Komplexe, sowie der interagierenden Proteine SWI1, BRU1 und SCC2 für Kernteilungen und die Entwicklung der Pflanze.

Mit den 35 analysierten T-DNA Linien in dieser Studie wird ein Überblick über die Möglichkeiten der Anwendung zytogenetischer Methoden gegeben. Aber ebenso wurden Nebeneffekte verdeutlicht, welche auftreten und die Analyse stören können, wie die Verminderung der Fluoreszenz Expression in den T-DNS Linien.

7. Literature

Accotto GP, Vaira AM, Noris E, Vecchiati M (1998) Using non-radioactive probes on plants: a few examples. J Biolumin Chemilumin 13:295-301

Agashe B, Prasad CK, Siddiqi I (2002) Identification and analysis of DYAD: a gene required for meiotic chromosome organisation and female meiotic progression in *Arabidopsis*. Development 129:3935-3943

Alonso JM, Stepanova AN (2003) T-DNA mutagenesis in *Arabidopsis*. Methods Mol Biol 236:177-188

Alonso JM, Stepanova AN, Leisse TJ, Kim CJ, Chen H, Shinn P, Stevenson DK, Zimmerman J, Barajas P, Cheuk R, Gadrinab C, Heller C, Jeske A, Koesema E, Meyers CC, Parker H, Prednis L, Ansari Y, Choy N, Deen H, Geralt M, Hazari N, Hom E, Karnes M, Mulholland C, Ndubaku R, Schmidt I, Guzman P, Aguilar-Henonin L, Schmid M, Weigel D, Carter DE, Marchand T, Risseeuw E, Brogden D, Zeko A, Crosby WL, Berry CC, Ecker JR (2003) Genome-wide insertional mutagenesis of *Arabidopsis thaliana*. Science 301:653-657

Andrews EA, Palecek J, Sergeant J, Taylor E, Lehmann AR, Watts FZ (2005) Nse2, a component of the Smc5-6 complex, is a SUMO ligase required for the response to DNA damage. Mol Cell Biol 25:185-196

Austin C, Novikova N, Guacci V, Bellini M (2009) Lampbrush chromosomes enable study of cohesin dynamics. Chromosome Res 17:165-184

Bai X, Peirson BN, Dong F, Xue C, Makaroff CA (1999) Isolation and characterization of SYN1, a RAD21-like gene essential for meiosis in *Arabidopsis*. Plant Cell 11:417-430

Bausch C, Noone S, Henry JM, Gaudenz K, Sanderson B, Seidel C, Gerton JL (2007) Transcription alters chromosomal locations of cohesin in *Saccharomyces cerevisiae*. Mol Cell Biol 27:8522-8532

Bernard P, Maure JF, Partridge JF, Genier S, Javerzat JP, Allshire RC (2001) Requirement of heterochromatin for cohesion at centromeres. Science 294:2539-2542

Bernard P, Schmidt CK, Vaur S, Dheur S, Drogat J, Genier S, Ekwall K, Uhlmann F, Javerzat JP (2008) Cell-cycle regulation of cohesin stability along fission yeast chromosomes. EMBO J 27:111-121

Berr A, Pecinka A, Meister A, Kreth G, Fuchs J, Blattner FR, Lysak MA, Schubert I (2006) Chromosome arrangement and nuclear architecture but not centromeric sequences are conserved between *Arabidopsis thaliana* and *Arabidopsis lyrata*. Plant J 48:771-783

Bevis BJ, Glick BS (2002) Rapidly maturing variants of the *Discosoma* red fluorescent protein (DsRed). Nat Biotechnol 20:83-87

Bhatt AM, Lister C, Page T, Fransz P, Findlay K, Jones GH, Dickinson HG, Dean C (1999) The DIF1 gene of *Arabidopsis* is required for meiotic chromosome segregation and belongs to the REC8/RAD21 cohesin gene family. Plant Journal 19:463-472

Blat Y, Kleckner N (1999) Cohesins bind to preferential sites along yeast chromosome III, with differential regulation along arms versus the centric region. Cell 98:249-259

Boateng K, Makaroff C (2004) The effect of the dys10 mutation on pairing and chromatid cohesion during meiosis in *Arabidopsis thaliana*. Faseb Journal 18:C125-C125

Buchholz WG, Thomashow MF (1984) Comparison of T-DNA oncogene complements of *Agrobacterium tumefaciens* tumor-inducing plasmids with limited and wide host ranges. J Bacteriol 160:319-326

Butaye KM, Goderis IJ, Wouters PF, Pues JM, Delaure SL, Broekaert WF, Depicker A, Cammue BP, De Bolle MF (2004) Stable high-level transgene expression in *Arabidopsis thaliana* using gene silencing mutants and matrix attachment regions. Plant J 39:440-449

Cai X, Dong F, Edelmann RE, Makaroff CA (2003) The Arabidopsis SYN1 cohesin protein is required for sister chromatid arm cohesion and homologous chromosome pairing. J Cell Sci 116:2999-3007

Canudas S, Houghtaling BR, Kim JY, Dynek JN, Chang WG, Smith S (2007) Protein requirements for sister telomere association in human cells. EMBO J 26:4867-4878

Chalfie M, Tu Y, Euskirchen G, Ward WW, Prasher DC (1994) Green fluorescent protein as a marker for gene expression. Science 263:802-805

Chelysheva L, Diallo S, Vezon D, Gendrot G, Vrielynck N, Belcram K, Rocques N, Marquez-Lema A, Bhatt AM, Horlow C, Mercier R, Mezard C, Grelon M (2005) AtREC8 and AtSCC3 are essential to the monopolar orientation of the kinetochores during meiosis. J Cell Sci 118:4621-4632

Chen S, Li X, Liu X, Xu H, Meng K, Xiao G, Wei X, Wang F, Zhu Z (2005) Green fluorescent protein as a vital elimination marker to easily screen marker-free transgenic progeny derived from plants co-transformed with a double T-DNA binary vector system. Plant Cell Rep 23:625-631

Ciosk R, Shirayama M, Shevchenko A, Tanaka T, Toth A, Shevchenko A, Nasmyth K (2000) Cohesin's binding to chromosomes depends on a separate complex consisting of Scc2 and Scc4 proteins. Mol Cell 5:243-254

Clough SJ, Bent AF (1998) Floral dip: a simplified method for *Agrobacterium*-mediated transformation of *Arabidopsis thaliana*. Plant J 16:735-743

Cobbe N, Heck MMS (2000) SMCs in the world of chromosome biology - From prokaryotes to higher eukaryotes. Journal of Structural Biology 129:123-143

Cortes-Ledesma F, Aguilera A (2006) Double-strand breaks arising by replication through a nick are repaired by cohesin-dependent sister-chromatid exchange. EMBO Rep 7:919-926

Cortes-Ledesma F, de Piccoli G, Haber JE, Aragon L, Aguilera A (2007) SMC proteins, new players in the maintenance of genomic stability. Cell Cycle 6:914-918

Cremer T, Tesin D, Hopman AH, Manuelidis L (1988) Rapid interphase and metaphase assessment of specific chromosomal changes in neuroectodermal tumor cells by *in situ* hybridisation with chemically modified DNA probes. Exp Cell Res 176:199-220

Csankovszki G, Collette K, Spahl K, Carey J, Snyder M, Petty E, Patel U, Tabuchi T, Liu H, McLeod I, Thompson J, Sarkeshik A, Yates J, Meyer BJ, Hagstrom K (2009) Three distinct condensin complexes control *C. elegans* chromosome dynamics. Curr Biol 19:9-19

D'Ambrosio C, Kelly G, Shirahige K, Uhlmann F (2008a) Condensin-dependent rDNA decatenation introduces a temporal pattern to chromosome segregation. Curr Biol 18:1084-1089

D'Ambrosio C, Schmidt CK, Katou Y, Kelly G, Itoh T, Shirahige K, Uhlmann F (2008b) Identification of cis-acting sites for condensin loading onto budding yeast chromosomes. Genes Dev 22:2215-2227

da Costa-Nunes JA, Bhatt AM, O'Shea S, West CE, Bray CM, Grossniklaus U, Dickinson HG (2006) Characterization of the three *Arabidopsis thaliana* RAD21 cohesins reveals differential responses to ionizing radiation. J Exp Bot 57:971-983

Daxinger L, Hunter B, Sheikh M, Jauvion V, Gasciolli V, Vaucheret H, Matzke M, Furner I (2008) Unexpected silencing effects from T-DNA tags in *Arabidopsis*. Trends Plant Sci 13:4-6

Dej KJ, Ahn C, Orr-Weaver TL (2004) Mutations in the Drosophila condensin subunit dCAP-G: defining the role of condensin for chromosome condensation in mitosis and gene expression in interphase. Genetics 168:895-906

Diaz-Martinez LA, Gimenez-Abian JF, Clarke DJ (2008) Chromosome cohesion - rings, knots, orcs and fellowship. J Cell Sci 121:2107-2114

Diaz-Pendon JA, Li F, Li WX, Ding SW (2007) Suppression of antiviral silencing by cucumber mosaic virus 2b protein in *Arabidopsis* is associated with drastically reduced accumulation of three classes of viral small interfering RNAs. Plant Cell 19:2053-2063

Dietrich C, Maiss E (2002) Red fluorescent protein DsRed from *Discosoma sp.* as a reporter protein in higher plants. Biotechniques 32:286, 288-290, 292-283

Dong F, Cai X, Makaroff CA (2001) Cloning and characterization of two *Arabidopsis* genes that belong to the RAD21/REC8 family of chromosome cohesin proteins. Gene 271:99-108

Dorsett D (2007) Roles of the sister chromatid cohesion apparatus in gene expression, development, and human syndromes. Chromosoma 116:1-13

Ellendorff U, Zhang Z, Thomma BPHJ (2008) Gene silencing to investigate the roles of receptor-like proteins in *Arabidopsis*. Plant Signaling & Behavior 3:10, 893-896

Fagan T (1996) Quickbasic program for exact and mid-P confidence intervals for a binomial proportion. Comput Biol Med 26:263-267

Freeman L, Aragon-Alcaide L, Strunnikov A (2000) The condensin complex governs chromosome condensation and mitotic transmission of rDNA. J Cell Biol 149:811-824

Fujimoto S, Yonemura M, Matsunaga S, Nakagawa T, Uchiyama S, Fukui K (2005) Characterization and dynamic analysis of *Arabidopsis* condensin subunits, AtCAP-H and AtCAP-H2. Planta 222:293-300

Gause M, Schaaf CA, Dorsett D (2008) Cohesin and CTCF: cooperating to control chromosome conformation? Bioessays 30:715-718

Gerlich D, Hirota T, Koch B, Peters JM, Ellenberg J (2006) Condensin I stabilises chromosomes mechanically through a dynamic interaction in live cells. Curr Biol 16:333-344

Gloyd M, Ghirlando R, Matthews LA, Guarne A (2007) MukE and MukF form two distinct high affinity complexes. J Biol Chem 282:14373-14378

Glynn EF, Megee PC, Yu HG, Mistrot C, Ünal E, Koshland DE, DeRisi JL, Gerton JL (2004) Genome-wide mapping of the cohesin complex in the yeast *Saccharomyces cerevisiae*. Plos Biology 2:1325-1339

Gonzalez-Barrera S, Cortes-Ledesma F, Wellinger RE, Aguilera A (2003) Equal sister chromatid exchange is a major mechanism of double-strand break repair in yeast. Mol Cell 11:1661-1671

Gorbunova VV, Levy AA (1999) How plants make ends meet: DNA double-strand break repair. Trends Plant Sci 4:263-269

Gullerova M, Proudfoot NJ (2008) Cohesin complex promotes transcriptional termination between convergent genes in *S. pombe*. Cell 132:983-995

Hamilton A, Voinnet O, Chappell L, Baulcombe D (2002) Two classes of short interfering RNA in RNA silencing. EMBO J 21: 4671–4679

Hartl TA, Sweeney SJ, Knepler PJ, Bosco G (2008) Condensin II resolves chromosomal associations to enable anaphase I segregation in *Drosophila* male meiosis. PLoS Genet 4:e1000228

Hartman T, Stead K, Koshland D, Guacci V (2000) Pds5p is an essential chromosomal protein required for both sister chromatid cohesion and condensation in *Saccharomyces cerevisiae.* J Cell Biol 151:613–626

Heidmann D, Horn S, Heidmann S, Schleiffer A, Nasmyth K, Lehner CF (2004) The *Drosophila* meiotic kleisin C(2)M functions before the meiotic divisions. Chromosoma 113:177-187

Hirano M, Anderson DE, Erickson HP, Hirano T (2001) Bimodal activation of SMC ATPase by intra- and inter-molecular interactions. EMBO J 20:3238-3250

Hirano M, Hirano T (2006) Opening closed arms: Long-distance activation of SMC ATPase by hinge-DNA interactions. Molecular Cell 21:175-186

Hirano T, Funahashi SI, Uemura T, Yanagida M (1986) Isolation and characterization of *Schizosaccharomyces pombe* cutmutants that block nuclear division but not cytokinesis. EMBO J 5:2973-2979

Hirano T, Kobayashi R, Hirano M (1997) Condensins, chromosome condensation protein complexes containing XCAP-C, XCAP-E and a *Xenopus* homolog of the *Drosophila* Barren protein. Cell 89:511-521

Hirano T (2005) Condensins: organizing and segregating the genome. Curr Biol 15:R265-275

Hirano T (2006) At the heart of the chromosome: SMC proteins in action. Nat Rev Mol Cell Biol 7:311-322

Hirota T, Gerlich D, Koch B, Ellenberg J, Peters JM (2004) Distinct functions of condensin I and II in mitotic chromosome assembly. J Cell Sci 117:6435-6445

Hudson DF, Marshall KM, Earnshaw WC (2009) Condensin: Architect of mitotic chromosomes. Chromosome Res 17:131-144

Jiang L, Xia M, Strittmatter LI, Makaroff CA (2007) The *Arabidopsis* cohesin protein SYN3 localises to the nucleolus and is essential for gametogenesis. Plant J 50:1020-1034

Johnson RD, Jasin M (2000) Sister chromatid gene conversion is a prominent double-strand break repair pathway in mammalian cells. EMBO J 19:3398-3407

Kadyk LC, Hartwell LH (1992) Sister chromatids are preferred over homologs as substrates for recombinational repair in *Saccharomyces cereviseae*. Genetics 132:387-402

Kim PM, Allen C, Wagener BM, Shen Z, Nickoloff JA (2001) Overexpression of human RAD51 and RAD52 reduces double-strand break-induced homologous recombination in mammalian cells. Nucleic Acids Res. 29:4352-60

Kim JS, Krasieva TB, LaMorte V, Taylor AM, Yokomori K (2002) Specific recruitment of human cohesin to laser-induced DNA damage. J. Biol. Chem. 277:45149-45153

Kimura K, Cuvier O, Hirano T (2001) Chromosome condensation by a human condensin complex in *Xenopus* egg extracts. J Biol Chem 276:5417-5420

Komari T, Hiei Y, Saito Y, Murai N, Kumashiro T (1996) Vectors carrying two separate T-DNAs for co-transformation of higher plants mediated by *Agrobacterium tumefaciens* and segregation of transformants free from selection markers. Plant J 10:165-174

Kueng S, Hegemann B, Peters BH, Lipp JJ, Schleiffer A, et al. (2006) Wapl controls the dynamic association of cohesin with chromatin. Cell 127:955–967

Kuhlmann M, Popova B, Nellen W (2006) RNA interference and antisense-mediated gene silencing in *Dictyostelium*. Methods Mol Biol. 346:211-26

Kurihara D, Matsunaga S, Uchiyama S, Fukui K (2008) Live cell imaging reveals plant aurora kinase has dual roles during mitosis. Plant Cell Physiol 49:1256-1261

Laloraya S, Guacci V, Koshland D (2000) Chromosomal addresses of the cohesin component Mcd1p. Journal of Cell Biology 151:1047-1056

Lam WS, Yang X, Makaroff CA (2005) Characterization of *Arabidopsis thaliana* SMC1 and SMC3: evidence that AtSMC3 may function beyond chromosome cohesion. J Cell Sci 118:3037-3048

Lee JY and Orr-Weaver TL (2001) The molecular basis of sister-chromatid cohesion. Annu Rev Cell Dev Bio. 17:753-777

Leitch AR, Mosgoller W, Schwarzacher T, Bennett MD, Heslop-Harrison JS (1990) Genomic *in situ* hybridisation to sectioned nuclei shows chromosome domains in grass hybrids. J Cell Sci 95 Pt 3:335-341

Lengronne A, Katou Y, Mori S, Yokobayashi S, Kelly GP, Itoh T, Watanabe Y, Shirahige K, Uhlmann F (2004) Cohesin relocation from sites of chromosomal loading to places of convergent transcription. Nature 430:573-578

Levitt JA, Matthews DR, Ameer-Beg SM, Suhling K (2009) Fluorescence lifetime and polarization-resolved imaging in cell biology. Curr Opin Biotechnol 20:28-36

Liu CM, McElver J, Tzafrir I, Joosen R, Wittich P, Patton D, Van Lammeren AA, Meinke D (2002) Condensin and cohesin knockouts in *Arabidopsis* exhibit a titan seed phenotype. Plant J 29:405-415

Liu Z, Makaroff CA (2006) *Arabidopsis* Separase AESP Is Essential for Embryo Development and the Release of Cohesin during Meiosis. Plant Cell 18:1213-1225

Losada A, Hirano T (2005) Dynamic molecular linkers of the genome: the first decade of SMC proteins. Genes Dev 19:1269-1287

Losada A (2007) Cohesin regulation: fashionable ways to wear a ring. Chromosoma 116:321-329

Maguire MP (1990) Sister chromatid cohesiveness: vital function, obscure mechanism. Biochem. Cell Biol. 68:1231-1242

Manuelidis L (1985) Individual interphase chromosome domains revealed by *in situ* hybridisation. Hum Genet 71:288-293

Mascarenhas J, Soppa J, Strunnikov AV, Graumann PL (2002) Cell cycle-dependent localisation of two novel prokaryotic chromosome segregation and condensation proteins in *Bacillus subtilis* that interact with SMC protein. EMBO J 21:3108-3118

Mascarenhas J, Volkov AV, Rinn C, Schiener J, Guckenberger R, Graumann PL (2005) Dynamic assembly, localisation and proteolysis of the *Bacillus subtilis* SMC complex. BMC Cell Biol 6:28

Matz MV, Fradkov AF, Labas YA, Savitsky AP, Zaraisky AG, Markelov ML, Lukyanov SA (1999) Fluorescent proteins from nonbioluminescent Anthozoa species. Nat Biotechnol 17:969-973

Matzke M, Matzke AJ (2003) RNAi extends its reach. Science 301:1060-1061

McClintock B (1953) Induction of Instability at Selected Loci in Maize. Genetics 38:579-599

McDonald WH, Pavlova Y, Yates JR, 3rd, Boddy MN (2003) Novel essential DNA repair proteins Nse1 and Nse2 are subunits of the fission yeast Smc5-Smc6 complex. J Biol Chem 278:45460-45467

McNairn AJ, Gerton JL (2008) The chromosome glue gets a little stickier. Trends Genet 24:382-389

Melby TE, Ciampaglio CN, Briscoe G, Erickson HP (1998) The symmetrical structure of structural maintenance of chromosomes (SMC) and MukB proteins: long, antiparallel coiled coils, folded at a flexible hinge. J Cell Biol 142:1595-1604

Mercier R, Vezon D, Bullier E, Motamayor JC, Sellier A, Lefevre F, Pelletier G, Horlow C (2001) SWITCH1 (SWI1): a novel protein required for the establishment of sister chromatid cohesion and for bivalent formation at meiosis. Genes & Development 15:1859-1871

Mercier R, Armstrong SJ, Horlow C, Jackson NP, Makaroff CA, Vezon D, Pelletier G, Jones GH, Franklin FC (2003) The meiotic protein SWI1 is required for axial element formation and recombination initiation in *Arabidopsis*. Development 130:3309-3318

Mette MF, van der Winden J, Matzke M, Matzke A (1999) Production of aberrant promoter transcripts contributes to methylation and silencing of unlinked homologous promoters *in trans*. EMBO J 18: 241–248

Mette MF, Aufsatz W, van der Winden J, Matzke M, Matzke A (2000) Transcriptional gene silencing and promoter methylation triggered by double-stranded RNA. EMBO J 19: 5194–5201

Mikkelsen L, Sarrocco S, Lubeck M, Jensen DF (2003) Expression of the red fluorescent protein DsRed-Express in filamentous ascomycete fungi. FEMS Microbiol Lett 223:135-139

Misulovin Z, Schwartz YB, Li XY, Kahn TG, Gause M, MacArthur S, Fay JC, Eisen MB, Pirrotta V, Biggin MD, Dorsett D (2008) Association of cohesin and Nipped-B with transcriptionally active regions of the *Drosophila melanogaster* genome. Chromosoma 117:89-102

Mito Y, Sugimoto A, Yamamoto M (2003) Distinct developmental function of two *Caenorhabditis elegans* homologs of the cohesin subunit Scc1/Rad21. Mol Biol Cell 14:2399-2409

Miyazaki WY, Orr-Weaver TL (1994) Sister-chromatid cohesion in mitosis and meiosis. Annu Rev Genet 28:167-187

Moriya S, Tsujikawa E, Hassan AK, Asai K, Kodama T, Ogasawara N (1998) A *Bacillus subtilis* gene-encoding protein homologous to eukaryotic SMC motor protein is necessary for chromosome partition. Mol Microbiol 29:179-187

Murashige T and Skoog F (1962) A revised medium for rapid growth and bioassays with tobacco tissue cultures. Physiol Plant 15: 473-497

Murray JM, Carr AM (2008) Smc5/6: a link between DNA repair and unidirectional replication? Nat Rev Mol Cell Biol 9:177-182

Nasmyth K (2001) Disseminating the genome: Joining, resolving, and separating sister chromatids during mitosis and meiosis. Annual Review of Genetics 35:673-745

Nasmyth K, Haering CH (2005) The structure and function of smc and kleisin complexes. Annu Rev Biochem 74:595-648

Niki H, Jaffe A, Imamura R, Ogura T, Hiraga S (1991) The new gene mukB codes for a 177 kd protein with coiled-coil domains involved in chromosome partitioning of E. coli. EMBO J 10:183-193

Ocampo-Hafalla MT, Katou Y, Shirahige K, Uhlmann F (2007) Displacement and re-accumulation of centromeric cohesin during transient pre-anaphase centromere splitting. Chromosoma 116:531-544

Onn I, Heidinger-Pauli JM, Guacci V, Unal E, Koshland DE (2008) Sister chromatid cohesion: a simple concept with a complex reality. Annu Rev Cell Dev Biol 24:105-129

Ono T, Losada A, Hirano M, Myers MP, Neuwald AF, Hirano T (2003) Differential contributions of condensin I and condensin II to mitotic chromosome architecture in vertebrate cells. Cell 115:109-121

Ono T, Fang Y, Spector DL, Hirano T (2004) Spatial and temporal regulation of Condensins I and II in mitotic chromosome assembly in human cells. Mol Biol Cell 15:3296-3308

Pacher M, Schmidt-Puchta W, Puchta H (2007) Two unlinked double-strand breaks can induce reciprocal exchanges in plant genomes via homologous recombination and nonhomologous end joining. Genetics 175:21-29

Palecek J, Vidot S, Feng M, Doherty AJ, Lehmann AR (2006) The Smc5-Smc6 DNA repair complex. bridging of the Smc5-Smc6 heads by the KLEISIN, Nse4, and non-Kleisin subunits. J Biol Chem 281:36952-36959

Palmer DK, O'Day K, Wener MH, Andrews BS, Margolis RL (1987) A 17-kD centromere protein (CENP-A) copurifies with nucleosome core particles and with histones. J Cell Biol 104:805-815

Parelho V, Hadjur S, Spivakov M, Leleu M, Sauer S, Gregson HC, Jarmuz A, Canzonetta C, Webster Z, Nesterova T, Cobb BS, Yokomori K, Dillon N, Aragon L, Fisher AG, Merkenschlager M (2008) Cohesins functionally associate with CTCF on mammalian chromosome arms. Cell 132:422-433

Pasierbek P, Jantsch M, Melcher M, Schleiffer A, Schweizer D, Loidl J (2001) A *Caenorhabditis elegans* cohesion protein with functions in meiotic chromosome pairing and disjunction. Genes & Development 15:1349-1360

Pebernard S, McDonald WH, Pavlova Y, Yates JR, Boddy MN (2004) Nse1, Nse2, and a novel subunit of the Smc5-Smc6 complex, Nse3, play a crucial role in meiosis. Molecular Biology of the Cell 15:4866-4876

Pebernard S, Wohlschlegel J, McDonald WH, Yates JR, 3rd, Boddy MN (2006) The Nse5-Nse6 dimer mediates DNA repair roles of the Smc5-Smc6 complex. Mol Cell Biol 26:1617-1630

Pecinka A, Schubert V, Meister A, Kreth G, Klatte M, Lysak MA, Fuchs J, Schubert I (2004) Chromosome territory arrangement and homologous pairing in nuclei of *Arabidopsis thaliana* are predominantly random except for NOR-bearing chromosomes. Chromosoma 113:258-269

Potts PR, Porteus MH, Yu H (2006) Human SMC5/6 complex promotes sister chromatid homologous recombination by recruiting the SMC1/3 cohesin complex to double-strand breaks. EMBO J 25:3377-3388

Puchta H (2005) The repair of double-stand breaks in plants: mechanisms and consequences for genome evolution. J Exp Bot 56:1-14

Radchuk V, Van D, Klocke E (2005) Multiple gene co-integration in *Arabidopsis thaliana* predominantly occurs in the same genetic locus after simultaneous in planta transformation with distinct *Agrobacterium tumefaciens* strains. Plant Science 168:1515-1523

Reddy GV, Roy-Chowdhury A (2009) Live-Imaging and Image Processing of Shoot Apical Meristems of *Arabidopsis thaliana*. Methods Mol Biol 553:305-316

Ribeiro SA, Gatlin JC, Dong Y, Joglekar A, Cameron L, Hudson DF, Farr CJ, McEwen BF, Salmon ED, Earnshaw WC, Vagnarelli P (2009) Condensin regulates the stiffness of vertebrate centromeres. Mol Biol Cell 20:2371-2380

Rodrigues F, van Hemert M, Steensma HY, Corte-Real M, Leao C (2001) Red fluorescent protein (DsRed) as a reporter in *Saccharomyces cerevisiae*. J Bacteriol 183:3791-3794

Rosso MG, Li Y, Strizhov N, Reiss B, Dekker K, Weisshaar B (2003) An *Arabidopsis thaliana* T-DNA mutagenized population (GABI-Kat) for flanking sequence tag-based reverse genetics. Plant Mol Biol 53:247-259

Rudnik R (2009) Die Zink-Finger Proteine C2H2 und REF6 stabilisieren die Chromatinstruktur in Interphase-Kernen von *Arabidopsis thaliana.* Diplomarbeit Universität Kassel: 93 Seiten

Savvidou E, Cobbe N, Steffensen S, Cotterill S, Heck MM (2005) *Drosophila* CAP-D2 is required for condensin complex stability and resolution of sister chromatids. J Cell Sci 118:2529-2543

Schmiesing JA, Gregson HC, Zhou S, Yokomori K (2000) A human condensin complex containing hCAP-C-hCAP-E and CNAP1, a homolog of *Xenopus* XCAP-D2, colocalises with phosphorylated histone H3 during the early stage of mitotic chromosome condensation. Mol Cell Biol 20:6996-7006

Schubert I, Pecinka A, Meister A, Schubert V, Klatte M, Jovtchev G (2004) DNA damage processing and aberration formation in plants. Cytogenet Genome Res 104:104-108

Schubert V, Klatte M, Pecinka A, Meister A, Jasencakova Z, Schubert I (2006) Sister chromatids are often incompletely aligned in meristematic and endopolyploid interphase nuclei of *Arabidopsis thaliana*. Genetics 172:467-475

Schubert V, Kim YM, Berr A, Fuchs J, Meister A, Marschner S, Schubert I (2007) Random homologous pairing and incomplete sister chromatid alignment are common in angiosperm interphase nuclei. Mol Genet Genomics 278:167-176

Schubert V, Kim YM, Schubert I (2008) *Arabidopsis* sister chromatids often show complete alignment or separation along a 1.2-Mb euchromatic region but no cohesion "hot spots". Chromosoma 117:261-266

Schubert V (2009) SMC proteins and their multiple functions in higher plants. Cytogenet Genome Res 124:202-214

Schubert V, Weißleder A, Ali H, Fuchs J, Lermontova I, Meister A, Schubert I (2009) Cohesin gene defects may impair sister chromatid alignment and genome stability in *Arabidopsis thaliana*. Chromosoma 118:591-605

Sebastian J, Ravi M, Andreuzza S, Panoli AP, Marimuthu MP, Siddiqi I (2009) The plant adherin AtSCC2 is required for embryogenesis and sister-chromatid cohesion during meiosis in *Arabidopsis*. Plant J doi: 10.1111/j.1365-313X.2009.03845.x

Seitan VC, Banks P, Laval S, Majid NA, Dorsett D, Rana A, Smith J, Bateman A, Krpic S, Hostert A, Rollins RA, Erdjument-Bromage H, Tempst P, Benard CY, Hekimi S, Newbury SF, Strachan T (2006) Metazoan Scc4 homologs link sister chromatid cohesion to cell and axon migration guidance. PLoS Biol 4:e242

Sergeant J, Taylor E, Palecek J, Fousteri M, Andrews EA, Sweeney S, Shinagawa H, Watts FZ, Lehmann AR (2005) Composition and architecture of the *Schizosaccharomyces pombe* Rad18 (Smc5-6) complex. Mol Cell Biol 25:172-184

Sheen J, Hwang S, Niwa Y, Kobayashi H, Galbraith DW (1995) Green-fluorescent protein as a new vital marker in plant cells. Plant J 8:777-784

Siddiqui NU, Stronghill PE, Dengler RE, Hasenkampf CA, Riggs CD (2003) Mutations in *Arabidopsis* condensin genes disrupt embryogenesis, meristem organisation and segregation of homologous chromosomes during meiosis. Development 130:3283-3295

Siddiqui NU, Rusyniak S, Hasenkampf CA, Riggs CD (2006) Disruption of the *Arabidopsis* SMC4 gene, AtCAP-C, compromises gametogenesis and embryogenesis. Planta 223:990-997

Sjögren C, Nasmyth K (2001) Sister chromatid cohesion is required for postreplicative double-strand break repair in Saccharomyces cerevisiae. Curr Biol. 11:991-995

Skibbens RV, Corson LB, Koshland D, Hieter P (1999) Ctf7p is essential for sister chromatid cohesion and links mitotic chromosome structure to the DNA replication machinery. Genes Dev 13:307–319

Southern EM (1975) Detection of specific sequences among DNA fragments separated by gel electrophoresis. J Mol Biol 98:503-517

Stedman W, Kang H, Lin S, Kissil JL, Bartolomei MS, Lieberman PM (2008) Cohesins localise with CTCF at the KSHV latency control region and at cellular c-myc and H19/Igf2 insulators. EMBO J 27:654-666

Ström L, Lindroos HB, Shirahige K, Sjogren C (2004) Postreplicative recruitment of cohesin to double-strand breaks is required for DNA repair. Molecular Cell 16:1003-1015

Ström L, Karlsson C, Lindroos HB, Wedahl S, Katou Y, Shirahige K, Sjogren C (2007) Postreplicative formation of cohesion is required for repair and induced by a single DNA break. Science 317:242-245

Ström L, Sjogren C (2007) Chromosome segregation and double-strand break repair - a complex connection. Curr Opin Cell Biol 19:344-349

Sutani T, Yuasa T, Tomonaga T, Dohmae N, Takio K, Yanagida M (1999) Fission yeast condensin complex: essential roles of non-SMC subunits for condensation and Cdc2 phosphorylation of Cut3/SMC4. Genes Dev 13:2271-2283

Takahashi N, Quimbaya M, Schubert V, Lammens T, Vandepoele K, Schubert I, Matsui M, Inzé D, Berx G, De Veylder L (submitted) The MCM-binding protein ETG1 aids sister chromatid cohesion for postreplicative DNA repair. PLoS Genet

Takeda S, Tadele Z, Hofmann I, Probst AV, Angelis KJ, Kaya H, Araki T, Mengiste T, Mittelsen Scheid O, Shibahara K, Scheel D, Paszkowski J (2004) BRU1, a novel link between responses to DNA damage and epigenetic gene silencing in *Arabidopsis*. Genes Dev 18:782-793

Talbert PB, Masuelli R, Tyagi AP, Comai L, Henikoff S (2002) Centromeric localisation and adaptive evolution of an *Arabidopsis* histone H3 variant. Plant Cell 14:1053-1066

Tanaka T, Cosma MP, Wirth K, Nasmyth K (1999) Identification of cohesin association sites at centromeres and along chromosome arms. Cell 98:847-858

Tao J, Zhang L, Chong K, Wang T (2007) OsRAD21-3, an orthologue of yeast RAD21, is required for pollen development in Oryza sativa. Plant J 51:919-930

Toth A, Ciosk R, Uhlmann F, Galova M, Schleiffer A, Nasmyth K (1999) Yeast cohesin complex requires a conserved protein, Eco1p(Ctf7), to establish cohesion between sister chromatids during DNA replication. Genes Dev 13:320-333

Traut (1991) Chromosomen Klassische und Molekulare Cytogenetik. Springer-Verlag, Berlin Heidelberg New York

Tsien RY (1998) The green fluorescent protein. Annu Rev Biochem 67:509-544

Tzafrir I, McElver JA, Liu Cm CM, Yang LJ, Wu JQ, Martinez A, Patton DA, Meinke DW (2002) Diversity of TITAN functions in *Arabidopsis* seed development. Plant Physiol 128:38-51

Uhlmann F (2007) What is your assay for sister-chromatid cohesion? EMBO J 26:4609-4618

Uhlmann F (2008) Molecular biology: cohesin branches out. Nature 451:777-778

Ülker B, Li Y, Rosso MG, Logemann E, Somssich IE, Weisshaar B (2008) T-DNA-mediated transfer of *Agrobacterium tumefaciens* chromosomal DNA into plants. Nat Biotechnol 26:1015-1017

Ünal E, Arbel-Eden A, Sattler U, Shroff R, Lichten M, Haber JE, Koshland D (2004) DNA damage response pathway uses histone modification to assemble a double-strand break-specific cohesin domain. Molecular Cell 16:991-1002

Vagnarelli P, Hudson DF, Ribeiro SA, Trinkle-Mulcahy L, Spence JM, Lai F, Farr CJ, Lamond AI, Earnshaw WC (2006) Condensin and Repo-Man-PP1 co-operate in the regulation of chromosome architecture during mitosis. Nat Cell Biol 8:1133-1142

Vass S, Cotterill S, Valdeolmillos AM, Barbero JL, Lin E, Warren WD, Heck MM (2003) Depletion of Drad21/Scc1 in *Drosophila* cells leads to instability of the cohesin complex and disruption of mitotic progression. Curr Biol 13:208-218

Verdel A, Vavasseur A, Le Gorrec M, Touat-Todeschini L (2009) Common themes in siRNA-mediated epigenetic silencing pathways. Int. J. Dev. Biol. 53: 245-257

Wassenegger M, Krczal G (2006) Nomenclature and functions of RNA-directed RNA polymerases. Trends Plant Sci 11:142-151

Watanabe K, Pacher M, Dukowic S, Schubert V, Puchta H, Schubert I (2009) The Structural Maintenance of Chromosomes 5/6 Complex Promotes Sister Chromatid Alignment and Homologous Recombination after DNA Damage in *Arabidopsis thaliana.* Plant Cell www.plantcell.org/cgi/doi/10.1105/tpc.108.060525

Watrin E, Peters JM (2006) Cohesin and DNA damage repair. Exp Cell Res 312:2687-2693

Weber SA, Gerton JL, Polancic JE, DeRisi JL, Koshland D, Megee PC (2004) The kinetochore is an enhancer of pericentric cohesin binding. Plos Biology 2:1340-1353

Wendt KS, Peters JM (2009) How cohesin and CTCF cooperate in regulating gene expression. Chromosome Res 17:201-214

Wendt KS, Yoshida K, Itoh T, Bando M, Koch B, Schirghuber E, Tsutsumi S, Nagae G, Ishihara K, Mishiro T, Yahata K, Imamoto F, Aburatani H, Nakao M, Imamoto N, Maeshima K, Shirahige K, Peters JM (2008) Cohesin mediates transcriptional insulation by CCCTC-binding factor. Nature 451:796-801

Yamanaka K, Ogura T, Niki H, Hiraga S (1996) Identification of two new genes, mukE and mukF, involved in chromosome partitioning in *Escherichia coli*. Mol Gen Genet 250:241-251

Yamazoe M, Onogi T, Sunako Y, Niki H, Yamanaka K, Ichimura T, Hiraga S (1999) Complex formation of MukB, MukE and MukF proteins involved in chromosome partitioning in *Escherichia coli*. EMBO J 18:5873-5884

Yeh E, Haase J, Paliulis LV, Joglekar A, Bond L, Bouck D, Salmon ED, Bloom KS (2008) Pericentric chromatin is organised into an intramolecular loop in mitosis. Curr Biol 18:81-90

Yeong FM, Hombauer H, Wendt KS, Hirota T, Mudrak I, Mechtler K, Loregger T, Marchler-Bauer A, Tanaka K, Peters JM, Ogris E (2003) Identification of a subunit of a novel Kleisin-beta/SMC complex as a potential substrate of protein phosphatase 2A. Curr Biol 13:2058-2064

Yong-Gonzalez V, Wang BD, Butylin P, Ouspenski I, Strunnikov A (2007) Condensin function at centromere chromatin facilitates proper kinetochore tension and ensures correct mitotic segregation of sister chromatids. Genes Cells 12:1075-1090

Zhang LR, Tao JY, Wang T (2004) Molecular characterization of OsRAD21-1, a rice homologue of yeast RAD21 essential for mitotic chromosome cohesion. Journal of Experimental Botany 55:1149-1152

Zhang T, Lim HH, Cheng CS, Surana U (2006) Deficiency of centromere-associated protein Slk19 causes premature nuclear migration and loss of centromeric elasticity. J Cell Sci 119:519-531

Zhang B, Chang J, Fu M, Huang J, Kashyap R, et al. (2009) Dosage Effects of Cohesin Regulatory Factor PDS5 on Mammalian Development: Implications for Cohesinopathies. PLoS ONE 4(5): e5232. doi:10.1371/journal.pone.0005232

Zilberman D, Cao X, Jacobsen S (2003) Argonaute4 control of locusspecific siRNA accumulation and DNA and histone methylation. Science 299: 716–719

8. Appendix

Gene	Locus	T-DNA insertion line	Primer	Sequence (5' - 3')
			SALK_LBb1	TGGTTCACGTAGTGGGCCATCG
			GABI_LB	CCCATTTGGACGTGAATGTAGACAC
SMC1	AT3G54670	SALK_017437	Co1	TCTTCTTGCTTGAGTTTTTGTGGTG
			Co2	AAAGTTCTCCCTGGTGAGGTGC
		GABI_269E12	Co3	GGACGTGGTAGAGTCTAAGGC
			Co4	CAGGCAAGGAGAGATTGAAAC
SMC3	AT2G27170	SALK_015308	Co5	TTTCAATTTGTATAGCACCCAAG
			Co6	GCTACTGAGGAGTTTAGCAACAAAG
		GABI_498B03	Co7	GGTCAGCCAATTAAATTAGGC
			Co8	TCCAATATGCATCACTCCAAAC
		SALK_087935	Co9	TGCCTTAGTTCGTGCAACTTC
			Co10	TCTTTGCCATTGCCCTATTTC
SYN1	AT5G05490	SALK_137095	Co11	TCTGCTCTGTTCACGAAGCTC
			Co12	TGACGTGTAACCTATGGGCTG
		SALK_006687	Co13	ACCAGCGAAAAAGAGAGCAAG
			Co14	AGGCATGGATCTCACATCATC
SYN2	AT5G40840	SALK_015096	Co15	TTCACCTGCTGAAGCAGAAAC
			Co16	AGATTCGTCTGCAGAGTTCCG
		SALK_044851	Co17	AAAACTTCGAAAAGGATTGGC
			Co18	GATGACATTCTTCTGGAACCG
SYN3	AT3G59550	SALK_119629	Co19	TCCTTGATCTCATGGATTTGC
			Co20	TGGATCAAAAAGCGAAAATTG
		GABI_095A10	Co21	CAGATCAAATTCCTACTGGCATTG
			Co22	CTAGGGATAGTGGGTTCCTTCTCA
SYN4	AT5G16270	SALK_076116	Co23	ACCCAAATGATTGTGAGGAGC
			Co24	GCACTAGCAGCATCTCGTATCC
		SALK_130085	Co23	ACCCAAATGATTGTGAGGAGC
			Co24	GCACTAGCAGCATCTCGTATCC
		SALK_020171	Co25	ATGATTGTGAGGAGCAACCTG
			Co26	AACCATTGAGAAATCATCGGG
SCC3	AT2G47980	SALK_021769	Co27	AGACTCTCCCAGCCTTGCTAC
			Co28	CAAATGCCCAGAGACTGAATG

Supplementary Table 1: PCR primers used to identify the T-DNA insertion alleles of the cohesin complex. SALK lines were genotyped with left border primer LBb1 and GABI lines with the respective left border primer from GABI.

Gene Locus	T-DNA insertion line	Sequence (5' - 3')
SMC1 AT3G54670	SALK_017437	TCTAAGCGTCAATTTGGAATTAGAAGACTCTATTTTATTC
	GABI_269E12	ACCACAATATATCCTGCAACTTCAGGTTCTAAGCTCTCAC
SMC3 AT2G27170	SALK_015308	GCAGTGAAGATAGGCATGCATTAACTTTAATATTCAGGATTTA
	GABI_498B03	TAGATTTCCCGGACATGAAATACAGAATGATGCACTTGAGC
	SALK_087935	TCTGCTAAAAGAGATAGACGCTTAGACAACTTAATAACACA
SYN1 AT5G05490	SALK_137095	GCTGATGCCGAGAATATTGTGGTGTAAACAAATTGACGCTT
	SALK_006687	ATGATGTGAGTCCATGCCACATTGCAGCCGTTCGTCTGTTT
SYN2 AT5G40840	SALK_015096	ATCAAGCTTAAAAACTGGGCAAATTACTAACAAGTTAATAA
	SALK_044851	CTGGTTCCAGAGACTTGCAAATTGACAATGTGATATTGTGGT
SYN3 AT3G59550	GABI_095A10	GAGAAATTGATGTTGAAACGGCTTCATGTCCGGGAAATCTACA
	SALK_119629	AAAACGTCCGCAATGTGTTCTTCCTCTCTCCAAAAGCACACAA
SYN4 AT5G16270	SALK_076116	ATGTGTTATAAGCGTCAGTTGGAGGCGTCTATGCAGATGGA
	SALK_130085	ATTAAGTTGTCTAAGCGTCAGTTGGAGGCG TGCATTACATG
	SALK_020171	GTCAATTTGTCTCCAATGTGTTATGGAGAGCATACTTCTCGT
SCC3 AT2G47980	SALK_021769	AAGTTGTCTAAGCGAATGTGCAACTAGTCACATCTTTCATTT

Supplementary Table 2: Sequences of the left border junctions of the T-DNA insertion lines of the cohesin genes. The red letters represent the sequence derived from the T-DNA and their position in each of the sequences reflects the orientation of the inserted T-DNA.

Gene	Locus	T-DNA insertion line	PCR method	Primer	Sequence (5' - 3')
SMC1	AT3G54670	SALK_017437 GABI_269E12	Real-time	CoI	GAAGGCGGTTCTCTATGCTG
				CoII	TTCCACCACTTGTACCACCA
SMC3	AT2G27170	SALK_015308	Real-time	CoIII	ACTCCATGAAGGTGCTGGTC
				CoIV	TCATCCTTCTTCAGGCCAAC
		GABI_498B03, SALK_087935	Real-time	CoV	CCGAGATAAATGGCTCAGGA
				CoVI	GCTCATCACGCTCTGTCAAG
SYN1	AT5G05490	SALK_137095	Semiquantitative RT	CoVII	TGTTCCGGATCCCACTTTAC
				CoVIII	GGTGGTGATGGGATGAGAGT
		SALK_006687	Semiquantitative RT	CoIX	CAGCGATGGATTATGAGCAA
				CoX	TCCAGAATAGAATGGCGTGA
SYN2	AT5G40840	SALK_044851	Semiquantitative RT	CoXI	CATCCGTCAGAGTCGTTGAA
				CoXII	CCATTTCCGCTTCATTATGG
		SALK_015096	Semiquantitative RT	CoXIII	GTTCTCGATCATCCCTACGC
				CoXIV	AGAGCAGCAGCCTGAGGAGT
SYN3	AT3G59550	SALK_119629	Semiquantitative RT	CoXV	ACATACGCTTTTGGCTCGAA
				CoXVI	TCATGAGCCGTTTCAACATC
		GABI_095A10	Real-time	CoXVII	GAACGCACTGAGTCATTGGA
				CoXVIII	GCACGTTCTTCCTCAGAACC
SYN4	AT5G16270	SALK_076116 SALK_130085 SALK_020171	Semiquantitative RT	CoXIX	GGAGCGGTGGAAGATAATGA
				CoXX	GTCCATCTCATTGAAAATGGG
			Semiquantitative RT	CoXXI	AGAAAACGGATGCATCAGCT
				CoXXII	CGAGAAGACCATCCACTGTTT
SCC3	AT2G47980	SALK_021769	Real-time	CoXXIII	TGGATGGACGCTTAATGACA
				CoXXIV	CAACATCATCAGCCATCTCG

Supplementary Table 3: Semiquantitative and Real-time PCR primers used to amplify transcripts of the cohesin genes. The positions of the primers are indicated in Figure 2. Homozygous lines were tested for the respective transcripts by Semiquantitative RT PCR and heterozygous lines by quantitative real-time PCR. All three T-DNA lines mutating *SYN4* were analysed for transcripts upstream and downstream of the T-DNA.

Gene	Locus	T-DNA insertion line	Primer	Sequence (5' - 3')
			SALK_LBb1	TGGTTCACGTAGTGGGCCATCG
			SALK_LB1.3	ATTTTGCCGATTTCGGAAC
			SAIL_LB3	AGCATCTGAATTTCATAACCAATC TCGATACAC
SMC2A	AT5G62410	SALK_052322	Cd1	TCTGGTTTCGATCCACATTTC
			Cd2	TCTCTTTTTCTCCCAGAAGGG
		SALK_103691	Cd3	CCTTGAGTTTATTCCCACTGTC
			Cd4	TAAATCTTTGGAAGCTGCCTG
		SALK_103701	Cd5	CCTTGAGTTTATTCCCACTGTC
			Cd6	TTTTTGTCATGGTCTTTGATGG
		SALK_095685	Cd7	GTTCTAGTTTTGCCATGGTGC
			Cd8	TTATGCTGTTCTTGCACTTCG
SMC2B	AT3G47460	SALK_101627	Cd9	AATTCCGCATTACCATTAGCC
			Cd10	CTACCAAATCTCAGAAGGCCC
		SALK_101643	Cd11	TCCGATATTTCACCCTGTGTC
			Cd12	GATACTTCCGTCTGGGTTTCC
		SALK_030653	Cd13	TCCTCTCACTCATGAGCTGTG
			Cd14	CTATGGCGCCTAATTCAGTTG
SMC4A	AT5G08010	SAIL_86_D02	Cd15	AGAAGCTGCCAGGGTAACAAG
			Cd16	CAAATGGTGAAATTAGCGGAG
		SALK_002313	Cd17	AAGACCTCCCAAGAAGAGCTG
			Cd18	TAACCGAAGGGAAGTACACCC
		SALK_002371	Cd19	GTAGACTCGCTGGACCCTTTC
			Cd20	TGAGACGGCTTACGAAAATAC
		SALK_002392	Cd21	GTAGACTCGCTGGACCCTTTC
			Cd22	TGAGACGGCTTACGAAAATAC
SMC4B	AT5G48600	SALK_105826	Cd23	AAACAAAGCCTAGAAATTGAGGG
			Cd24	ATACATTTCGCAAATGCTTGG
CAP-H	AT2G32590	SALK_017766	Cd25	TGGAGGTTGATGAGATTCCTG
			Cd26	TCGAAAAACAAAAGGTATGCG
		SALK_072400	Cd27	TGGAGGTTGATGAGATTCCTG
			Cd28	TCGAAAAACAAAAGGTATGCG
CAP-H2	AT3G16730	SALK_059304	Cd29	TTTCCGCTCTCTTCAACAGTC
			Cd30	AAAAAGATTGGATGGAGCATTAC
CAP-D2A	AT3G57060	SALK_077796	Cd31	AGATTGCTCTTCCTCGGACTC
			Cd32	TCTGCATCCTCATCAATCTCC

Supplementary Table 4: PCR primers used to identify the T-DNA insertion alleles of the condensin complex. SALK lines were genotyped with left border primer LBb1 and LB 1.3 and the SAIL line with the left border primer SAIL_LB3.

Gene Locus	T-DNA insertion line	Sequence (5' - 3')
SMC2A AT5G62410	SALK_052322	TGTTTACACCACAATATATCCTGAAATATTGCCGGCTCTCGAGA
	SALK_095685	TGAAACCTATATTATATTGTCGCTTAGACAACTTTGACGC
	SALK_103691	CGTTGTCTCTGGTTCGTCATGGGCGGTGAGGGCATCAGCTGT
	SALK_103701	CGTTGTCTCTGGTTCGTCATAGTGGTGATTTTGTGCCGAGC
SMC2B AT3G47460	SALK_101643	GGGGATTGATGGTACTTAGCCGCTGGGTTTCCATTTCTAGGGTT
	SALK_101627	AGAGTCCCCCGTGTTCTAACAACCGAAATGAACCGATCCAAA
	SALK_030653	ACAAGTTTAGATCAGAATTATGGAAGTCGCAGGAGAATCATTA
SMC4A AT5G08010	SALK_002313	TAGATTGGTGGGAATCTAGCTGCCTGTATCGAGTGGTGAT
	SAIL_86_D02	CAAAGAAATTATATAAACTCAGCTGCCTGTATCGAGTGGTG
	SALK_002371	TATTTTCGTAAGCCGTTCTTTAAAATCGGCAAAATCCCTTAT
	SALK_002392	ACACCACAATATATCCTGCTTAGTCTACCAAATGGCATCTCTAC
SMC4B AT5G48600	SALK_105826	ATTTAATTATGCAATTTGTCGAAGCCTTTTTCTGTGTTTC
CAP-H AT2G32590	SALK_017766	TGGGAGGAAAAAGACAACACAACTCAAGCTTTAGGTCAAC
	SALK_072400	AACACTTCCAGTCATTAAGATAATAACAAATTGCGGACGTTTT
CAP-H2 AT3G16730	SALK_059304	TAAAGACGAGAAGACATCCCTTATTACGAGAAGGTCTGTGTTT
CAP-D2A AT3G57060	SALK_077796	CGGTATATAACAATTTCTAAAATAGTGGTGTAAACAAATTGTG

Supplementary Table 5: Sequences of the left border junctions of the T-DNA insertion lines mutating condensin genes. The red letters represent the sequence derived from the T-DNA and their position in each of the sequences reflects the orientation of the inserted T-DNA.

Gene	Locus	T-DNA insertion line	PCR method	Primer	Sequence (5' - 3')
SMC2A	AT5G62410	SALK_052322	Semiquantitative RT	CdI	CCGGAGATATTGTCCATGCT
				CdII	TTTTCTCCCAGAAGGGTGTC
		SALK_103691, SALK_103701	Real-time	CdIII	CCATCAAAGCTCAAATGCAG
				CdIV	TTGCTTCTTCCTCCATCACA
		SALK_095685	Semiquantitative RT	CdV	AGTCTCTTGCCGAGCTCAAG
				CdVI	CGATATCAGAGCATTGTATTCATC
SMC2B	AT3G47460	SALK_101627, SALK_101643	Semiquantitative RT	CdVII	GTTTTGACCCGCATTTCAAC
				CdVIII	GGATGCCTGAATACGAGCTT
		SALK_030653	Real-time	CdIX	TGCGGCTAAGGAAGTAGCAT
				CdX	CTCGGCCAGATCATGAAGTT
SMC4A	AT5G08010	SAIL_86_D02	Real-time	CdXI	GAACAGAGAGACAGCTTGCAGA
				CdXII	CATCCATTTTCACTCGCTCA
		SALK_002313	Real-time	CdXIII	GCTCAGTTCATTATCATCAG
				CdXIV	TGCAAAACTTCCAGGATTGA
		SALK_002371 SALK_002392	Semiquantitative RT	CdXV	ATCACTCTGGGAGGTGATGC
				CdXVI	TTTTCTGACAAACTGCAAAACT
SMC4B	AT5G48600	SALK_105826	Semiquantitative RT	CdXVII	TTTTGATGAAACCGTGTCCA
				CdXVIII	TTTATGGCTCCAAGGTGAGC
CAP-H	AT2G32590	SALK_017766	Real-time	CdXIX	CTATTGGCTAGCTTCCCAGA
				CdXX	AGGCTGAGATTGTGCTCGTT
		SALK_072400	Real-time	CdXXI	CACGCCAGGTCAACAAAAT
				CdXXII	TCCTGAAGACACTCCCAAAGA
CAP-H2	AT3G16730	SALK_059304	Semiquantitative RT	CdXXIII	GAAACCAACCTTGTGGTGCT
				CdXXIV	ACTGGAGAAGCGCAGAGAAG
CAP-D2A	AT3G57060	SALK_077796	Semiquantitative RT	CdXXV	AGCGGAGTCACAGGTATGCT
				CdXXVI	CTGAGGACAGCAAGGGATTC

Supplementary Table 6: Semiquantitative and Real-time PCR primers used to amplify transcripts of condensin T-DNA lines. Homozygous lines were tested for the respective transcripts by semiquantitative RT PCR and heterozygous lines by quantitative real-time PCR.

Gene	Locus	T-DNA insertion line	Primer	Sequence (5' - 3')
SWI1	AT5G51330	GABI_206H06	IP29	TCTTCCCCATAAGCTCTCTGC
			IP30	AGCCATCACATGACTCTCGTC
SCC2	AT5G15540	SALK_058767	IP31	CGAATAATGGCCATTGAGTTG
			IP32	ACTAACCTGTCATGGCCAATG
		SALK_151609	IP33	GACACAGACGGATATTCAGGAAG
			IP34	ATGTAAGCGCAAAAATTGTGC
BRU1	AT3G18730	SALK_034207	IP35	GCACATTTTGCATTTTCAATC
			IP36	ACGACGACCAGTTGTTTCAAC

Supplementary Table 7: PCR primers used to identify the T-DNA insertion alleles of cohesin and condensin interacting proteins.

Gene Locus	T-DNA insertion line	Sequence (5' - 3')
SWI1 AT5G51330	GABI_206H06	ACATAGTTCTGAATATAAAAATTGGGTTTGTTCTTACAGTTG
SCC2 AT5G15540	SALK_058767	AAGTCAATGTGTTATTAATTTGTTTACTTCGTTCTTGCTATC
	SALK_151609	TCAAGGACCTGGGAAATTGACGCTTAGACAACTATTGCGG
BRU1 AT3G18730	SALK_034207	TTAAGTTGTCTAAGCGTCAAACTTAGATCAGAACGGTTAGCA

Supplementary Table 8: Sequences of the left border junctions of the T-DNA insertion lines of cohesin and condensin interacting proteins. The red letters represent the sequence derived from the T-DNA and their position in each of the sequences reflects the orientation of the inserted T-DNA. Annotated positions in the database were not always correct. Some insertions were shifted to the neighbouring intron or exon.

Gene	Locus	T-DNA insertion line	PCR method	Primer	Sequence (5' - 3')
SWI1	AT5G51330	GABI_206H06	Semiquantitative RT	IPXXV	GAAGCAAGGAAGCTGATTGG
				IPXXVI	CATCCCATGTCTTCCTCCAT
			Semiquantitative RT	IPXXVII	CGATGTTCGTGAAACGGAAT
				IPXXVIII	CATGAGGTGCGATTCTTCTG
SCC2	AT5G15540	SALK_151609	Real-time	IPXXIX	GCACCAAATGATGGCTGTTA
				IPXXX	CATCACCTTCAAATGCCAAA
		SALK_058767	Real-time	IPXXXI	CATTGCCAGACTGAAAGCAA
				IPXXXII	TCCAAGGGCTAAAGTAATCTGC
BRU1	AT3G18730	SALK_034207	Semiquantitative RT	IPXXIX	ACCGAATATGAGCTGGGATG
				IPXXX	ATGATGAATGATCGGCAACA

Supplementary Table 9: Semiquantitative and Real-time PCR primers used to amplify transcripts of proteins interacting with cohesin or condensin. Homozygous lines were tested for the respective transcripts by Semiquantitative RT PCR and heterozygous lines by quantitative real-time PCR.

Vector	Primer	Sequence (5' - 3')	Product size
pBIN-pROK2 (SALK)	35Spromoter forward	GGTCTTGCGAAGGATAGTGG	374 bp
	35Spromoter reverse	GGTGGAGCACGACACACTT	
pAC161 (GABI)	Right border forward	GCAGAGCGAGGTATGTAGGC	496 bp
	Right border reverse	AAGCCCTCCCGTATCGTAGT	

Supplementary Table 10: Primers to amplify the Southern hybridisation probe. Probes were amplified from genomic DNA of corresponding mutant plants.

Vector	Primer	Sequence (5' - 3')	Product size
pLH7000	EYFP forward	TATATCATGGCCGACAAGCA	96 bp
	EYFP reverse	GTTGTGGCGGATCTTGAAGT	
pLH9000	YFP forward	GGTGATGTTAATGGGCACAA	92 bp
	YFP reverse	TCACCTTCACCCTCTCCACT	
pLH9000	DsRed forward	GCGTGATGAACTTCGAGGAC	95 bp
	DsRed reverse	GCCGATGAACTTCACCTTGT	

Supplementary Table 11: Primers used to amplify the EYFP, YFP and DsRed transcripts for Real-time PCR. Transcript standards were amplified from plasmid DNA. Transcripts were amplified from pooled seedlings of corresponding mutant plants.

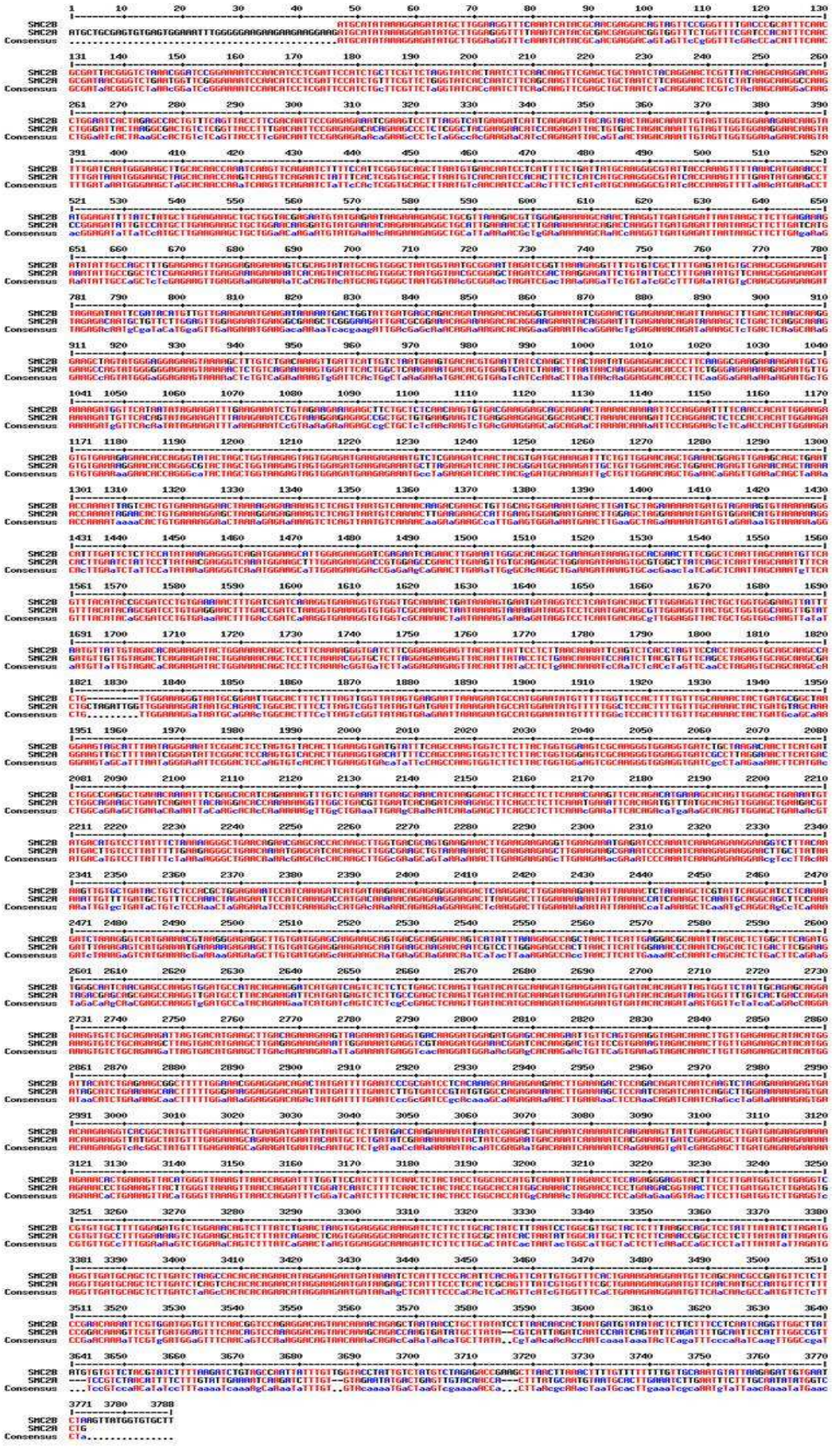

Supplementary Figure 1: cDNA alignment of *SMC2* homologs of the condensin complex. *SMC2A* and *–B* show a high homology (>90% on cDNA level).

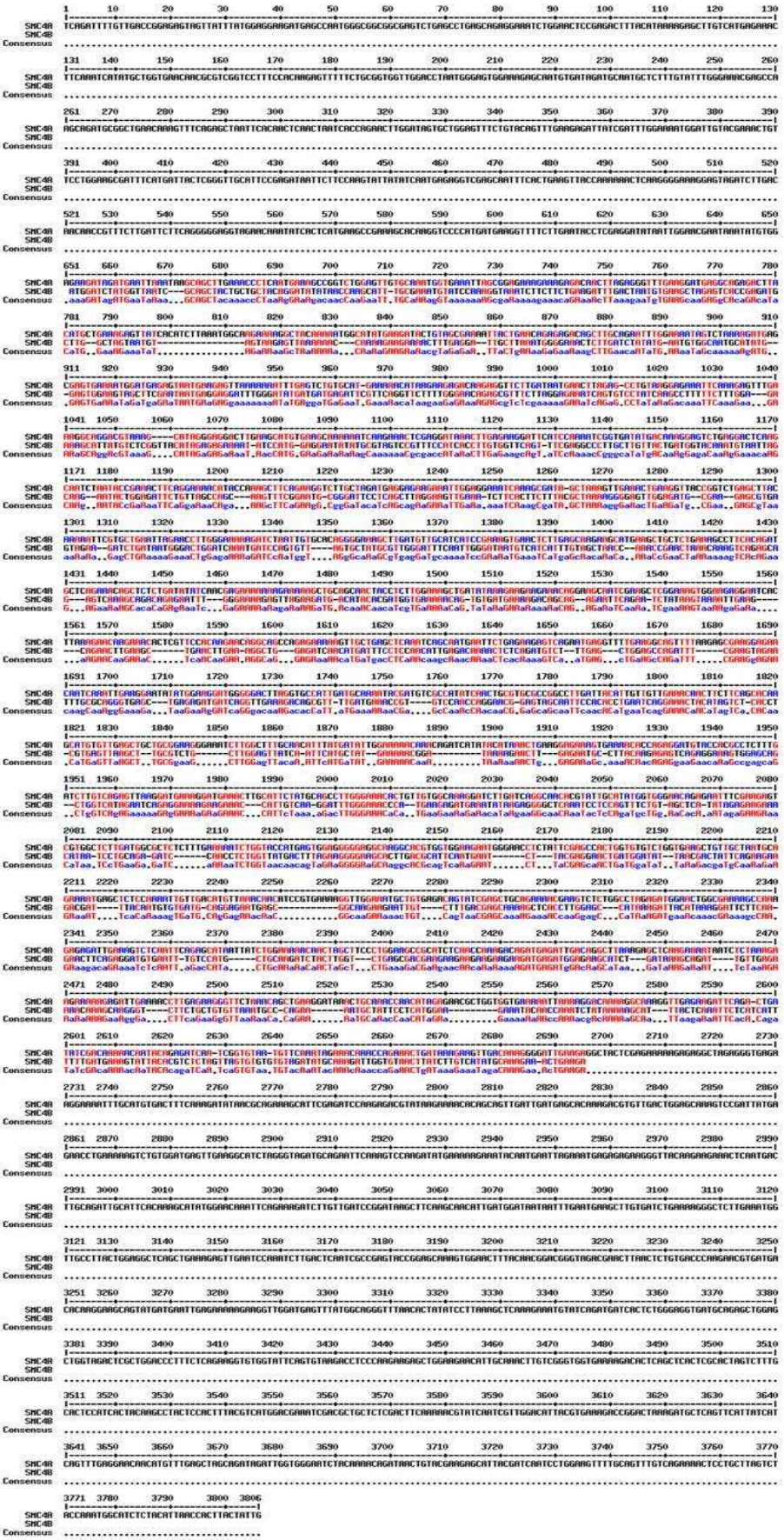

Supplementary Figure 2: cDNA alignment of *SMC2* homologs of the condensin complex. *SMC4A* and *SMC4B* are different in sequence and length.

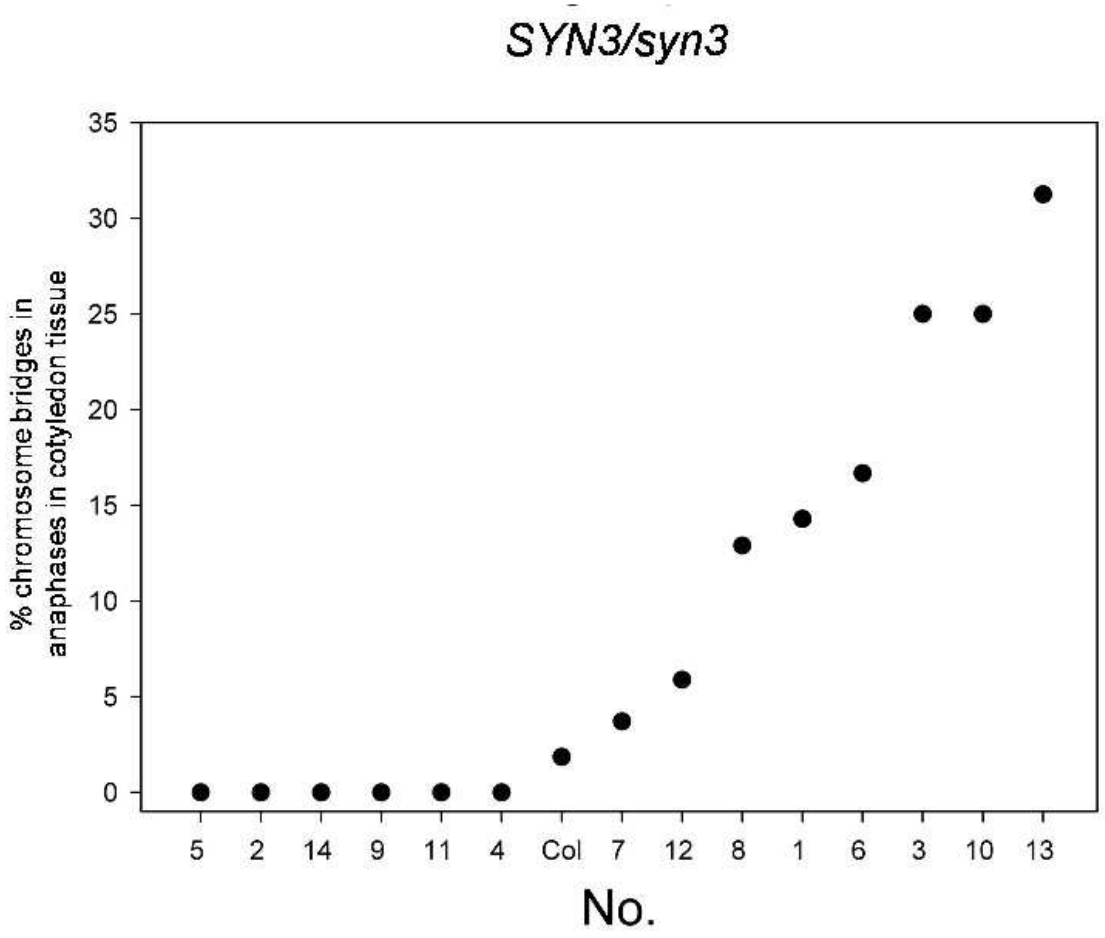

Supplementary Figure 3: A representative example for distribution of anaphase bridges in a plant population derived from a heterozygous *syn3* mutant plant. Plants number 8, 1, 6, 3, 10 and 13 deviate significantly from wt, indicating heterozygosity for these plants. Values were calculated with help of the two-sided Fisher´s Exact Test.

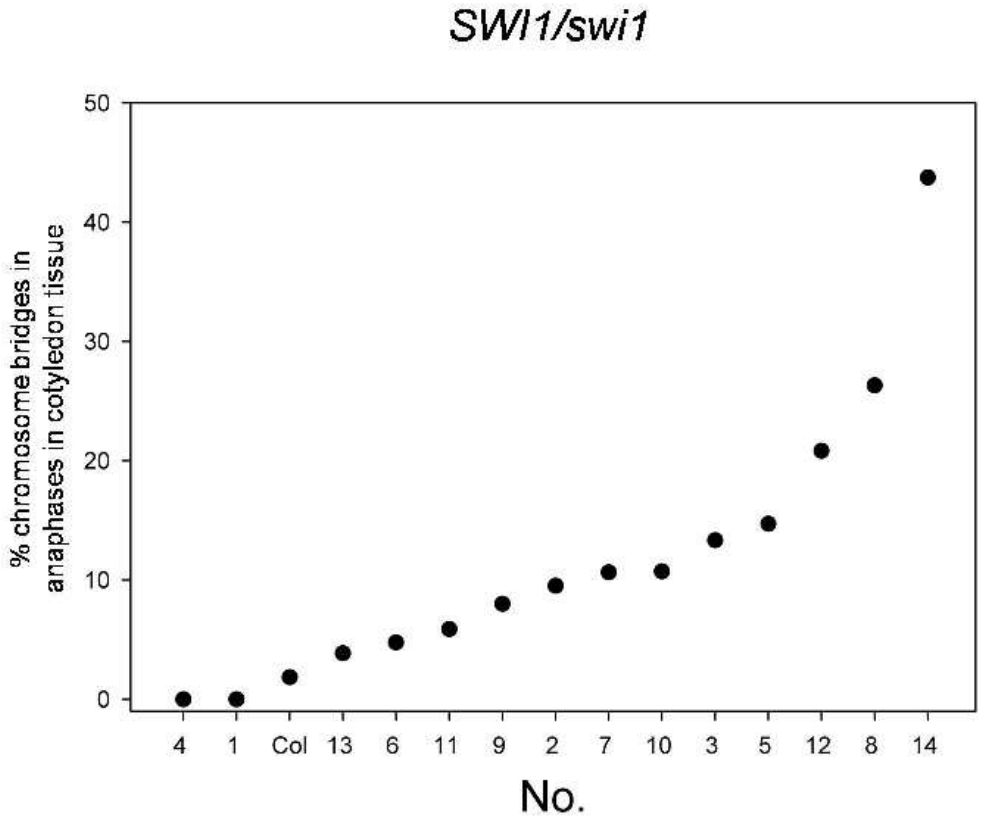

Supplementary Figure 4: A representative example for distribution of anaphase bridges in a plant population derived from a heterozygous *swi1* mutant plant. Homozygous *swi1* mutants were sterile. Thus, propagation of the line was done via heterozygotes. Plants number 7, 3, 5, 12, 8 and 14 deviate significantly from wt. Plant number 14 displays a putative homozygous mutant. Values were calculated with help of the two-sided Fisher´s Exact Test.